Global limits on silicate weathering and implications for the silicate weathering feedback

Dissertation

zur Erlangung des akademischen Grades doctor rerum naturalium
(Dr. rer. nat.)

vorgelegt dem Rat der Chemisch-Geowissenschaftlichen Fakultät der
Friedrich-Schiller-Universität Jena

von cand.scient. Susanne Kathrine Munk Arens
geboren am 15. Februar 1976 in Nykøbing Falster, Dänemark

Gutachter:

1. Dr. habil. Victor Brovkin, Max-Planck-Institut für Meteorologie
2. Jun.-Prof. Dr. Anke Hildebrandt, Friedrich-Schiller-Universität Jena

Tag der öffentlichen Verteidigung: 29. Mai 2013

The more comfortable we become with being stupid,
the deeper we will wade into the unknown
and the more likely we are to make big discoveries.[1]
Martin A. Schwartz

---

[1] The importance of stupidity in scientific research, J Cell Sci 121, 1771. 2008

Abstract

Chemical weathering of silicate rocks is considered responsible for the stabilization of atmospheric CO_2 and climate on geological time scales. The details of the function of this negative feedback are hard to establish on a global scale due to the spatial variability of controlling factors of weathering such as climate, physical erosion and biotic activity. We set out to investigate if there is a simple way of including spatial variability of climatic and tectonic drivers of weathering in a global model of silicate weathering and regolith formation. We did this from the perspective that the physical transports of the ingredients of chemical weathering (water, carbon and minerals) set limitations for weathering and thereby control silicate weathering rates at large scales. This is in contrast to previous global models of the geological carbon cycle, in which chemical kinetics and thus temperature is considered of primary importance and physical transports are considered secondary in nature.

We therefore developed a new model of the regolith, which specifically considers these physical transports as boundary conditions for chemical weathering rates. The climate related transports of water and carbon are estimated based on a global dynamic vegetation and soil hydrology model. The tectonic related transport of minerals are estimated with empirical formulations of physical erosion rates.

The model is able to satisfactorily simulate river concentrations of elements relevant to the silicate weathering feedback for a present day scenario, in which effects of recent glaciations are considered. It also illustrates how the limitations set by physical transports of water, carbon and minerals control steady state chemical weathering rates. In steady state chemical weathering is either limited by the climatic carbon and water fluxes, which set the potential for dissolution of minerals and transport of dissolved load, or by the tectonic mineral supply flux. Thus if chemical weathering is limited by mineral supply, an increase in the climatic potential for dissolution and transport has no effect on chemical weathering rate. We hereby show that mineral supply limitation weakens the silicate weathering feedback. We also show that biotic enhancement of weathering, which strongly affects carbon

fluxes in soils and regoliths, is limited by mineral supply and by inference tectonic uplift.

By considering chemical weathering as co-limited by the physical transports associated with climatic and tectonic boundary conditions, we illustrate that there are some inherent problems associated with the use of factorial laws in global models of the geological carbon cycle. Even though it is possible to deduce a factorial law from the spatially explicit model developed here, the quality of the fit of the factorial law to the model output decreases markedly, when mineral supply limitation is included. This indicates that an integrated approach, in which all drivers of weathering are considered simultaneously is preferable to separate empirical parameterizations, because a change in one driver might lessen the impact of the other drivers. This can only be achieved with process based models. The resulting quantification of the silicate weathering feedback may depend on the characteristics of the model used, such as resolution, lithological description, kinetic rate laws used, and climate sensitivity to atmospheric CO_2, but the principle of co-limitation associated with the physical transports of water, carbon, and minerals seems universal in setting the boundaries for the potential feedback.

KURZFASSUNG

Die Chemische Verwitterung von Silikatgesteinen bewirkt eine Stabilisierung der atmospärischen CO_2-Konzentration und des Klimas auf geologischen Zeitskalen. Die funktionellen Details dieses negativen Rückkopplungsmechanismus sind auf globalen Skalen schwierig zu beschreiben, weil die für die Verwitterung wichtigen Prozesse wie Klima, Erosion und biotische Einflüsse, große räumliche Variabilitäten aufweisen. Ziel dieser Arbeit war es zu prüfen, ob es einfache Möglichkeiten gibt, die räumliche Variabilität klimatischer und tektonischer Einflussfaktoren auf Verwitterung in einem globalen Modell zu beschreiben. Grundlage war die Hypothese, dass der physikalische Transport der chemischen Verwitterungsprodukte (Wasser, Kohlenstoff, Mineralien), die Verwitterung begrenzt und somit die Verwitterungs- raten von Silikaten auf großen Skalen bestimmt. Im Gegensatz dazu wurde in bisherigen Beschreibungen der Verwitterung davon ausgegangen, dass chemische Kinetik und somit die Temperatur die Haupteinflussfaktoren bilden und physikalischer Transport in der Natur eine untergeordnete Rolle spielt.

Im Rahmen dieser Arbeit wurde ein neues Regolithmodell entwickelt, welches den physikalischen Transport explizit als Randbedingung für chemische Verwitterung berücksichtigt. Der Transport von Wasser und Kohlenstoff, der auch vom Klima beeinflusst wird, wurde mit Hilfe eines globalen dynamischen Vegetations-Bodenhydrologiemodells bestimmt. Der tektonisch bedingte Transport von Mineralien wurde durch empirische Modelle physikalischer Erosionsraten quantifiziert.

Das Modell kann in Flüssen gemessene Konzentrationen von für die Silikatverwitterung wichtigen Elementen in zufriedenstellender Weise reproduzieren. Dazu wurde ein present-day Szenario gewählt, in dem Einflüsse der letzten Eiszeiten berücksichtigt. Das Modell demonstriert auch, wie der physikalische Transport von Wasser, Kohlenstoff und Mineralien die chemischen Verwitterungsraten im stationären Zustand maßgeblich bestimmt. Im stationären Zustand ist die chemische Verwitterungsrate entweder durch klimatische Kohlenstoff- und Wasserflüsse begrenzt, welche das Potenzial für die Lösung von Mineralien und den Abtransport der gelösten Stoffe bestimmen, oder durch die Rate, mit der tektonisch neue Mineralien bereitgestellt

werden. Zudem schwächt die tektonische Begrenzung der Mineralbereitstellung den Rückkopllungsmechanismus der Silikatverwitterung ab. Insbesondere wird die biotische Erhöhung von Verwitterungraten, die die Kohlenstoffflüsse im Boden und Regolith stark beeinflusst, über die Mineralbereitstellung durch tektonische Hebung begrenzt ist.

Mit der Berücksichtigung dass chemische Verwitterung auch durch physikalischen Transport begrenzt ist, wird gezeigt, dass es grundsätzliche Probleme bei der Anwendung von Faktorgesetzen in Modellen des globalen Kohlenstoffkreislaufs gibt. Obwohl es möglich ist, aus dem hier entwickelten Modell ein faktorielles Gesetz herzuleiten, sinkt die Qualität der Regression des faktoriellen Gesetzes erheblich, sobald eine Begrenzung der Mineralbereitstellung berücksichtigt wird. Dies deutet darauf hin, dass ein integrierter Ansatz in dem alle Einflussfaktoren von Verwitterung gleichzeitig berücksichtigt werden, der Verwendung von separaten, empirischen Parametrisierungen vorzuziehen ist, da die Änderung eines Einflussfaktors die Auswirkungen der anderen Faktoren verringern kann. Ein solcher Ansatz kann nur mit prozessbasierten Modellen realisiert werden. Die resultierende quantitative Bestimmung des Rückkopplungsmechanismus der Silikatverwitterung hängt zwar von spezifischen Modellcharakteristika wie Modellauflösung, Beschreibung der Lithologie, den verwendeten kinetischen Reaktionsgesetzen und Klimasensitivität gegenüber erhöhtem atmosphärischen CO_2 ab, das Prinzip der Begrenzung durch physikalischen Wasserß Kohlenstoffß und Mineraltransport jedoch scheint für die Bestimmung der Grenzen eines potentiellen Rückkopplungsmechanismus universell zu sein.

Contents

1 Introduction

1.1 Silicate weathering and the geological carbon cycle

Chemical weathering of silicate rocks has a stabilizing effect on the Earth's climate, through the role it plays in the geological carbon cycle (Ebelmen, 1845; Urey, 1952; Walker et al., 1981). One major aspect is the ability of the Earth to sustain liquid water on geological time scales, a feature which is unique in the solar system. The Earth is the only planet within the solar system with a rigorous water cycle, in which water is transferred between the liquid, solid and gaseous phases. The Earth is also the only planet where energy and matter are continuously exchanged between the atmosphere and interior through plate tectonics. Perhaps not surprisingly the two features are connected. The existence of plate tectonics relies on the presence of water for lubrication of the lithospheric plates and initiation of subduction (Regenauer-Lieb et al., 2001). The stability of liquid water on the Earth's surface depends on the greenhouse effect, which modulates the temperature profile of the atmosphere, and thus the exchange of water both vertically and laterally in the atmosphere. The greenhouse effect is dominated by water vapor (which is a strong greenhouse gas) and modulated by carbon dioxide (CO_2), which is the other major natural and photochemically stable polyatomic greenhouse gas of the troposphere (Edmond and Huh, 2003). On geological time scales the concentration of CO_2 in the atmosphere is affected by the exchange of matter with the Earth's interior, through volcanism and the burial and subduction of carbon.

The amount of CO_2 released into the atmosphere by volcanic activity and metamorphic degassing on geological time scales ($4 - 10 \times 10^{18}$ mol/Ma, Marty and Tolstikhin 1998) must be balanced by removal of CO_2 from the atmosphere. Otherwise the CO_2 level of the atmosphere and thus temperatures would fluctuate much more than indicated by the constant presence of liquid water on the Earth's surface throughout Earth history (Walker et al., 1981;

Holland, 2004). Considering that the size of the combined atmosphere-ocean-soil-biosphere carbon reservoir is on the same order of magnitude (3×10^{18} mol C, Berner and Caldeira 1997) as the flux from the Earth's interior on this long time scale, the need for a mechanism responsible for the balanced removal of CO_2 from the atmosphere becomes even more evident. The clue is hidden in the rock record, specifically in the appreciable size of the carbon reservoirs of carbonate (5000×10^{18} mol C, Berner and Caldeira 1997) and organic carbon (1300×10^{18} mol C, Berner and Caldeira 1997).

The formation of carbonate minerals (Ca,Mg)CO_3 primarily takes place in the Earth's oceans, through both inorganic precipitation and organic deposition of calcareous plankton, corals, and shells:

$$(Ca, Mg)^{2+} + 2HCO_3^- \rightarrow (Ca, Mg)CO_3 + CO_2 + H_2O \qquad (1.1)$$

Note that for 2 moles of dissolved CO_2 (HCO_3^-), one is bound in carbonate and one is released back into the atmosphere-ocean reservoir. Also, a continuous external source of Ca^{2+} and Mg^{2+} is needed to sustain a net formation of carbonates[1].

The source of Ca^{2+} and Mg^{2+} is primarily the dissolution of rocks containing Ca and Mg minerals. If the source is carbonate rocks there is no net consumption of CO_2 as this simply corresponds to the reverse reaction of 1.1. If the source is silicate rocks, the result is a net consumption of CO_2 from the atmosphere. An often-used generalized form of the partaking chemical weathering reactions is (Berner, 1999):

$$(Ca, Mg)SiO_3 + 2CO_2 + H_2O \rightarrow (Ca, Mg)^{2+} + 2HCO_3^- + SiO_2 \qquad (1.2)$$

As 2 moles of CO_2 are consumed during the dissolution of (Ca,Mg)SiO_3 and 1 mole of CO_2 is released during the subsequent formation of (Ca,Mg)CO_3

---

[1] The role of Mg fluxes is somewhat ambiguous. Mg-carbonate is observed in greater quantities in the sedimentary rock record, e.g. in the Dolomites in the Eastern European Alps. However, magnesian calcite is only produced in limited quantities today (0.5-5 mole % $MgCO_3$ of marine carbonates, Morse and MacKenzie 1990), and dolomitization (the substitution of Ca with Mg) rarely forms in modern carbonate environments (McKenzie and Vasconcelos, 2009). Hereto comes reverse weathering reactions in marine sediments, which may remove as much as 50 % of Mg from weathering (Wollast and Mackenzie, 1983).

(reaction 1.1), the net result of the two reactions is that CO_2 is removed from the atmosphere and bound in $(Ca,Mg)CO_3$ (Ebelmen, 1845; Urey, 1952):

$$(Ca, Mg)SiO_3 + CO_2 \rightarrow (Ca, Mg)CO_3 + SiO_2 \tag{1.3}$$

Finally, it is worth noting that this geological cycle of carbon is closed when the carbonates formed on ocean floors are subjected to metamorphism in subduction zones. Hereby, new silicate minerals are formed and CO_2 is

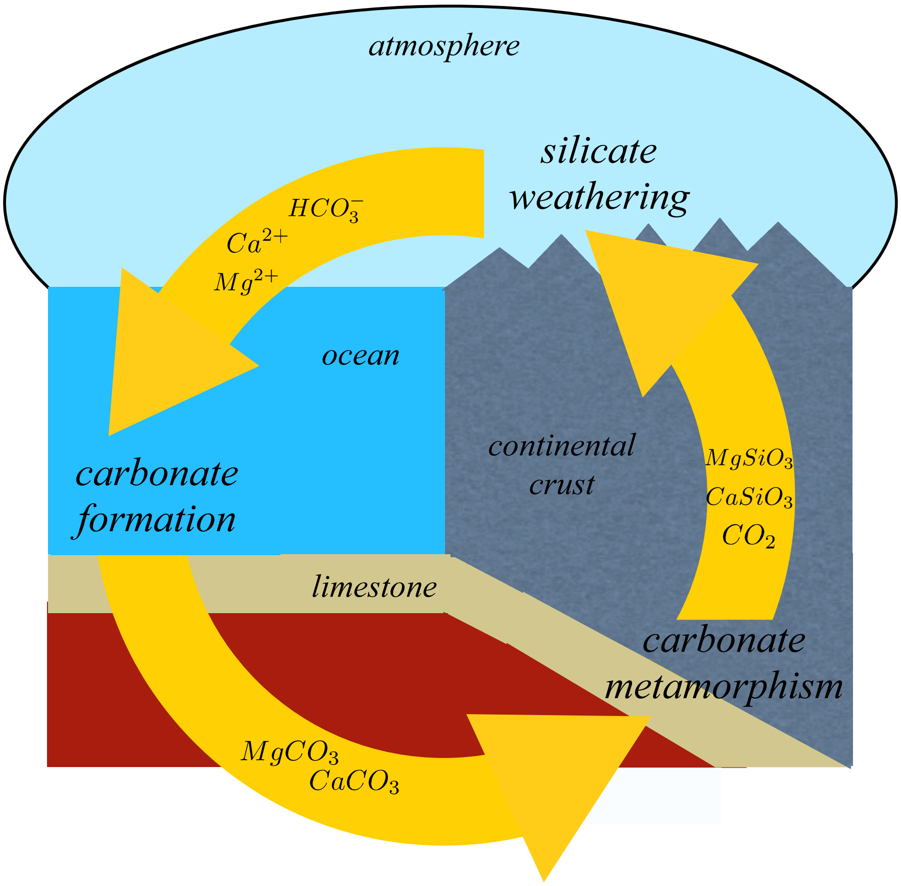

Figure 1.1: The geological cycle of carbon (C), calcium (Ca) and magnesium (Mg). Silicate rocks formed in the Earth's crust are uplifted, exposed and weathered at the surface, leading to the export of dissolved Ca, Mg and CO_2 to the oceans. In the oceans Ca, Mg and CO_2 are bound in carbonate minerals. These carbonate minerals are eventually subducted and metamorphosed by which CO_2 is released back into the atmosphere and new silicate minerals are formed.

released back into the atmosphere:

$$(Ca, Mg)CO_3 + SiO_2 \rightarrow (Ca, Mg)SiO_3 + CO_2 \tag{1.4}$$

Figure 1.1 illustrates the connection and flow of matter between the three processes involved in the geological carbon cycle: carbonate formation (reaction 1.1), silicate weathering (reaction 1.2) and carbonate metamorphism (reaction 1.4). Each of the three processes may form a bottleneck, that can slow down or speed up the rate of the whole cycle. However, the time scale of the whole cycle is $10^7 - 10^8$ years, due to the slow rate of subduction (Edmond and Huh, 2003; Kasting and Catling, 2003). The much shorter time scale of silicate weathering and carbonate formation ($10^5 - 10^6$ years Kasting and Catling 2003) means that these processes and their impact on atmospheric CO_2 are usually modeled with the rate of metamorphic release of CO_2 as a boundary condition estimated from rates of seafloor spreading and subduction (e.g. Berner 1994). This is because the surface processes and their fast response to the slow changes in metamorphic release of CO_2 control the partitioning of C within the atmosphere-ocean reservoir rather than the actual fluxes of CO_2 into and out of the atmosphere-ocean reservoir.

1.1.1 The silicate weathering feedback

As a solution to the stabilization of atmospheric CO_2 on geological time scales, the silicate weathering hypothesis (Walker et al., 1981) suggests a negative feedback involving climatic effects on the dissolution of silicate minerals on land. The flux of calcium and magnesium from land to ocean thus plays a critical role in the stabilization of atmospheric CO_2 by driving the formation of carbonate minerals in the oceans. The silicate weathering feedback is illustrated and described in figure 1.2.

In Walker et al. (1981) the silicate weathering feedback is defined as a purely climatic feedback, depending on temperature, partial pressure of CO_2 and runoff. It is assumed that silicate weathering rate is limited by reaction kinetics, and that higher temperature and partial pressure of CO_2 will lead to higher weathering rates, due to the dependence of kinetic parameters on temperature and CO_2. The formulation for this dependence was found under

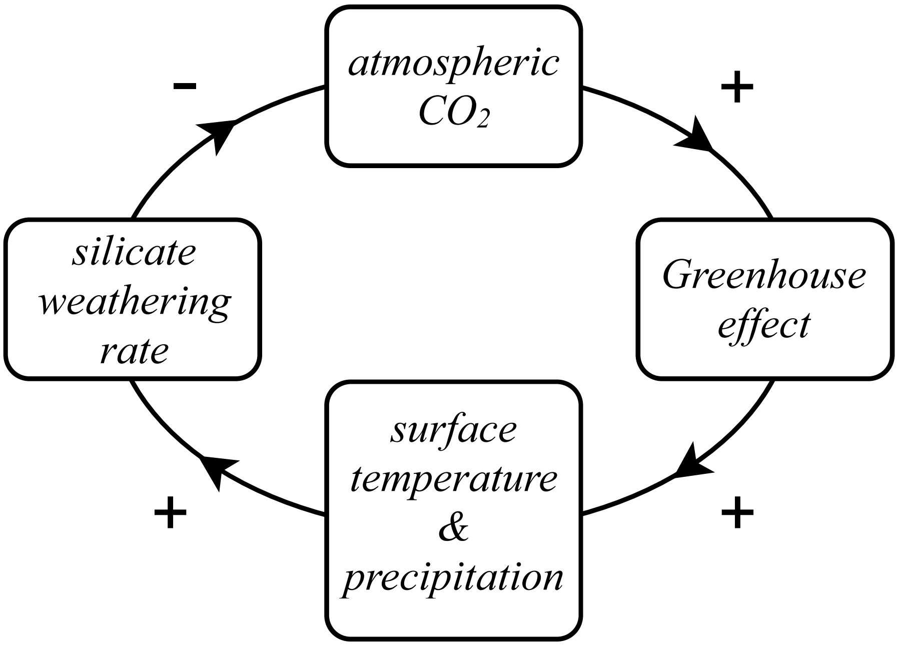

Figure 1.2: The silicate weathering feedback. + indicates a direct response, i.e. a positive effect of one parameter on another. - indicates an inverse response, i.e. a negative effect of one parameter on another. The overall negative feedback results because an increase or decrease in CO_2 results in a dampening of this increase or decrease through the inverse response (-) of atmospheric CO_2 to silicate weathering rate. Thus, an increase in atmospheric CO_2 will lead to an increase in the greenhouse effect, with resulting increases in temperature and precipitation. This will lead to a corresponding increase in silicate weathering rate and in the rate of removal of CO_2 from the atmosphere through carbonate formation as described in reactions 1.1 and 1.2. Thus an initial increase in atmospheric CO_2 will lead to a decrease in and thus stabilization of atmospheric CO_2. Conversely, the negative feedback loop also stabilizes an initial decrease in atmospheric CO_2 with a decrease in silicate weathering rate and CO_2 consumption.

far-from-equilibrium laboratory conditions. Extrapolating from laboratory conditions to the field has proven difficult, as weathering rates found under laboratory conditions commonly are 2 to 4 orders of magnitude faster than those measured in the field (Schnoor, 1990; Brantley, 1992; White et al., 1996; White and Brantley, 2003). This indicates that other processes must play a crucial role in limiting chemical weathering rates on the land surface.

A key observation is that a disproportionately large fraction of dissolved fluxes to the oceans come from areas of high topographic relief (Raymo and Ruddiman, 1992). This can be explained by the need for a continued supply of minerals to sustain chemical weathering rates on long time scales. Uplift of the continental crust drives physical erosion, which keeps the regolith shallow and rich in weatherable silicate minerals. Thus the rate of uplift plays an important role in moderating atmospheric CO_2 through it's impact on topographic relief and physical erosion (Raymo et al., 1988; Gaillardet et al., 2011).

The original view of the silicate weathering feedback (Walker et al., 1981) is now an integral part of any global model of silicate weathering and the geological carbon cycle, but many other characteristics of the land surface have now been taken into account. Notably, Schwartzman and Volk (1989); Berner (1991) and Von Bloh et al. (2003) included land surface area and biotic enhancement of weathering, and Berner (1994) included a factor for continental relief in response to the potential role of tectonic uplift in modulating the weathering rate. However, at the core of these models is still the assumption that weathering is kinetically limited. Also, debate continues regarding the role of uplift in modifying the silicate weathering feedback and atmospheric CO_2 on geological time scales (e.g. Berner and Caldeira, 1997; Edmond and Huh, 2003; Zeebe and Caldeira, 2008; Willenbring and von Blanckenburg, 2010).

1.2 Motivation

It is the working hypothesis of this thesis that limitations associated with the physical transport of dissolved and solid material shape global patterns of chemical weathering rates rather than the complexity of a suite of reaction kinetics, and that these limitations play an important role in shaping the response of silicate weathering to changes in atmospheric CO_2 and climate. This can be motivated by the following thought experiment: if there were no topographical gradients on the surface of the Earth, there would be no lateral transport of liquid or solid matter along the surface. Chemical gradients would soon be depleted as reactants were used up or isolated from each other by accumulating products of the chemical reaction. A chemical equilibrium would hereby be reached putting a stop to further weathering reactions. Thus, without topographical gradients to remove the products of reaction, chemical weathering would cease.

In order to understand the connection between physical transport processes and observed global patterns of chemical weathering, we consider these processes in terms of the limitations they set for chemical weathering. This is motivated by our understanding of limits on chemical weathering rates described in the following section.

1.2.1 On the role of limits

If chemical weathering is kinetically limited, it is the rate laws of the chemical reactions involved that define the rate at which products of the reaction are exported from the regolith. However, as chemical reactions come to a halt when saturation is reached with respect to the products of reaction, e.g. Ca^{2+} and HCO_3^-, chemical weathering instead becomes dependent on the exchange of reactants and products with the surrounding environment. The flow of water through the regolith plays an important role as it removes dissolved products and replaces saturated water with unsaturated water in which the chemical reactions may continue. If the flow of water is fast enough, saturation is never reached, and chemical weathering is kinetically limited. If the flow of water is so slow that saturation is reached, chemical weathering is limited by transport of water, or simply transport limited.

Another form of transport limitation is associated with the supply of reactants. Chemical weathering can only occur if there are minerals to weather. The supply of minerals in the regolith depends on the physical breakdown and transport of minerals from the bedrock into the regolith. This regolith production rate or *physical weathering rate* depends on a number of factors, including temperature variability, frost, root activity and chemical weathering. A common feature of these processes is that their activity decreases exponentially with depth and so does regolith production rate (Ahnert, 1977; Heimsath et al., 1997; Humphreys and Wilkinson, 2007). This means that physical weathering rate is tightly connected to regolith depth and thereby to physical erosion rate, which is modified by topographic relief and uplift. Thus if physical erosion rate is limited by low topographic relief, chemical weathering rates may become limited by the availability or supply of weatherable minerals. This type of behavior is commonly termed *supply limited* chemical weathering (Riebe et al., 2004).

Finally, chemical weathering as described here can also be limited by the transport of carbon (CO_2) into the regolith. Vegetation and microbial activity is a strong modifier of CO_2 concentration in soils and regoliths, leading to biotic enhancement of weathering. There are a multitude of other ways in which biota might increase chemical weathering (Taylor et al., 2009), but these are not the main focus here. Instead the potential for biotic enhancement of weathering will be considered from a limitations perspective.

We can therefore conclude that there are four potential limitations on chemical weathering rate in any given chemical weathering scenario involving carbon: 1) a kinetic limitation, 2) a hydrological limitation, 3) a carbon limitation and 4) a mineral supply limitation. These limitations govern the input, output and the rate of transformation in the weathering "reactor" of the regolith (figure 1.3).

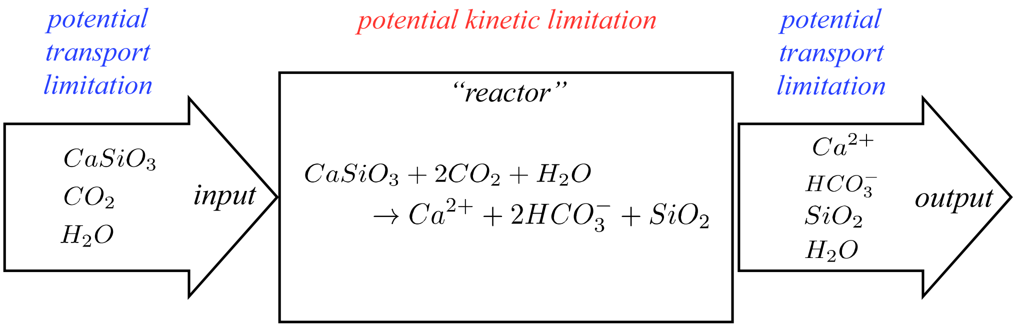

Figure 1.3: Potential limitations, inputs and outputs associated with the silicate weathering "reactor" of the regolith. The input fluxes are provided by uplift ($CaSiO_3$), precipitation (H_2O) and the biosphere (CO_2), the output fluxes are controlled by runoff (Ca^{2+}, HCO_3^-, H_2O) and physical erosion (SiO_2).

As mentioned in section 1.1.1 weathering rates measured under far from equilibrium laboratory conditions are commonly 2 to 4 orders of magnitude faster than those found in regoliths in the field (Schnoor, 1990; Brantley, 1992; White et al., 1996; White and Brantley, 2003). Furthermore, the effect of temperature has proven difficult to establish empirically for river catchments, probably due to correlation between temperature and runoff (Hartmann, 2009; Hartmann and Moosdorf, 2011). This is a strong indication that the kinetic rate limitation is not the dominant limitation under field conditions. It does not rule out that kinetic limitations may exist under some conditions, but does suggest that they are generally negligible. It would therefore be interesting to test if chemical weathering rates can be parameterized in a process based model without the specific consideration of kinetic rate laws. Can the known patterns in the transport limitations be used to model patterns of chemical weathering rates?

In practice this can be done by the application of climate data or a climate model and an integrated vegetation and soil hydrology model to calculate the physical transport of carbon and water through the regolith, thereby defining the hydrological and carbon limitation on weathering rate. Here, the term *eco-hydrological limitation* is used when both carbon and water are considered simultaneously. Assuming that uplift is equal to erosion in steady state (a common assumption in geomorphology, e.g. Whipple 2001; Willett and Brandon 2002), topographic data and an empirical formulation of erosion can be used to calculate the transport of minerals through the regolith. The *mineral supply limitation* can thereby be defined. For this method to be considered successful, it should result in weathering rates consistent with river basin discharge of dissolved load. This means that the timing and evolution of regoliths should also be considered, as not all regoliths are in or close to a steady state.

Finally, it should also be investigated how the limitations that shape patterns of weathering rates would affect the response of chemical weathering to changes in atmospheric CO_2 and climate. That is, how do transport limitations affect the silicate weathering feedback? This can be motivated by the following thought experiment illustrated in figure 1.4. Let us assume that chemical weathering is either limited by the transport of water and carbon through the regolith or by mineral supply. The limit that would result in the slowest chemical weathering rate defines the chemical weathering rate

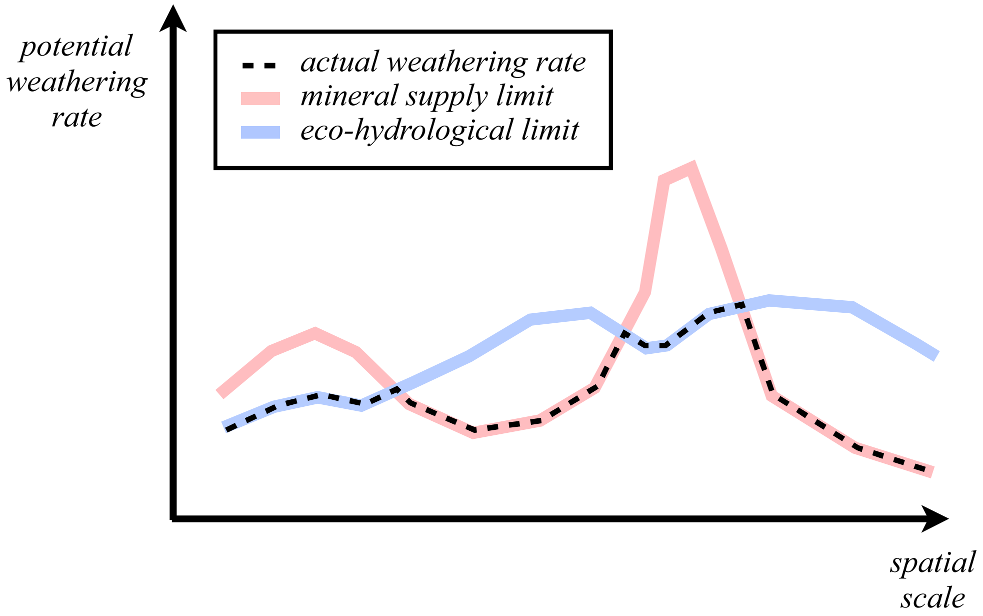

Figure 1.4: Schematic illustration of how the actual steady state weathering rate results from one of the two limitations: (1) the *eco-hydrological limitation* associated with climate (and vegetation), which provides the fluxes of water and CO_2 into the weathering "reactor" (figure 1.3); (2) the *mineral supply limitation* associated with uplift, which provides the flux of $CaSiO_3$ into the weathering "reactor" (figure 1.3). The chemical weathering rate (dashed line) is defined by the lower of the two limits for each point on the surface. Thus chemical weathering is either limited by eco-hydrology (blue) or mineral supply (red).

in steady state. If one of these limitations is changed, for example if the eco-hydrological limit is changed by a change in climate, this may change the chemical weathering rate, but only where the new eco-hydrological limit becomes the lowest or defining limit. If both limits are changed simultaneously, still only one limit will define the steady state chemical weathering rate. Thus only one change in limitation will have an impact on the chemical weathering rate at a given point.

This means that one should be careful when considering simultaneous changes in different drivers of chemical weathering, as is done in global box models of the geological carbon cycle (e.g. Berner 1991, 1994; Berner and Kothavala 2001). In our thought experiment we assume that the two limitations are independent of each other, which is certainly not always the case (e.g. physical erosion and thus mineral supply limit depends on runoff as well as topographic relief). However, if we multiply the change in drivers as is done in global box models, we risk overestimating the impact of a change in each individual driver.

To sum up: In this thesis we will take a closer look at the potential for modeling global silicate weathering rates by considering only the limitations associated with the physical transport of water, carbon and minerals. It will be illustrated how these limitations define potential changes in weathering, using biotic enhancement of weathering as an example. Finally, the implications this view has for the silicate weathering feedback will be analyzed. In the following the open research questions that are addressed in this thesis are presented.

1.2.2 Research questions

The physical transport of dissolved and solid matter is an important control on chemical weathering rates on the surface of the Earth. This control can be understood in terms of the limitations these transport processes set for chemical weathering rates. In order to elucidate how important the limitations set by physical transports are for the chemical weathering process, we will try to answer the following questions:

1. How does transport limitation of dissolved compounds shape the response of global chemical weathering rates to atmospheric CO_2?
2. Can global spatial variability of chemical weathering be modeled by considering only transport limitation of liquid and solid phases?

The land surface can not be considered to be governed purely by physical transports, as one of the most prominent features is vegetation. Vegetation affects the land surface in a multitude of ways, including modifying the water and carbon cycles and the erosion and deposition of sediment, which means that vegetation affects the physical transports in and out of the weathering “reactor” (figure 1.3). Vegetation thereby has a direct impact on the chemical reactions in the weathering “reactor” through the addition of reactive species such as H^+ and organic acids to the soil solution, impacts on soil CO_2 through respiration, removal of dissolved species though root water uptake, effects on precipitation on regional scales, and stabilization of soils and regolith by roots (Taylor et al., 2009). Many of these processes potentially lead to the enhancement of weathering, however, they cannot take place if there are no weatherable minerals in the soil/regolith. Therefore the potential for biotic enhancement of weathering could be limited by mineral supply, i.e. the potential for physical transport set by topography. This leads us to ask the following question:

3. What effect does mineral supply limitation have on the potential for biotic enhancement of weathering at the global scale?

Physical transports also play an important role in the context of the climate system, particularly in shaping the spatial variability of weathering rates. As discussed in section 1.2.1 physical erosion affects chemical weathering rates by exposing the bedrock and thus weatherable minerals to the surface environment. If physical erosion is limited by low topographic relief, chemical weathering rates may become limited by the supply of weatherable minerals. The prime example of this type of behavior is the low weathering rate of the highly weathered soils of the Amazon basin.

It is important to consider what role mineral supply limitation plays in shaping the response of weathering rates to changes in climate, as areas that are limited by the supply of weatherable minerals should not respond to small changes in runoff or temperature (West et al., 2005). Thus only areas in which silicate weathering is sensitive to climatic variations will contribute to the silicate weathering feedback. This poses the question:

4. How does mineral supply limitation affect the global sensitivity of silicate weathering rates to atmospheric CO_2 and climate?

This sensitivity defines the strength of the silicate weathering feedback. Furthermore, if we consider that mineral supply limitation should have an impact on the potential for biotic enhancement of weathering (cf. question 3), we may ask the question:

5. How does mineral supply limitation affect the global sensitivity of biotic enhancement of weathering to atmospheric CO_2?

Evidently, there is a bit of a leap between the complexity of a spatially explicit method, as the one applied in this thesis, and the parameterizations of the silicate weathering feedback applied in global scale box models of the carbon cycle. It is therefore relevant to consider if and how simple parameterizations needed for direct application in a box model can be deduced, if the information from the complex model is to be applied on geological time scales. It is worth noting that, if this approach is a success, the origin and thus meaning of the silicate weathering parameterization will be considerably different to previous parameterizations (Walker et al., 1981; Berner, 1991).

In global scale box models of the geological carbon cycle such as Berner (1991) the information gained from different studies is usually compiled into a set of parameterizations for each of the processes that may control silicate weathering rates. Since these empirical laws have been obtained under a vast range of conditions, there is often the need to extrapolate to conditions relevant to the Earth's surface environments. After the proper extrapolation has been applied, these state-of-the-art global geochemical models, multiply the empirical laws in order to get a parameterization that covers all controlling factors. By doing so, it is inherently assumed that the processes involved do not interact and different scales are considered simultaneously. Thus any point on the land surface will respond to any change in any of the driving factors. One could argue, that since the act of discretizing the land surface into a set of points leads to the loss of sub-scale heterogeneity, this heterogeneity should instead be represented by the simultaneous consideration of all driving factors, because some part of the land surface will be controlled by one driving factor or another. However, an equally weighed contribution from all drivers, as is assumed by multiplying their potential impacts, is a very strong assumption. This calls for a careful analysis of the coupling of processes and of the impact of integrating processes that have previously been left out in global models of the geological carbon cycle, such as the shielding of bedrock from chemical weathering by the accumulation of regolith (Godderis et al., 2008).

In this study the potential physical limitations associated with each of the driving factors climate and tectonics are considered through their impacts on physical transports. It should therefore be possible to determine which transport process is potentially the limiting one by a direct comparison. In doing so, it is not assumed that all limitations are equally important at all locations. However, as the limitations are considered both individually and combined their individual impacts can be assessed within the framework. Thus it may be possible to answer the following question:

6. Can a spatially explicit model of silicate weathering be simplified into a factorial law applicable in a box model of the geological carbon cycle?

1.3 Thesis overview

This thesis consists of four chapters written in the form of journal articles. Each chapter therefore contains its own introduction, methodology, results, discussion and conclusions, and can be read individually.

In Chapter 2 the sensitivity of global chemical weathering rates to atmospheric CO_2 given by the transport capacity of rivers is analyzed with a global climate model and a simple formulation of saturated Ca concentration. An abridged version of this chapter has been published in *Mineralogical Magazine*[2].

In Chapter 3 the integrated effects of solid and liquid transport limitation on chemical weathering rates are investigated with a new mechanistic global regolith model[34].

Chapter 4 contains an analysis of the role of mineral supply limitation in shaping the potential for biotic enhancement of weathering. This chapter has been published in *Applied Geochemistry*[5].

In Chapter 5 the impact of mineral supply limitation on the silicate weathering feedback is investigated with a model that considers chemical weathering as a co-limited process of tectonic and climatic drivers[6].

Chapter 6 concludes the thesis with a summary of the findings by addressing the above research questions and an outlook on directions for future research.

---

[2] S. Arens and A. Kleidon: Global sensitivity of weathering rates to atmospheric CO_2 under the assumption of saturated river discharge, *Mineralogical Magazine*, **72**(1), 301-304, 2008

[3] The eco-hydrological modeling framework applied for the weathering analyses of chapters 3-5 was developed in collaboration with colleagues of the Biospheric Modelling and Theory group at the Max Planck Institute for Biogeochemistry and documented in Porada et al. (2010). My primary contribution was the development of parameterizations for the soil CO_2 balance.

[4] Arens, S. and Kleidon A.: Integrating eco-hydrological effects and supply-limitation on chemical weathering in a global dynamic regolith model (*in prep.*)

[5] S. Arens and A. Kleidon: Eco-hydrological versus supply-limited weathering regimes and the potential for biotic enhancement of weathering at the global scale, *Applied Geochemistry*, **26**, Supplement, June 2011, S274-S278, 2011

[6] Arens, S. and Kleidon A.: The impact of mineral supply limitation on the silicate weathering feedback (*in prep.*)

2 Global sensitivity of weathering rates to atmospheric CO_2 under the assumption of saturated river discharge

The sensitivity of the global river-borne flux of Ca^{2+} to atmospheric pCO_2 was obtained from model simulations under the assumption of saturation of $CaCO_3$. The response was subdivided into contributions from changes in runoff, temperature and partial CO_2 pressure. These responses were then used to parameterize the different direct and indirect effects of a changing climate on carbonate weathering and equilibria. The sensitivity of saturated weathering fluxes to atmospheric CO_2 is weaker than what has previously been formulated by application of kinetic rate laws for silicate weathering (Walker et al., 1981). This suggests that the strength of the silicate weathering feedback could be overestimated if saturated states are not considered.

2.1 Introduction

On time scales of $10^5 - 10^6$ years the CO_2 level of the atmosphere is controlled by a negative geological feedback (Walker et al., 1981). Simply put, weathering of silicate rocks supplies Ca^{2+} and Mg^{2+} to the oceans, where CO_2 is removed from the combined ocean-atmosphere reservoir through the formation of (mostly) biogenic carbonate rocks such as calcite ($CaCO_3$) and dolomite ($CaMg(CO_3)_2$). The feedback loop is closed by the assumption that higher levels of atmospheric CO_2 yield an increase in silicate weathering rates due to higher surface temperatures and an accelerated hydrological cycle associated with the greenhouse effect. The relative effects of runoff, temperature and the biosphere have previously been parameterized based on relative functions that relate to present day values (Walker et al., 1981; Schwartzman and Volk, 1989; Berner, 1991). These studies all used a semi-empirical approach, applying a combination of laboratory and field studies and modelling.

Here, we base our parameterizations on the assumption of saturated states and apply it in a spatially resolved Earth system model. This is a markedly different approach, because we focus on the end state of the water and not on the details of the actual weathering processes.

2.2 Carbonate weathering

The role of carbonate weathering in the geological feedback loop is complex. Carbonate weathering circulates Ca^{2+}, Mg^{2+}, HCO_3^- and CO_3^{2-} back to the ocean and brings meteoric water closer to equilibrium with carbonates, which leads to reduced weathering rates of silicate rocks. Once the water reaches saturation with respect to carbonates, the most important way to increase the concentration of Ca^{2+} and Mg^{2+} in the water is by evaporation. This extensive evaporation can be reflected in river water concentrations of Ca^{2+} and HCO_3^-, as is the case for the Rio Grande river (Holland 1978). However, this effect is ignored here, since it does not affect the actual flux of elements and precipitation of $CaCO_3$ on the continents is negligible in the context of global scale studies.

The equilibrium state of water in contact with atmospheric CO_2 and $CaCO_3$ (calcite) can be calculated for a given temperature according to the reaction scheme:

$$\begin{aligned} &CaCO_3(s) + CO_2(g) + H_2O \\ &\quad \Leftrightarrow Ca^{2+} + 2HCO_3^- \end{aligned} \tag{2.1}$$

It is thereby assumed that the water has enough time to reach equilibrium and that $CaCO_3$ is available for weathering in sufficient amounts. In reality the ambient CO_2 level changes as the water moves through the soil until it reaches the river. In Figure 2.1, the change in CO_2 concentration in a packet of water responding to ambient CO_2 level along the path is outlined.

The water entering the soil has a concentration corresponding to that of the atmosphere. As it percolates into the soil, the CO_2 increases due to heterotrophic and autotrophic respiration. Once the water enters the river it again comes into contact with atmospheric levels and releases CO_2 accordingly. The concentration of CO_2 in water reaching the ocean depends on the length of the river path, i.e. if the CO_2 in the water has enough time to again reach equilibrium with respect to the CO_2 of the atmosphere. Decomposition of organic matter within the river is an additional source of CO_2 in the river water and may thus keep it away from equilibrium with the atmosphere.

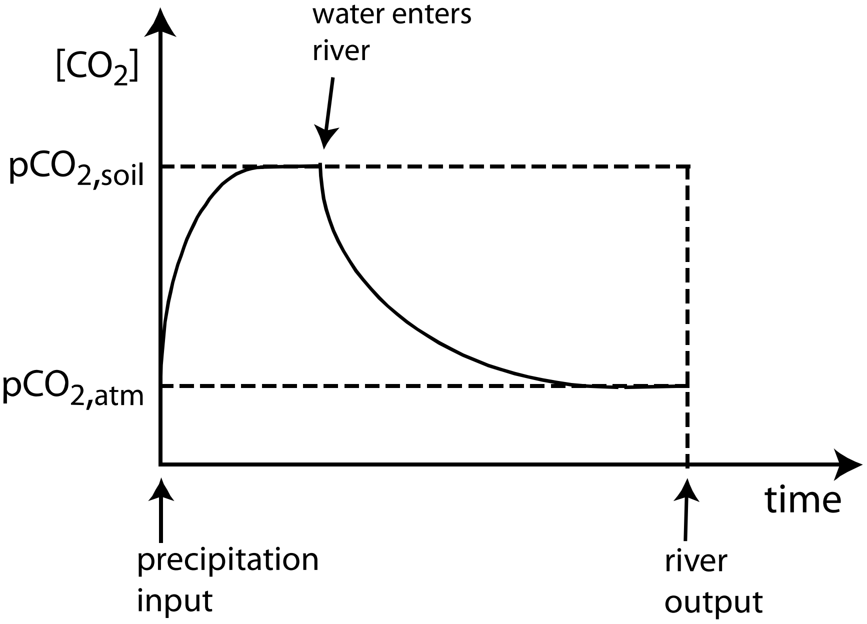

Figure 2.1: Schematic change in concentration of CO_2 in a packet of water as it moves through the soil and the river, when the residence time of water is long enough for it to first reach saturation with respect to soil CO_2 and second with atmospheric CO_2. The concentration of water entering the ocean depends on the actual path including the length of the river. The time axis is not necessarily to scale.

The concentration of Ca^{2+} in a packet of water as a function of time is shown in Figure 2.2. The path to saturation depends on the ambient conditions along the path, including composition of the soil and biotic effects.

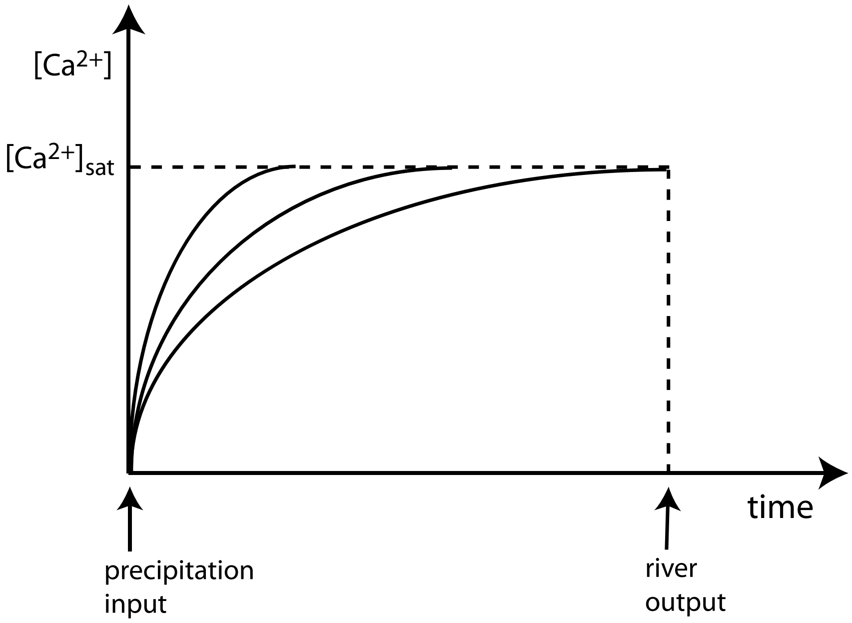

Figure 2.2: Concentration of [Ca^{2+}] in a packet of water as a function of time. The path to saturation depends on the ambient conditions along the path and so the water may reach saturation of [Ca^{2+}] at a faster or slower rate. Once the water reaches saturation the concentration of [Ca^{2+}] is basically unchanged (unless evaporation occurs).

The water may overshoot the saturation level of Ca^{2+} corresponding to atmospheric CO_2 levels where soil levels are higher. The water can remain in an supersaturated state because $CaCO_3$ does not reform spontaneously until very high levels of supersaturation. An example is the observed formation of travertine at hot springs (e.g. Fouke et al., 2000), where the emerging solution degasses CO_2, whereby $CaCO_3$ spontaneously forms (removing CO_2 pushes reaction 2.1 towards the left). Conversely, the water might not saturate if the path is too short, i.e. if the water reaches the river before it saturates. Many rivers are close to saturation of $CaCO_3$ with respect to atmospheric CO_2 levels and the world average is only slightly below (Holland 1978). We therefore use the concentration of Ca^{2+} at saturation of $CaCO_3$ as an indicator of the capacity of rivers to transport Ca^{2+} at different atmospheric CO_2 levels.

In the following, we test this approach using climate model simulations and discuss the obtained sensitivities of Ca^{2+} flux in relation to the weathering sensitivities of (Walker et al., 1981) and (Schwartzman and Volk, 1989).

2.3 Method for simulation of saturated Ca fluxes

The Planet Simulator (Lunkeit et al., 2004; Fraedrich et al., 2005a,b) is an Earth system model of intermediate complexity with a low-resolution (approximately 5.6^o lon. by 5.6^o lat.) general circulation model and prognostic schemes for radiative transfer, the atmospheric hydrological cycle and clouds. The version used here applies 10 atmospheric layers. The atmospheric component is coupled with a mixed-layer ocean model with prescribed heat transport, a simple land surface model, a dynamic vegetation model and a dynamic sea ice model.

We ran the Planet Simulator for atmospheric CO_2 levels of 100, 200, 280, 360, 540, 720, 1000, 1500, 2000, 5000 and 10000 ppm (parts per million) with a 50 m deep mixed layer ocean and fixed present day ice sheets. This would keep the poles artificially cold in high CO_2 simulations, which should be kept in mind by interpretation of the results. The simulations were run for 20 years and we took the 360 ppm run as our control or reference run. Based on the annual means of the last 5 years of the simulations the equilibrium concentration of Ca^{2+} was calculated for each grid cell using the 2m temperature and the corresponding temperature dependent equilibrium constant K(T):

$$\frac{[Ca^{2+}][HCO_3^-]^2}{pCO_2} = K(T) \tag{2.2}$$

This can be simplified because $2[Ca^{2+}] \approx [HCO_3^-]$ for pH values < 10

$$\frac{[Ca^{2+}]^3}{pCO_2} \approx \frac{K(T)}{4} \tag{2.3}$$

K(T) was calculated from energy of formation associated with reaction (2.1):

$$logK(T) = \frac{-\Delta_r H^o_{298}}{2.30259RT} + \frac{\Delta_r S^o_{298}}{2.30259R} \tag{2.4}$$

where $\Delta_r H^o_{298} = -40.10$ kJ/mol is the enthalpy change of the reaction, $\Delta_r S^o_{298} = -245.81$ J/mol/K is the entropy change of the reaction and R is the gas constant (R = 8.314 J mol^{-1} K^{-1}). The flux was then calculated from runoff rates for each grid cell.

For the sensitivity analysis with respect to temperature, atmospheric CO_2 and runoff rates, we included each factor individually by keeping the others constant at their respective values for the control (360 ppm) run. In order to analyse the results in view of previous studies (Walker et al., 1981; Schwartzman and Volk, 1989) exponential and power fits were made for relative variations of Ca^{2+} flux with respect to the control against relative variations of pCO_2 or global mean temperature ($T(pCO_2)$) in order to get a parameterization of the form:

$$\frac{F}{F_{360}} = \left(\frac{P}{P_{360}}\right)^{\alpha} e^{\beta * \Delta T} \tag{2.5}$$

where F is the Ca^{2+} flux, P is pCO_2 and α and β are fitting parameters. F_{360} and P_{360} are the Ca^{2+} flux and pCO_2 for the control run.

2.4 Sensitivity of saturated Ca fluxes to atmospheric CO_2

The global mean temperature for the different atmospheric CO_2 levels is displayed in figure 2.3 (top). The relationship between temperature and atmospheric CO_2 can be fitted with a simple equation, relating temperature change ΔT to P/P_{360}:

$$\Delta T = 3.833 * ln \frac{P}{P_{360}} \tag{2.6}$$

The temperature sensitivity is close to the range of previous studies for General Circulation Models (Oglesby and B., 1990; Kothavala et al., 1999). Figure 2.3 (top) also shows the sensitivity of global annual continental precipitation, evaporation and runoff to atmospheric CO_2. The runoff does not strictly follow a simple exponential form as assumed in (Walker et al., 1981). This is probably due to the setup of the model, with present day vegetation,

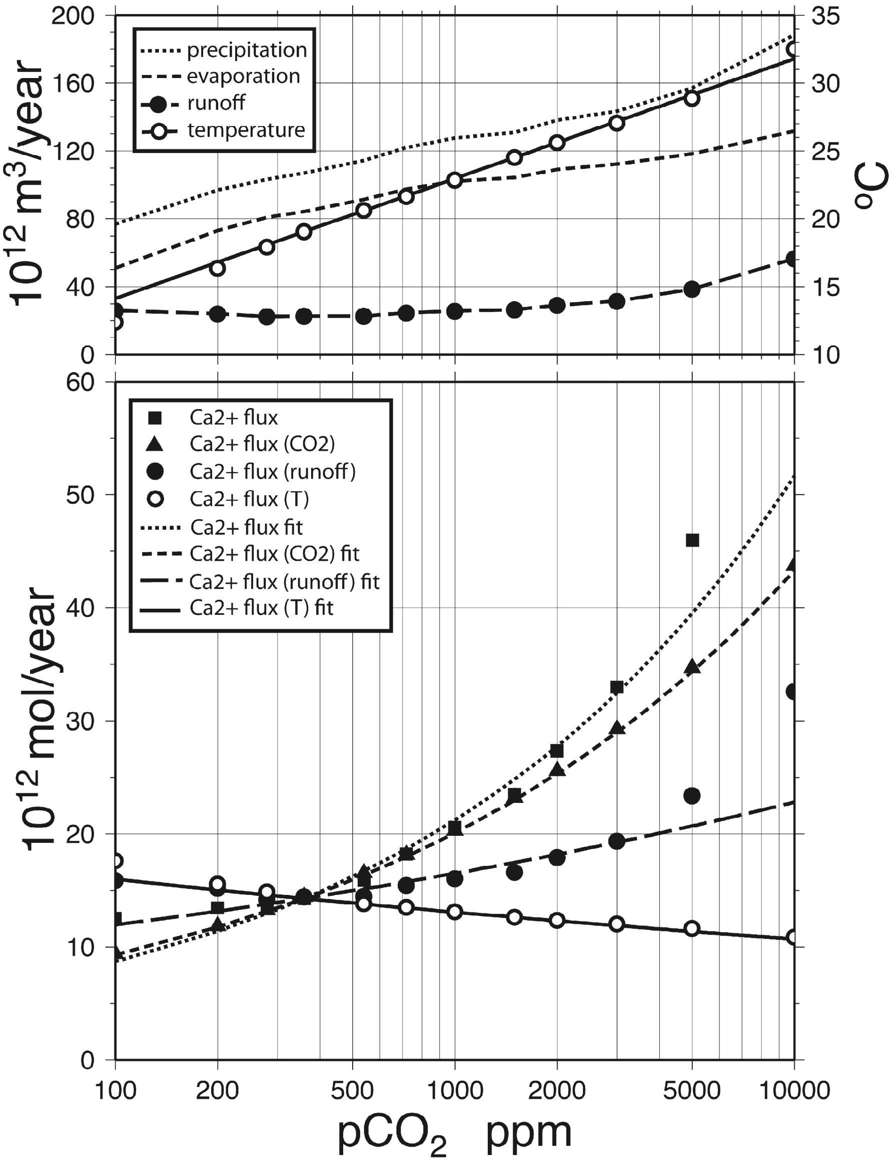

Figure 2.3: Model outputs for different CO_2 levels. Top: Temperature scale on the right, water flux scale on the left. Open circles: global mean temperature, full line: temperature fit according to equation (3.6), dots: total continental precipitation, dashed line: total continental evaporation and closed circles: total continental runoff per year. Bottom: Model outputs of total global riverine fluxes of Ca^{2+} (squares). Ca^{2+} fluxes corresponding to the separate effects of atmospheric pCO_2 (triangles), global mean temperature (open circles) and continental runoff (closed circles) are also plotted. The line fits for the separate effects and the total flux correspond to the parameterizations of equation (3.7).

that does not include effects such as stomatal response to atmospheric CO_2 levels.

The global relationship between atmospheric CO_2 levels and Ca^{2+} fluxes for our model runs is depicted in 2.3 (bottom). The contributions to variation in fluxes have been separated into those of atmospheric CO_2 level, runoff and temperature. Flux variations due to CO_2 level and runoff exhibit positive trends with increasing pCO_2, while temperature have the opposite effect due to the inverse relation of dissolution of CO_2 in water with temperature.

The exponential and power fits of the three contributions to Ca^{2+} flux variation yield the following equation:

$$\begin{aligned}\frac{F}{F_{360}} &= \left(\frac{P}{P_{360}}\right)^{0.33} e^{-0.023*\Delta T} e^{0.037*\Delta T} \\ &= \left(\frac{P}{P_{360}}\right)^{0.33} e^{0.014*\Delta T} \qquad (2.7)\end{aligned}$$

The first term on the right is a multiplier for the direct dependence of Ca^2+ concentration on ambient/atmospheric CO_2 level. The second term represents the temperature dependence of Ca^2+ concentration and the third term is due to the dependence of runoff on atmospheric CO_2. These functions have been transformed to a pure pCO_2 dependence by applying Equation 2.6 and are also plotted in figure 2.3 (bottom). Equation 2.7 can be compared to the parameterization of (Walker et al., 1981):

$$\frac{W}{W_0} = \left(\frac{P}{P_0}\right)^{0.3} e^{0.056*\Delta T} e^{0.017*\Delta T} \qquad (2.8)$$

where W is silicate weathering rate. However, the origins of the terms are very different to those of (Walker *et al.* 1981). In the parameterizations of (Walker et al., 1981) the first exponent has been estimated to 0.3 (0.4 in (Schwartzman and Volk, 1989)), but is based on the dependence of dissolution of silicates on pCO_2. The second term is the dependence of the dissolution of silicates on temperature and the third represents the relation between global runoff and global mean temperature. For the first and second terms high-pCO_2 and high-temperature laboratory data were extrapolated to the real world pCO_2 and temperature range. The third term was based on runoff sensitivity to global temperature in climate models (as is the case in our approach). It is perhaps rather surprising that the terms relating weathering rate to atmospheric CO_2 in both parameterisations are so similar despite their different origins.

The relationship in equation 2.7 yields a dependence of potential Ca^{2+} flux on atmospheric CO_2 level and temperature, but should be viewed with the inherent limitations of our approach kept in mind. The basic assumption that dissolved CO_2 in runoff is in equilibrium with atmospheric CO_2 implies that the water does not come into contact with higher levels of CO_2 long enough for the water to reach supersaturation with respect to atmospheric CO_2. One could argue that this could be the case on an Earth without a biosphere and that the difference to what is observed yields the biospheric enhancement of weathering. That would be the case if the amount of weatherable material was not depending on weathering history, which is clearly not the case. Rather the availability of weatherable material depends on lithology and soil history. An example is the present day tropical rainforests, where soils are old and weathering rates are low despite high temperatures, high runoff rates and high biospheric productivity. Conversely, high latitude rivers often exhibit concentrations of $[Ca^{2+}]$ much higher than for the equilibrium state at atmospheric CO_2 levels. This demonstrates that the state of soils and aquifers feeding the rivers play a key role, because the rate of weathering is influenced by ambient conditions and rock composition in the weathering zone.

The main difference between the assumptions behind our parameterisation and those of (Walker et al., 1981) is that we assume transport limited weathering, whereas they assume a strong influence of kinetic rate limitation on weathering. Since a saturated state should dictates the upper limit of Ca2+ flux, the weaker sensitivity of weathering rate at saturation to atmospheric CO_2 suggests that we risk overestimating the silicate weathering feedback if we consider weathering rates purely governed by kinetic rate laws. That in mind, $CaCO_3$ dissolves much more readily than silicates and can change the composition of a river within a few kilometres. If river composition is measured at the river outlet, it is more likely that the river passed through carbonate terrain and saturation could be expected. However, it is only the part of the Ca^{2+} flux that originates in silicates that will have an influence on the long-term (10^6 years) carbon cycle. This silicate weathering flux can be obscured by carbonate dissolution. The actual part of the Ca^{2+} flux originating in silicate rocks has been estimated to around 15% for the whole world (Schlesinger, 1997). This percentage has likely not been a constant through time.

On a final note, it should be said that our model setup with the fixed ice sheets acts to enhance atmospheric circulation at high atmospheric CO_2 levels and we would therefore tend to overestimate precipitation and evapotranspiration, whereby runoff is also affected increasingly with increasing CO_2 levels. This could lead to an overestimation of the exponent of the third term of equation (7), which describes the sensitivity through runoff changes.

2.5 Conclusion

It has been shown that it is possible to get a simple carbonate weathering pCO_2 relationship from an Earth system model of intermediate complexity. In this approach we have ignored the actual path of meteoric water through soils and water reservoirs of different ages and lithologies. By assuming that saturation is reached in any case, the temperature dependence of dissolution rates can be ignored and only the final temperature dependence of the saturated state becomes important. In order to get similar relationships for silicate weathering, (such as those applied in (Walker et al., 1981; Schwartzman and Volk, 1989; Berner, 1991), we would need to include more detail about the residence time of water in and composition of the sub-surface. The coupling between the hydrological cycle, soil formation and the biosphere is especially important in this context.

The sensitivity of saturated weathering fluxes to atmospheric CO_2 would suggest a weaker feedback than what has previously been formulated by application of kinetic rate laws. This indicates a need to consider the partitioning of natural waters between kinetically limited and transport limited weathering regimes in order to assess the strength of the silicate weathering feedback.

3 Integrating eco-hydrological effects and supply-limitation on chemical weathering in a global dynamic regolith model

Chemical weathering of silicate minerals is potentially crucial to the stabilization of atmospheric CO_2 and climate on geological time scales. Here, we present a new process based approach that considers climatic, biotic and tectonic limitations on chemical weathering by formulating the physical transports of water, CO_2, and minerals in and out of the regolith. A sensitivity study illustrates the impact of different limits on chemical weathering rates. The model is applied to the global scale and is able to simulate present day river concentrations of dissolved Ca and bicarbonate consistent with observations. The model thus captures variability in weathering rates and CO_2 consumption across climatic and tectonic gradients. This suggests that chemical weathering rates on long time scales are controlled by limitations set by climate and tectonic activity rather than by specific reaction kinetics.

3.1 Introduction

It has been suggested that chemical weathering of silicate rocks results in the stabilization of atmospheric CO_2 on geological time scales (Walker et al., 1981; Berner, 1991). The basis for this hypothesis is the notion that the warmer, wetter climates associated with higher atmospheric CO_2 levels should lead to higher chemical weathering rates, and thus higher consumption of CO_2. Biotic effects play a key role in shaping this response (Schwartzman and Volk, 1989; Taylor et al., 2009). However, chemical weathering rates are not only controlled by climate and vegetation. A continued supply of silicate minerals is needed to sustain chemical weathering rates on long time scales. Uplift of the continental crust drives physical erosion, which keeps the regolith shallow and rich in weatherable silicate minerals. Thus the rate of uplift plays an important role in moderating atmospheric CO_2 as well (Raymo et al., 1988; Gaillardet et al., 2011).

It is therefore crucial to consider both physical transports and chemical reactions, which include biotic effects when modeling chemical weathering rates and associated consumption of atmospheric CO_2. This has traditionally been done with a factorial approach (Berner, 1991; Donnadieu et al., 2006; Taylor et al., 2012), in which the driving factors have been parameterized separately and then multiplied to provide an overall weathering function of the surface. The actual chemical weathering rate results from the interplay between the supply of primary weatherable minerals and the rate of transformation from primary to secondary minerals.

The supply cannot be considered constant on geological time scales, but depends on large scale isostatic processes associated with tectonic uplift and exhumation. If we assume that the landscape is in a steady state, erosion rates should balance uplift rates, whereby we can infer uplift rates to a first order from an empirical formulation of erosion rates.

The rate of transformation from primary to secondary minerals may be controlled by reaction kinetics if the flow of water through the regolith is fast. However, if the flow of water is slow compared to reaction kinetics, a state of saturation may be reached, and the rate of transformation is controlled by the exchange of saturated water with unsaturated fresh water. Therefore, in far from equilibrium conditions where reaction kinetics control weathering rates, it is inherently a consequence, that the rate of water exchange does not control weathering rates.

On a regional scale it is difficult to distinguish between the contributions from unsaturated, kinetically controlled water and from saturated water, when the sources are integrated over large river systems. Many large rivers seem to be controlled by a $CaCO_3$ saturation state, as indicated by observed concentrations of calcium Ca^{2+} and bicarbonate HCO_3^- (Holland, 1978). Control by reaction kinetics would be indicated by a clear temperature dependence, but this is not supported by large scale data sets (Bluth and Kump, 1994; Kump et al., 2000; Hartmann et al., 2010; Moosdorf et al., 2011a). Although, it is problematic to make temporal conclusions from spatial analysis (cf. Moosdorf et al. (2011b)), this suggests that the relative contribution from kinetically controlled water is small on larger scales, and that the silicate weathering feedback is not necessarily a direct consequence of the temperature dependence of reaction kinetics.

Here, we present an integrated process-oriented approach to modeling of CO_2 consumption by chemical weathering of silicate minerals in regoliths. This method equally weighs chemical and physical processes. We use a global vegetation and soil hydrology model (Porada et al., 2010), which simulates the eco-hydrological fluxes of water and carbon. In this model we have implemented a chemical weathering scheme, which considers saturated states and the potential supply limitation of silicate minerals. This enables us to make a comparison of climatic/biotic and tectonic effects. We first describe the weathering reactions in Section 3.2, then the model setup in section 3.3. In our results section we first focus on the characteristic dynamics of the model illustrated by a set of single point sensitivity experiments in section 3.4.1. We do this in order to identify and explore the relative importance of the drivers, which shape the overall response of the model. We then move on to a global scale simulation in section 3.4.2 and the results on river waters in section 3.4.3. A discussion of the limitations of our approach and implications of our results are found in section 3.5. The paper concludes in section 3.6.

3.2 Model description

Regolith weathering is illustrated in figure 3.1. Ca^{2+} ions are released through the interaction of water and dissolved CO_2 with primary minerals originating in the bedrock. Ca^{2+} (and Mg^{2+}) will later combine with CO_3^{2-} in oceans to form carbonate that is buried at the sea floor, whereby CO_2 is sequestered from the atmosphere. The land regolith is formed through physical and chemical weathering processes. When the regolith solution is saturated with respect to secondary minerals these form as a residue in the regolith. With time these clay residues isolate fresh water from primary minerals and the weathering zone from temperature variations at the surface, leading to a de-

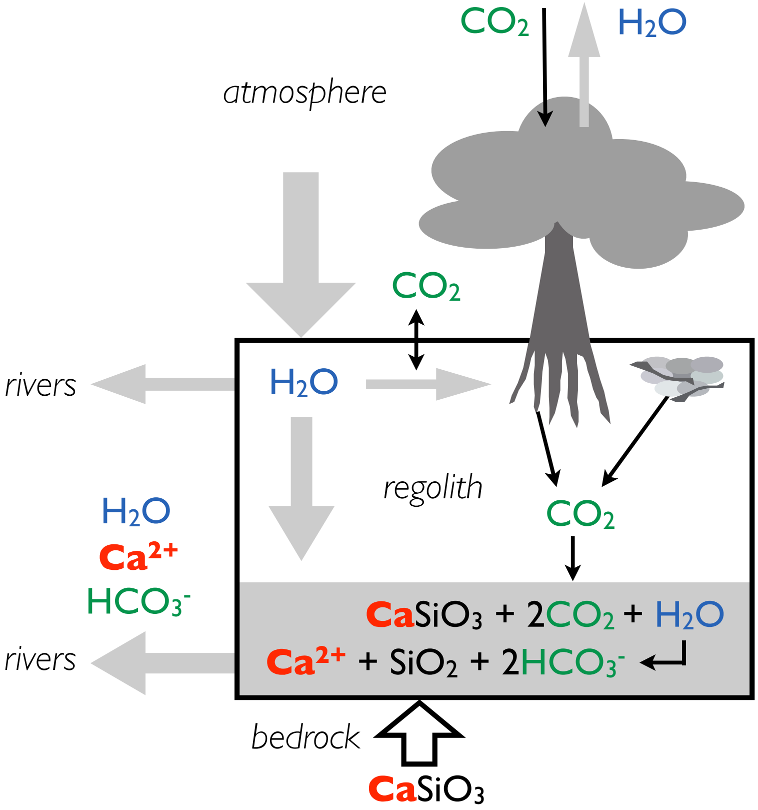

Figure 3.1: Regolith weathering illustrated with a simplified chemical weathering reaction. Respired CO_2 is dissolved in regolith water and reacts with calcium silicate minerals. This leads to a flux of dissolved Ca^{2+} and HCO_3^- with regolith water discharge, and the accumulation of regolith (here SiO_2). Grey arrows: water fluxes incl. drainage and discharge.

crease in weathering rates unless the clays are removed by physical erosion.

Here, we view chemical weathering as the export of dissolved load from soils/regoliths to rivers and eventually the ocean. Therefore chemical weathering needs water and particularly enough water that drains the regolith. In order to model weathering on a large scale we therefore use a land surface model (Porada et al., 2010), which also covers the effects of vegetation on the water balance of the regolith. Into this model we implement a chemical weathering scheme, which considers only the most abundant elements and a simplification of the reactions in which they partake. In the model we also consider the impact of physical erosion of secondary minerals on chemical weathering rate. The parameters, variables and balance equations used in the model are shown in tables 3.2, 3.3 and 3.4.

3.2.1 Water balance

The land surface model JeSSy-SimBA (Porada et al., 2010) calculates the surface water budget. This includes the fluxes: evapotranspiration, uptake of water by vegetation, snow accumulation and melt, surface runoff calculated as saturation excess flow, and drainage. The water balance of the regolith is calculated with a leaking bucket scheme, i.e. surface runoff is generated when precipitation in general exceeds evapotranspiration. The leak in the bucket leads to subsurface/groundwater drainage, which is used in the calculation of exports of dissolved load from the regolith. For the saturation excess flow we assume no re-immersion, which means that the surface runoff does not carry a dissolved load in the model. Also, frost inhibits immersion of water into the regolith in the model. This effect is important in mountainous and polar regions, where frost has a large impact on the water balance of the regolith.

3.2.2 Mass balance equations

An overview of the mass balance equations is presented in table 3.4. These equations represent the connections between the pools and fluxes listed in table 3.2. The most important parameters are listed in table 3.3. Subscripts used in notation are listed in table 3.1.

In the following we introduce the parameterisations used for chemical weathering, regolith production, and erosion.

3.2.3 Chemical weathering

There are two forms of weathering considered in the model: carbonate weathering and silicate weathering. The two are not exclusive in nature, but they have been separated in the description below.

Carbonate solubility and thus weathering as a function of ambient CO_2

subscript	definition
a	atmosphere
b	bedrock
d	dissolved
r	river (export)
s	soil/regolith
v	vegetation
dc	dissolved concentration
aw	atomic weight
pp	partial pressure
p	primary
q	secondary

Table 3.1: Repeating subscripts and their definitions.

can be calculated from the equillibrium equation:

$$CaCO_3 + CO_2 + H_2O \Leftrightarrow Ca^{2+} + 2HCO_3^- \tag{3.1}$$

because we can ignore the speciation of CO_3^{2-} for pH values < 10. The equilibrium constant is:

$$K_{eq} = \frac{(a_{Ca^{2+}})(a_{HCO_3^-})^2}{a_{CaCO_3} pCO_2} \simeq \frac{[Ca^{2+}][HCO_3^-]^2}{a_{CaCO_3} pCO_2} \tag{3.2}$$

where a_{CaCO_3} is the activity of $CaCO_3$ and pCO_2 is the partial pressure of CO_2 in the adjacent air. For pure $CaCO_3$ $a_{CaCO_3} = 1$. Here, we substitute the activity of the ions in solution with their concentrations. This leads to an underestimate of the concentrations that increases fractionally with increasing concentrations and for which we add a simple curve fitted correction. At pH values less than 10 we use the approximation $2[Ca^{2+}] \backsimeq [HCO_3^-]$ in which case

$$[Ca^{2+}]^3 \backsimeq \frac{K_{eq}}{4} * pCO_2 \tag{3.3}$$

where $K_{eq} = 10^{-5.9}$ at $T = 25^oC$ (Shvartsev, 2001).

When modeling silicate weathering the effects of the accumulation of secondary minerals on weathering rates need to be considered, especially on

	variable	description	unit / value
pools	H_2O_s	water volume	m/m^2
	Ca_p	primary Ca	kg/m^2
	Ca_d	dissolved Ca	mol/m^2
	NaK_p	primary Na + K	kg/m^2
	NaK_d	dissolved Na + K	mol/m^2
	FeO	iron oxides	kg/m^2
	$HCO_{3,d}$	dissolved HCO_3^-	mol/m^2
	$SiO_{2,p}$	non-erodible SiO_2 bound in primary rock	kg/m^2
	$SiO_{2,s}$	erodible SiO_2	kg/m^2
	Si_p	non-erodible kaolinite bound in primary rock	kg/m^2
	Si_q	kaolinite	kg/m^2
	x	any mineral	kg/m^2
fluxes	fH_2O_{as}	precipitation	m/s
	fH_2O_{sa}	evaporation	m/s
	fH_2O_{sv}	water uptake by vegetation	m/s
	fH_2O_{sr}	surface runoff	m/s
	fH_2O_{br}	drainage	m/s
	fCa_{br}	Ca to river	mol/m^2/s
	fCa_{bs}	Ca bedrock to regolith	kg/m^2/s
	fCa_{pd}	Ca dissolution	kg/m^2/s
	$fNaK_{br}$	Na + K to river	mol/m^2/s
	$fNaK_{bs}$	Na + K bedrock to regolith	kg/m^2/s
	$fNaK_{pd}$	Na + K dissolution	kg/m^2/s
	fFe_{bs}	Fe bedrock to regolith	kg/m^2/s
	fFe_{pd}	Fe dissolution	mol/m^2/s
	$fFeO_{sr}$	erosion of Fe oxides	kg/m^2/s
	$fHCO_{3,d}$	HCO_3^- from weathering	mol/m^2/s
	$fHCO_{3,br}$	HCO_3^- to river	mol/m^2/s
	$fCO_{2,cons}$	CO_2 consumption	mol/m^2/s
	$fSiO_{2,bs}$	SiO_2 bedrock to regolith	kg/m^2/s
	$fSiO_{2,ss}$	solid SiO_2 release from rock to erodible pool	kg/m^2/s
	$fSiO_{2,pd}$	SiO_2 dissolution (stoichiometric excess)	mol/m^2/s
	$fSiO_{2,sr}$	erosion of SiO_2	kg/m^2/s
	$fSi_{p,bs}$	kaolinite bedrock to regolith	kg/m^2/s
	$fSi_{p,ss}$	kaolinite release from rock to erodible pool	kg/m^2/s
	$fSi_{q,ss}$	formation of kaolinite	kg/m^2/s
	$fSi_{q,sr}$	erosion of kaolinite	kg/m^2/s
other	zCa_{dc}	Ca^{2+} concentration	mol/l
	zNaK_{dc}	Na^+ + K^+ concentration	mol/l
	$\mathrm{zSiO}_{2,dc}$	dissolved SiO_2 concentration	mol/l
	$\mathrm{zHCO}^-_{3,dc}$	HCO_3^- concentration	mol/l
	$\mathrm{zCO}_{2,pp}$	regolith CO_2 partial pressure	ppm
	D_s	regolith depth	m
	U	regolith production rate	m/s

Table 3.2: Model variables.

parameter	description	unit / value
cCa_{aw}	standard atomic weight of Ca	40.0784 g/mol
$cSi_{q,aw}$	standard atomic weight of kaolinite	258.1608 g/mol
c_{NaK}	$[Y^{+}]/[X^{2+}]$ in bedrock	mol/mol
c_{Fe}	$[Fe^{2+}]/[Ca^{2+}]$ in bedrock	mol/mol
cm_{carb}	molal fraction of solid Ca that is $CaCO_3$	mol/mol
cm_{pyr}	molal fraction of solid Ca that is pyroxene	mol/mol
p_{Ca}	weight fraction of Ca minerals in bedrock	kg/kg
p_{NaK}	weight fraction of Na + K minerals in bedrock	kg/kg
p_{Fe}	weight fraction of Fe minerals in bedrock	kg/kg
p_{SiO_2}	weight fraction of quarts in bedrock	kg/kg
p_{Sip}	weight fraction of kaolinite in bedrock	kg/kg
$frac_{SiO_2}$	volume fraction of secondary minerals that is SiO_2	m^3/m^3
$frac_{Siq}$	volume fraction of secondary minerals that is kaolinite	m^3/m^3
$frac_{FeOx}$	volume fraction of secondary minerals that is Fe oxide	m^3/m^3
ρ_{SiO_2}	density of SiO_2	1602 kg/m^3
ρ_{Siq}	density of kaolinite	1746 kg/m^3
ρ_{FeOx}	density of Fe oxides	1746 kg/m^3

Table 3.3: Model parameters.

geological time scales. We simplify the complexity of the primary and secondary mineralogies to a feldspar/pyroxene - kaolinite/iron oxide sequence, which we utilize to describe the long term evolution of Ca^{2+} leaching from regoliths.

The feldspar anorthite contains Ca^{2+}, which is released through weathering according to the reaction:

$$\begin{aligned} CaAl_2Si_2O_8 \quad &+ \quad 2CO_2 + 3H_2O \\ &\Rightarrow \quad Ca^{2+} + 2HCO_3^- + Al_2Si_2O_5(OH)_4 \end{aligned} \tag{3.4}$$

As a result of this reaction kaolinite ($Al_2Si_2O_5(OH)_4$) forms. The reaction happens in two steps. In the first step Al^{3+} and H_4SiO_4 is released into solution, and in the second these compounds bind to form kaolinite. Under the assumption that all aluminum from dissolution of anorthite is bound in kaolinite it can be modeled as a one-step process.

Basaltic rock contains a large proportion of pyroxes which typically weather according to the reaction:

$$XSiO_3 + 2CO_2 + 3H_2O \Rightarrow X^{2+} + 2HCO_3^- + H_4SiO_4 \tag{3.5}$$

variable	mass balance	flux equations
H_2O	$\frac{d}{dt}H_2O_s = fH_2O_{as} - fH_2O_{sa} - fH_2O_{sv} - fH_2O_{sr} - fH_2O_{br}$	Porada et al. (2010)
Ca	$\frac{d}{dt}Ca_d = fCa_{pd} - fCa_{br}$	$fCa_{br} = fH_2O_{br} \cdot zCa_{dc}$
	$\frac{d}{dt}Ca_p = fCa_{bs} - fCa_{pd}$	$fCa_{bs} = p_{Ca} \cdot U \cdot \rho_{rock}$
Na + K	$\frac{d}{dt}NaK_d = fNaK_{pd} - fNaK_{br}$	$fNaK_{br} = fH_2O_{br} \cdot zNaK_{dc}$ $fNaK_{pd} = c_{NaK} * fCa_{pd}$
	$\frac{d}{dt}NaK_p = fNaK_{bs} - fNaK_{pd}$	$fNaK_{bs} = p_{NaK} \cdot U \cdot \rho_{rock}$
Fe	$\frac{d}{dt}Fep_s = fFe_{bs} - fFe_{pd}$	$fFe_{bs} = p_{Fe} \cdot fmass_{bs}$
	$\frac{d}{dt}FeO = fFe_{pd} - fFeO_{sr}$	$fFeO_{sr} = \varepsilon * frac_{FeO} * \rho_{FeO}$ $fFe_{pd} = c_{Fe} * fCa_{pd}$
HCO_3^-	$\frac{d}{dt}HCO_{3,d} = fHCO_{3,d} - fHCO_{3,br}$	$fHCO_{3,br} = fH_2O_{br} \cdot zHCO_{3,dc}$ $fHCO_{3,d} = 2 \cdot (fCa_{pd} + fFe_{pd}) + fNaK_{pd}$ $fCO_{2,cons} = fCa_{pd} + 2 \cdot fFe_{pd} + fNaK_{pd}$
$SiO_{2,p}$	$\frac{d}{dt}SiO_{2,p} = fSiO_{2,bs} - fSiO_{2,ss}$	$fSiO_{2,bs} = p_{SiO_2} \cdot U \cdot \rho_{rock}$
$SiO_{2,s}$	$\frac{d}{dt}SiO_{2,s} = fSiO_{2,ss} - fSiO_{2,sr}$	$fSiO_{2,ss} = fCa_{pd} \cdot cCa_{aw}/p_{Ca} \cdot p_{SiO_2}$ $fSiO_{2,sr} = \varepsilon \cdot frac_{SiO_2} \cdot \rho_{SiO_2}$
Si_p	$\frac{d}{dt}Si_p = fSi_{p,bs} - fSi_{q,ss} - fSi_{p,ss}$	$fSi_{p,bs} = p_{Sip} \cdot U \cdot \rho_{rock}$ $fSi_{q,ss} = (fCa_{pd} \cdot (1 - cm_{carb} - cm_{pyr}) + fNaK_{pd}) \cdot cSi_{q,aw}$
Si_q	$\frac{d}{dt}Si_q = fSi_{q,ss} + fSi_{p,ss} - fSi_{q,sr}$	$fSi_{p,ss} = fCa_{pd} \cdot cCa_{aw}/p_{Ca} \cdot p_{Sip}$ $fSi_{q,sr} = \varepsilon \cdot frac_{SiO_2} \cdot \rho_{Siq}$
D_s	$\frac{d}{dt}D_s = \sum \frac{fx_{bs} - fx_{sr}}{\rho_x} - \sum \frac{fx_{p,ss}}{\rho_{x,p}} + \sum \frac{fx_{q,ss}}{\rho_{x,q}}$	x's are minerals

Table 3.4: Mass balance equations.

where X is Ca, Mg or Fe. This does not necessarily lead to the formation of aluminum clays unless aluminum is available in the solution, but the dissolved Fe^{2+} quickly oxidizes into hematite Fe_2O_3 or limonite $FeO(OH)$, which leads to the to the reddish color of the regoliths formed on top of basaltic bedrock.

The dissolution of silicates and thus the release of Ca^{2+} and Mg^{2+} ions into rivers depends on the composition of the bedrock and the regolith. The applied initial composition of the bedrock is described in section 3.3.3 and table 3.5.

The equilibrium equation of anorthite with the solution is

$$[Ca^{2+}] * [HCO_3^-]^2 \backsimeq K'_{eq} * pCO_2^2 * \frac{a_{CaAl_2Si_2O_8}}{a_{Al_2Si_2O_5(OH)_4}} \tag{3.6}$$

where $K'_{eq} = 10^{1.1}$ at $T = 25^oC$ (Shvartsev, 2001). Note that K'_{eq} is much larger than the equilibrium constant associated with the calcite equilibrium described in equations (3.2) and (3.3). Also, because all dissolved CO_2 comes from the air, the dependence on atmospheric pCO_2 is quadratic. This means that concentrations of Ca^{2+} needs to be many orders of magnitude larger to fulfill this equilibrium than the calcite equilibrium. However, as calcites start to form when the calcite equilibrium is reached, we assume that this is the upper bound to concentration of calcium in solution (Shvartsev, 2008b). We therefore apply the carbonate weathering equilibrium as an upper limit to silicate weathering as given by the carbonate weathering equilibrium equation (3.2). Higher concentrations are possible, but this usually only occurs on a large scale due to other processes such as extensive evaporation (Taylor and Eggletom, 2001). This special case is not treated here. Instead we assume that secondary calcite formed in regoliths is negligible at the global scale.

The concentration of cations $[X^{2+}]$ and $[Y^+]$ in solution is balanced by $[HCO_3^-]$ in order to keep the solution neutrally charged:

$$[HCO_3^-] \backsimeq 2[X^{2+}] + [Y^+] \tag{3.7}$$

If we insert equation (3.7) into equation (3.2) and set the activity of the solid phase to 1, we get:

$$[Ca^{2+}] * \left(2[X^{2+}] + [Y^+]\right)^2 \backsimeq K_{eq} * pCO_2 \tag{3.8}$$

We assume that the minerals behave as a solid solution and thus dissolve at a rate proportional to their composition, i.e. that the proportion of elements in solution is the same as in the parent rock $[Y^+]/[X^{2+}] = c_{NaK}$ and $[Fe^{2+} +$

$Mg^{2+}]/[Ca^{2+}] = c_{Fe} + c_{Mg} = c_{FeMg}$. We make this assumption because we are not aiming at modeling detailed weathering profiles. We then get

$$[Ca^{2+}][X^{2+}]^2(2 + c_{NaK})^2 \backsimeq K_{eq} * pCO_2 \tag{3.9}$$

$$[Ca^{2+}][Ca^{2+}]^2(1 + c_{FeMg})^2(2 + c_{NaK})^2 \backsimeq K_{eq} * pCO_2 \tag{3.10}$$

if we assume that $[X^{2+}] = [Ca^{2+}] + [Mg^{2+}] + [Fe^{2+}]$. We then get the following solution for the concentration of Ca in solution:

$$[Ca^{2+}]^3 \backsimeq \frac{K_{eq} * pCO_2}{(2 + c_{NaK})^2(1 + c_{FeMg})^2} = \frac{K_{eq} * pCO_2}{c_{min}} \tag{3.11}$$

where $c_{min} = (2 + c_{NaK})^2(1 + c_{FeMg})^2$. Note that $(2 + c_{NaK})^2 \rightarrow 4$ for $c_{NaK} \rightarrow 0$, and $(1 + c_{FeMg})^2 \rightarrow 1$ for $c_{FeMg} \rightarrow 0$ in which case the solution of equation (3.11) approximates the carbonate equilibrium solution of equation (3.3). This is what we would expect if pure anorthite is dissolved. Thus, c_{min} is simply a correction term for the simultaneous dissolution of other minerals that produce HCO_3^-. Finally, since the minerals are in a solid solution we need to consider their activity. For ideal solid solutions the activity of a mineral can be represented by the corresponding molal fraction of the mineral (Anderson, 2005). We therefore consider the activity of Ca-minerals by including the molal fraction of Ca-minerals m_{Ca} to all reacting primary minerals of the bedrock m_p

$$[Ca^{2+}]^3 \backsimeq \frac{K_{eq} * pCO_2}{c_{min}} \left(\frac{m_{Ca}}{m_p}\right) \tag{3.12}$$

Thus the upper limit on the concentration of dissolved Ca^{2+} in the regolith becomes:

$$zCa_{lim} = [Ca^{2+}] = \left(\frac{K_{eq} * pCO_2}{c_{min}} * \frac{m_{Ca}}{m_p}\right)^{1/3} \tag{3.13}$$

We then calculate the dissolution of Ca-minerals (fCa_{pd}) needed to fulfill this concentration. It is limited by the amount of Ca available in the regolith, which depends on the physical weathering processes associated with regolith production described in section 3.2.4. Thus chemical weathering may become limited by physical weathering in which case the actual concentration of dissolved Ca, zCa_{dc} is less than the upper limit zCa_{lim} (eq. 3.13). The export of Ca^{2+} (fCa_{br}) from the regolith is then calculated by multiplying the concentration of Ca^{2+} with the drainage fH_2O_{br}:

$$fCa_{br} = zCa_{dc} \cdot fH_2O_{br} \tag{3.14}$$

The corresponding concentration of HCO_3^- is

$$\begin{aligned} zHCO^-_{3,dc} = [HCO_3^-] &\backsimeq 2[X^{2+}] + [Y^+] \\ &= 2 \cdot zCa_{dc}(1 + c_{FeMg}) + zCa_{dc} \cdot c_{NaK} \end{aligned} \tag{3.15}$$

and the export of HCO_3^- becomes

$$fHCO_{3,br} = zHCO^-_{3,dc} \cdot fH_2O_{br} \tag{3.16}$$

The production of secondary minerals kaolinite $fSi_{q,ss}$ and iron oxides $fFeO_{ss}$ follow the rate of dissolution, thus

$$\begin{aligned} fSi_{q,ss} &= fCa_{pd} * (1 - cm_{carb} - cm_{pyr}) * m_{kaol} \\ fFeO_{ss} &= fFe_{pd} * m_{FeO} \end{aligned}$$

where m_{kaol} is the molar mass of kaolinite and m_{FeO} is the molar mass of iron oxides. The dissolution of iron fFe_{pd} is calculated from the relative abundance of pyroxenes in the bedrock, i.e. $fFe_{pd} = c_{Fe} * fCa_{pd}$.

CO_2 consumption

In order to calculate the net sink of atmospheric CO_2 by weathering, we need to consider that part of the HCO_3^- formed through weathering is released again into the atmosphere during the formation of carbonates in the oceans (Ridgwell and Zeebe, 2005). There is therefore no net sink of atmospheric CO_2 for the weathering of carbonates. Only half of the CO_2 that is transferred to HCO_3^- can eventually be bound in carbonates for (Ca,Mg)-silicates and potentially all CO_2 for the (Na,K)-silicates as illustrated by the unbalanced weathering equations (Hartmann et al., 2009):

$$\begin{aligned} NaAlSi_3O_8 + CO_2 + \frac{11}{2}H_2O &\rightarrow Na^+ + HCO_3^- \\ CaAl_2Si_2O_8 + 2CO_2 + 3H_2O &\rightarrow Ca^{2+} + 2HCO_3^- \\ &\rightarrow CaCO_3 + H_2O + CO_2 \end{aligned} \tag{3.17}$$

How much CO_2 is really consumed by this process naturally depends on other chemical processes in the oceans. Nevertheless, here we assume that weathering rates on land can be directly translated into CO_2 consumption.

3.2.4 Regolith production

Physical weathering or soil production rate is often described as the “uplift” of material from the bedrock into the soil column/regolith. It should not be equalized with large scale uplift of the landscape, as the driving forces are quite different though not independent of each other, especially under steady state assumptions.

Here, we assume that soil or regolith production is basically driven by chemical weathering. That means that regolith production rate cannot exceed chemical weathering rate in the regolith on long time scales. This excludes chemical weathering in river basins and alluvial fans, which is also sustained by deposition of primary minerals from upstream. However, as the regolith accumulates, the active chemical weathering zone becomes increasingly isolated from the surface environment and this may also impose a limitation on chemical weathering (Stallard and Edmond, 1983). This is seen in the often observed exponential decrease in regolith production rate with depth (e.g. Heimsath et al. (1997)). It can be related to decreasing temperature variations, borrowing, or water infiltration with depth, but the actual processes responsible for this decrease are site specific.

We thus describe the regolith production U as a function of regolith depth, assuming that it can be described globally by an exponentially decaying function with depth D_s

$$U = U_0 \cdot exp\Big(ln(5 \times 10^{-5})\frac{D_s}{20}\Big) \tag{3.18}$$

where U_0 is the regolith production rate for $D_s = 0$. The release of Ca minerals into the regolith is thus:

$$fCa_{bs} = U \cdot \rho_{rock} \cdot p_{Ca} \tag{3.19}$$

where ρ_{rock} is the density of the bedrock and p_{Ca} is the fraction by weight of the rock that are Ca-minerals. Our formulation does not take into account the observed increase in regolith production with depth for shallow regoliths. This is not necessarily an issue as chemical weathering rates in shallow regoliths more likely are limited by processes associated with the climatic and hydrologic conditions than by mineral supply.

The regolith production rate is used to calculate regolith depth from the general scheme:

$$\frac{dD_s}{dt} = U - W - \varepsilon \tag{3.20}$$

where W is chemical weathering rate and ε is the physical transport of particulate matter away from the regolith described in the following section.

3.2.5 Physical erosion

Physical erosion is the transport or loss of particulate matter from regoliths. The empirical formulation of physical erosion ε used in the model is that of (Hilley and Porder, 2008):

$$\begin{aligned} \varepsilon &= 2.0 \times 10^{-4} R_z && \text{for} R_z \leq 494 \text{ m} \\ \varepsilon &= 1.4 \times 10^{-6} R_z^{1.8} && \text{for} R_z \geq 494 \text{m} \end{aligned} \tag{3.21}$$

yielding a maximum of 2.8 mm/yr for local relief R_z at 2000 m. A minimum physical erosion rate of 2×10^{-6} mm/yr is imposed in order to secure that the model can reach a steady state. In this formulation erosion is solely dependent on the topographic gradient R_z. Only secondary minerals are eroded and we assume no lateral transport from one land grid cell to another, i.e. we assume no deposition in neighbouring grid cells. This will lead to an underestimate of weathering in regions where lateral transport is a large source of weatherable minerals, such as in the forelands of large mountain ranges. Also, it changes the formulation of physical erosion into a potential, which is only fulfilled when chemical weathering rates can sustain the physical fluxes in steady state. Physical erosion rate thereby becomes limited by chemical weathering rate and thus also dependent on factors controlling chemical weathering such as biotic enhancement of weathering. We calculate the physical erosion of secondary minerals normalized to their relative abundance in the regolith:

$$fx_{q,sr} = \varepsilon * frac_x * \rho_{x_q} \tag{3.22}$$

where $fx_{q,sr}$ is the loss of the secondary mineral x_q from the regolith, $frac_x$ is the fraction of secondary minerals in the regolith that is mineral x_q by volume and ρ_{x_q} is the density of mineral x_q.

3.2.6 Biological influence on weathering

The biosphere potentially has a profound impact on chemical weathering rates (Drever, 1994; Gislason et al., 1996; Moulton et al., 2000; Lenton et al., 2012). Apart from the effect of vegetation on the regolith water balance, we implement an indirect effect of vegetation on weathering rates through the influence of autotrophic and heterotrophic respiration on the partial pressure of CO_2 in the regolith. This was schematically illustrated in figure 3.1. We consider biotic enhancement of weathering through the impact of biotic processes on the export of dissolved Ca and C from regoliths. The passive effect of the biotic increase of soil/regolith CO_2 has an important effect on Ca^{2+} and HCO_3^- fluxes, because of the direct influence on the saturation level of $[Ca^{2+}]$ and $[HCO_3^-]$ in the regolith solution. The uptake of nutrients by vegetation plays a role locally in the regolith, but not globally if uptake is balanced by leaching from soil organic matter. This would be the case when the vegetation is in steady state, which is the ordinary assumption for the 1Ma geological time scale considered in global mass balance models of the carbon cycle (Berner, 1991, 1994; Berner and Kothavala, 2001; Wallmann, 2001).

3.2.7 Limits of weathering rates

The physical and chemical processes included in the model may together or singularly impose a limitation on the transformation rate of primary to secondary minerals and associated exports of dissolved and solid loads from the regolith. We therefore define two overall limits of weathering rates:

1) the *eco-hydrological limit*
2) the *supply limit*

The eco-hydrological limit is the maximum possible chemical weathering rate given by the eco-hydrological conditions: regolith drainage, CO_2, temperature. This limit yields the upper limit for chemical weathering in the case, where there is no limitation by the supply of weatherable minerals. It therefore corresponds to the export of Ca calculated in equation 3.14 in the case where $zCa_{dc} = zCa_{lim}$ (cf. equation 3.13).

The supply limit is given by the potential physical transport of secondary minerals away from the regolith. This limit is set by the topographic relief (cf. equation 3.21) and yields the upper limit to the chemical weathering rate in the case, where the potential physical transport rate of secondary minerals is exactly balanced by the formation rate of secondary minerals through chemical weathering. The corresponding chemical weathering rate can be calculated by combining the erosion rate of secondary minerals calculated in equation 3.22 with the mass balances associated with the transformation from primary to secondary minerals.

As we shall later demonstrate in section 3.4.1, the steady state solution falls within the bounds of these two limits.

3.3 Model Setup

The model is set up as in figure 3.2. Climate data are used to force a land surface model consisting of a vegetation model (SimBA), simulating the productivity and water balance of the vegetation, and a soil hydrology and carbon model (JeSSy) (Porada et al., 2010). The balance of water and carbon in the soil/regolith is then used to simulate chemical weathering rates in the regolith with the weathering module. In this simple setup the consumption of CO_2 by weathering is not included in the carbon balance of the regolith, as this flux is in general considered small compared to the other carbon fluxes. However, we cannot rule out that it may be important for the regolith carbon balance in areas that are covered by carbonate. Since carbonate weathering has no net influence on the long term carbon cycle, we do not consider this effect important in this context.

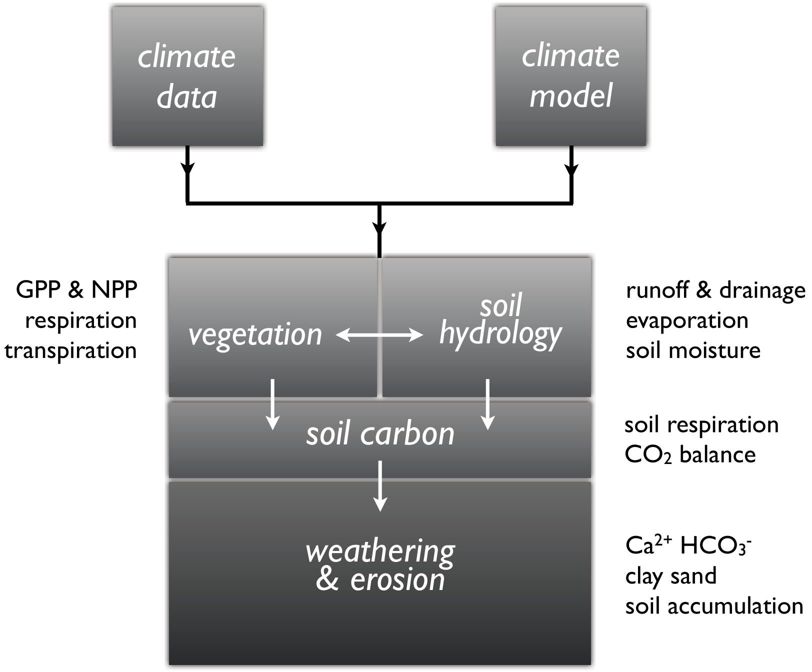

Figure 3.2: Flowchart of model setup. Climate data or output from a climate model can be used to force the model.

3.3.1 Climate

The model is forced with climate data from the NASA Land Surface and Hydrology archive (Sheffield et al., 2006) for the time period 1960-1989 rescaled to $1.125° \times 1.125°$. We use daily means of temperature, precipitation, relative humidity and longwave and shortwave radiation as input to the coupled land surface/weathering model. The glacial cover of the last glacial maximum (figure 3.3) is used to define areas where regoliths are necessarily much younger than in the rest of the world. Areas that were covered by glacial lakes is treated in the same way as areas that were covered by ice.

3.3.2 Biosphere

The representation of the biosphere is simplified to vascular plants and their productivity based on temperature and the availability of solar energy and

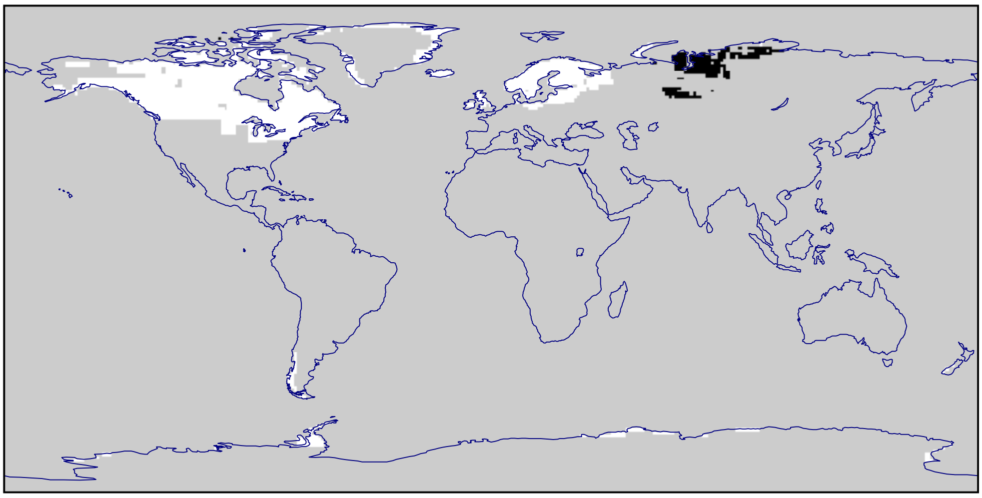

Figure 3.3: Current freely exposed land areas that were covered by glaciers (white) and glacial lakes (black) during the last glacial maximum. Data from ECHAM5 (courtesy of Uwe Mikolajewicz and Veronika Gayler).

water. The vegetation-soil hydrology model used for this purpose is the JeSSy-SimBA model (Porada et al., 2010). The model includes a scheme for calculation of soil CO_2 levels according to (Fang and Moncrieff, 1999) but for a 1-layer soil/regolith. This scheme yields reasonable subsurface CO_2 levels in the range of 1-215 times the atmospheric CO_2 which is set to 360 ppm for interglacial periods and 280 ppm for glacial periods.

3.3.3 Lithologies

We use the lithologies of (Amiotte Suchet and Probst, 1995) rescaled to $1.125° \times 1.125°$ and extrapolated to cover all possible land points in both the glacial and interglacial climate state. This map of lithologies is rather corse compared to more recent maps (Hartmann and Moosdorf, 2012), but given the limitations set by model resolution, sufficient for this study. The six lithological classes are listed in table 3.5 as well as the bulk mineral composition assumed for each class. The mineralogy has been simplified, so that the bedrock consists of a combination of non-weatherable and weatherable minerals, of which a part form secondary minerals when weathered. This

Class	Ca-feldspar	K,Na-feldspar	Pyroxenes	Quartz	Secondary	Carbonate
1 - sandstone	0.01	0.11	-	0.86	0.01	0.01
2 - carbonate	-	-	-	-	-	1.0
3a - shale a	0.0005	0.0055	-	0.104	0.8405	0.0495
3b - shale b	0.001	0.011	-	0.108	0.781	0.099
4 - granite	0.05	0.55	-	0.40	-	-
5 - acid volcanic	0.05	0.55	-	0.40	-	-
6 - basalt	0.25	0.55	0.20	-	-	-

Table 3.5: Characterization of lithologies by mineral weight fractions. After Nockolds (1954).

is achieved by representing the primary rock as a combination of quartz, feldspar, pyroxene ($CaFeSi_2O_6$) and carbonate ($CaCO_3$) and letting the secondary minerals hematite, limonite and kaolinite form through chemical weathering (e.g. Equation 3.4). Note that in this simple setup, we have not included Mg-minerals.

3.3.4 Topographic relief

We assume that local topographic relief (Farr et al., 2007) scales with topographic gradient between grid cells. The topographic relief has been scaled to yield a maximum of 1920 meters, which is within the range used in Montgomery and Brandon (2002). Using the gradient between grid cells will lead to the loss of sub-grid variability, however, we should be able to capture the overall geographical variability in chemical weathering rates associated with variations in topography.

3.4 Results

We first look at the model behavior for a single grid point in order to understand the importance of drivings factors and parameter settings. We then analyze the model output for regional and global scales.

3.4.1 Model Behavior

The inherent sensitivities of the model to the parameters in table 3.6 have been tested for a single grid point. Results for Ca export from regoliths are displayed in figures 3.4 to 3.8. This grid point is characterized by a wet tropical climate: drainage 48 cm/yr, average temperature 24.3°C, average regolith CO_2 level is 75.7 times atmospheric CO_2 (27257 ppm) and a relatively high erosion rate (0.24 mm/yr). This leads to a steady state weathering rate after some 20.000 years of simulated time and a relative shallow soil (cf. figures 3.4 and 3.7). In the control simulation (figure 3.4) the Ca flux or weathering rate is initially defined by the eco-hydrological limit, which is set by the water and carbon balance as described in section 3.2.7. This limit is marked by the upper boundary of the shaded area. After about 2000 years, secondary minerals have accumulated to an extent where regolith production rate becomes a limiting factor. Around 20.000 years the regolith is close to steady state and defined by the supply limit, which is indicated by the lower limit of the shaded area. Thus for the control simulation, weathering rate is ultimately supply limited. Figure 3.4 also shows the time evolution with lower temperature or drainage rate. Decreasing the temperature by 15 °C leads to a larger initial Ca flux, but the supply limit still defines the rate in the end of the simulation. This is also the case for a scenario with half

parameter/variable	description	equation	value/range	units	internal/external
K_{eq}	equilibrium constant	Eq. (3)	$10^{-5.9}$	-	internal
U_0	regolith production constant	Eq. (19)	2×10^{-3}	[mm/yr]	internal
pCO_2	regolith partial pressure of CO_2	Eq. (12)	$1-214.4$	$\times$360 [ppm]	external
Q_d	drainage		$0-3.32 \times 10^{-8}$	[m/s]	external
R_z	topographic relief	Eq. (22)	$0-1920$	[m]	external
Lithology	bedrock lithology	Table 5	class $1-6$	-	internal/external

Table 3.6: Internal and external parameters and variables tested for sensitivity analysis. Internal parameters are those directly applied in the formulation of the model. The external variables depend on the climatic and topographic boundary conditions as well as the vegetation model. Lithological classes are defined internally in the model but geographic distribution is prescribed by an external input file.

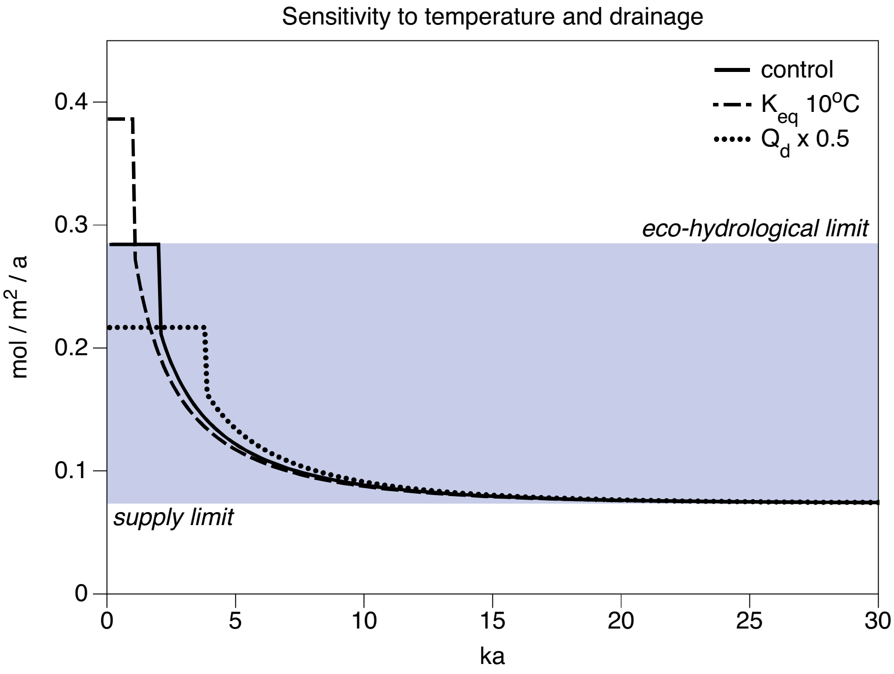

Figure 3.4: Sensitivity of Ca flux to temperature and drainage Q_d. The solubility of Ca^{2+} is higher in colder water. Thus a decrease in temperature to 10 °C ($K_{eq} = 10^{-5.5}$) leads to higher initial concentrations and a higher eco-hydrological limit, but has no effect in the supply-limited steady state. A decrease in drainage exports less dissolved compounds, whereby the eco-hydrological limit is lowered, but this also has no impact on the supply-limited steady state. The shaded area marks the limits for the control run. The upper limit is the eco-hydrological limited flux and the lower limit is the supply-limited flux.

the drainage, where a lower initial weathering rate is observed. Note that a change in the drainage does not simply mean that the export of dissolved calcium is changed proportionally, because the water balance of the regolith is changed and thus the productivity of the vegetation and the carbon balance of the regolith as well.

If we change the regolith production constant U_0, we may change the time it takes the regolith to reach steady state, but we will not change the steady state itself. This is illustrated in figure 3.5. Here, the control simulation is also compared to simulations, where the topographic relief is changed by

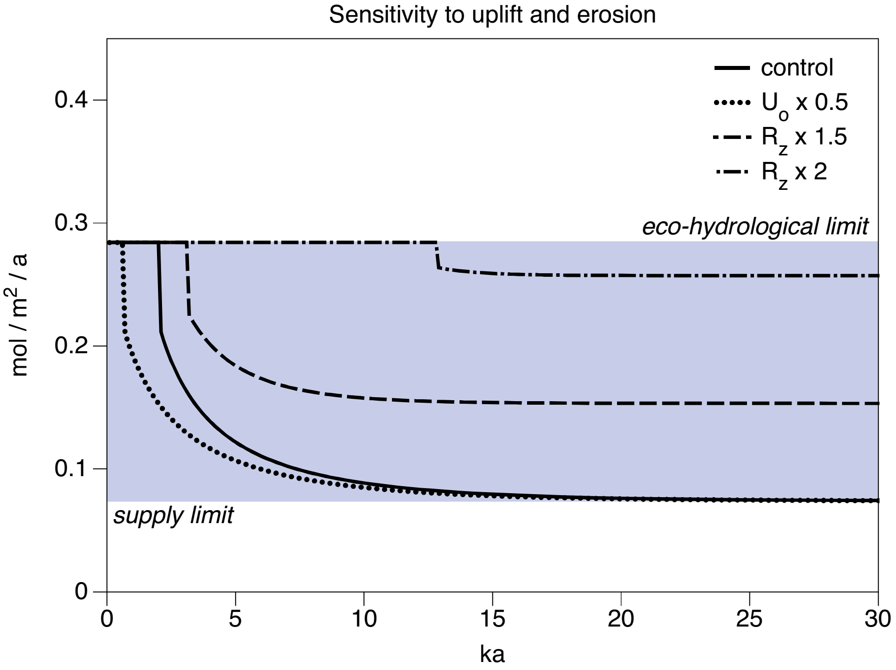

Figure 3.5: Sensitivity of Ca flux to physical weathering modulated by the regolith production constant U_0, and erosion modulated by topographic relief. A decrease in U_0 only affects the transient state of the regolith, whereas increasing the topographic relief influences the "end" steady state by increasing the supply limit compared to the control, which is marked by the lower limit of the shaded area.

a factor of 1.5 and 2. Erosion rate is thereby increased. This leads to an increase in steady state Ca flux. If topographic relief is increased further, the supply limitation can exceed the limitation set by the eco-hydrological conditions, i.e. the water and carbon balance, whereby these conditions will control weathering rates.

If the regolith CO_2 level is doubled, the eco-hydrological limit increases as in the case of a temperature decrease, figure 3.6. If the biotic effects are removed, the eco-hydrological limit lies below the supply limit and thus controls the Ca flux. In this case the CO_2 level is the same level as in the atmosphere, and results in the much lower chemical weathering rates than in the control simulation.

In figure 3.7 we trace the effects of the parameter study on accumulated

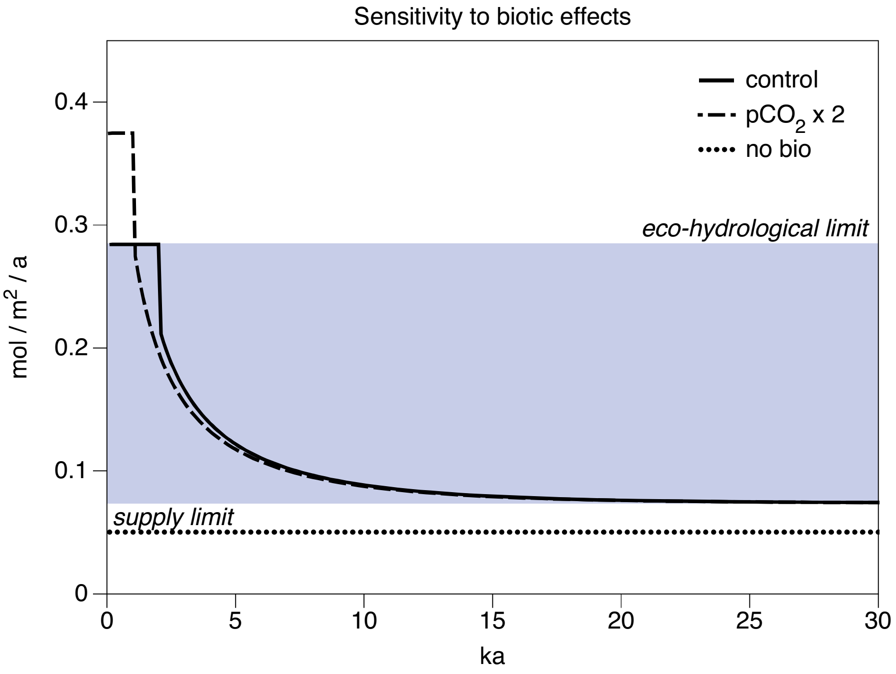

Figure 3.6: Sensitivity of Ca flux to changes in biotic effects. By an increase in regolith CO_2 the eco-hydrological limit is increased compared to the control, which is marked by the upper limit of the shaded area. The supply limit and thus the steady state remains the same. Removing all biotic effects, including effects on hydrology, leads to a significant decrease of the eco-hydrological limit below the supply limit.

Ca flux. Note, that the accumulated Ca flux for a change in the regolith production constant U_0 is delayed compared to the other tests that did not change the steady state Ca flux. The rate of increase is the same. The reason for this becomes clear when we look at the corresponding regolith depths shown in figure 3.7. Changing the regolith production constant U_0 results in a more shallow steady state regolith. Thus shallower regoliths are accompanied by lower accumulated chemical weathering rates. Changing the topographical relief also leads to a decrease in regolith depth, as the regolith accumulates at a slower rate due to the increased erosion. Note also that in the simulation with no biotic effects regolith does not accumulate at all. This is because the regolith produced through chemical weathering is eroded

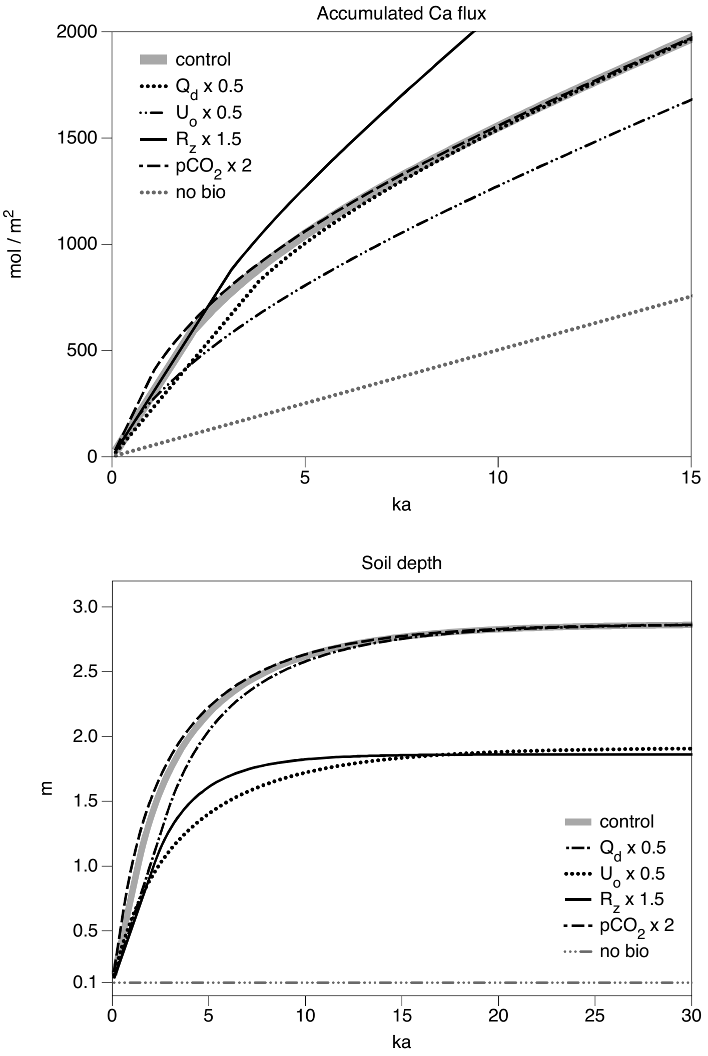

Figure 3.7: Top: accumulated Ca flux for single point simulation. A change in temperature (not shown), drainage or regolith CO_2 does not affect the long term accumulated weathering flux. Changing U_o yields a "delay" in accumulated weathering. The largest impact is caused by erosion rate and the combined biotic effects. Bottom: regolith depths for single point simulation. Steady state regolith depths can be changed by changing uplift rate or erosion rate. Drainage, temperature (not included) or regolith CO_2 have no direct influence on steady state regolith depth in the model for this grid point. When biotic effects are excluded regolith does not accumulate beyond the initial state. Note the difference in time scale in a) and b).

as fast as it is created.

Figure 3.8 shows the Ca fluxes of a test with the lithological definitions of table 3.5. We have included two definitions for shale in which *shale b* contains twice as much Ca as *shale a*. The higher the fraction of Ca in the bedrock, the higher the steady state Ca flux. There is also differences in the time it takes before weathering rate becomes supply-limited. This leads to the sudden exponential drop in the Ca flux. Carbonate weathering is per definition not supply limited, and even adding small amounts of other secondary minerals to this lithology will not make it supply-limited, unless erosion rate is very low (figure 3.8).

Overall these sensitivity simulations show that the response of chemical weathering rates to variations in the different drivers does not support a simple factorial function for single grid points. Instead they elucidate the importance of limiting factors in shaping the steady state response. The transient response may be affected by some parameter selection as is the

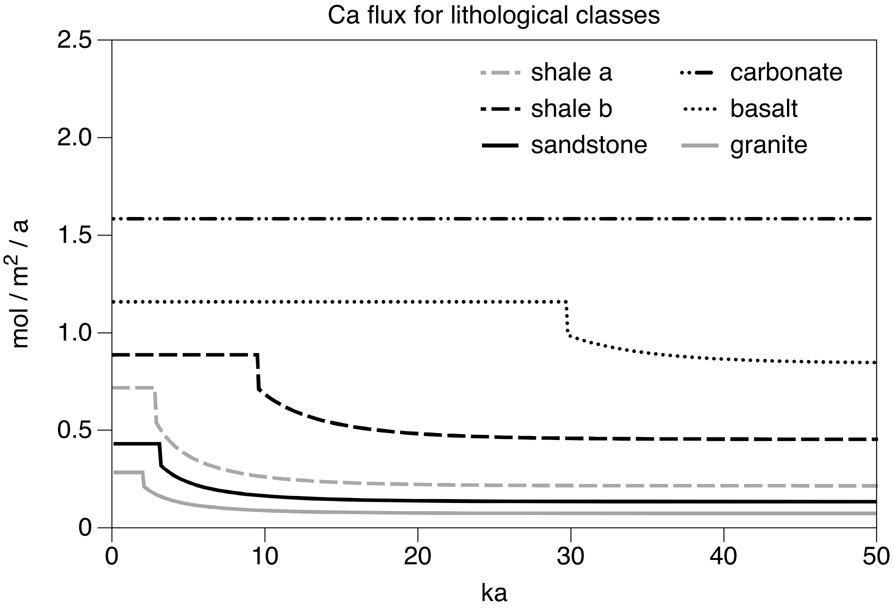

Figure 3.8: Evolution of Ca fluxes for single point test of lithological classes in table 3.5.

case for U_0, but in the end it is the two limits (defined in section 3.2.7) that set the steady state weathering rate in the model.

3.4.2 Global weathering rates

Global weathering rates were obtained by a 1Ma model run for all land points that were not glaciated or covered by water in the last glacial maximum, and a subsequent continued 10ka model run for all present day land points.

In table 3.7 the global fluxes of Ca^{2+}, Na+K, HCO_3^- and CO_2 consumption are shown for the different lithological classes. The fluxes are consistent with previous estimates from observations (Livingston, 1963; Gaillardet et al., 1999). Most of the Ca exported from land to ocean has an origin in carbonate, as only about $\sim$ 9.4% comes from silicate weathering. This is about half of the fraction of Ca originating in silicate weathering estimated in Berner and Berner (1987), but in agreement with Gaillardet et al. (1999). Since CO_2 is also consumed by weathering of other silicate minerals, than those containing Ca, $\sim$ 25% of the dissolved HCO_3^- is a result of silicate weathering, also in agreement with Gaillardet et al. (1999).

Figure 3.9 shows the global pattern of annual export of Ca from regoliths (top) and CO_2 consumption by weathering (bottom). Carbonate areas of China and Europe show particular high Ca fluxes as does basalt covered areas such as Iceland, and the shale covered part of Siberia. Areas charac-

lithology	Ca^{2+}_{tot}	Ca^{2+}_{sil}	$(Na,K)^+$	HCO_3^-	CO_2
1 - sandstone	0.27	0.03	0.33	0.88	0.36
2 - carbonate	7.62	0	0	15.2	0
3 - shale (a)	0.57	0.00	0.02	1.16	0.03
4 - granite	0.35	0.35	3.97	4.67	4.32
5 - acid volcanic	0.02	0.02	0.26	0.31	0.29
6 - basalt	0.47	0.47	0.55	1.93	1.24
global total	9.30	0.87	5.15	24.2	6.24

Table 3.7: Simulated rates of total Ca, silicate Ca, Na+K, HCO_3^- flux and CO_2 consumption by lithological class and globally. All units are in 10^{12} moles pr. year.

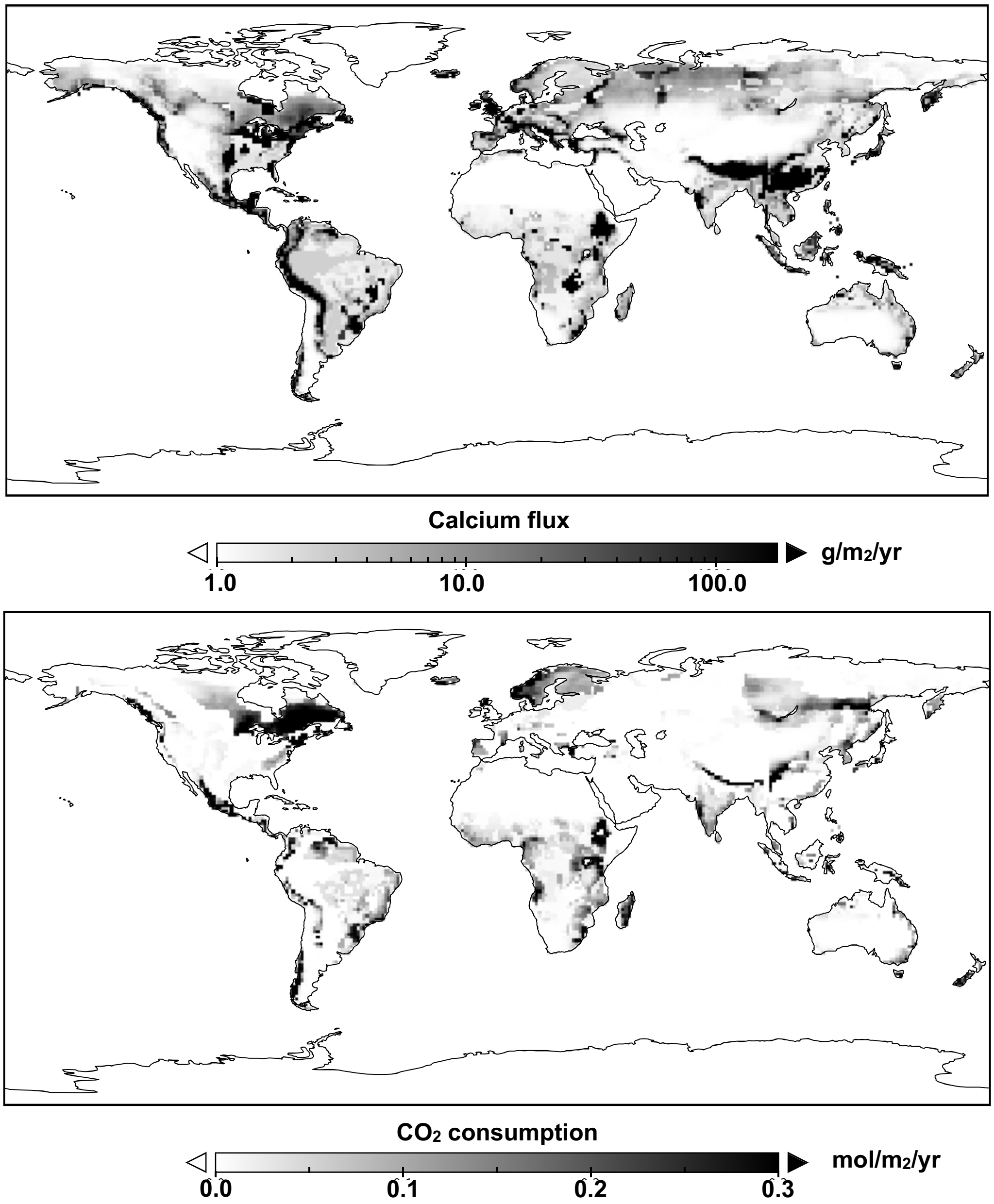

Figure 3.9: Top: Global map of annual export of Calcium from regoliths. Maximum Ca denudation is 176.4 g/m_2/yr. Bottom: Global map of CO_2 consumption by silicate weathering. Maximum CO_2 consumption is 2.7 mol/m_2/yr.

terized by low exports of Ca are the deserts, and areas of low topographic relief, such as large regions of the Amazon Basin. The pattern for CO_2 consumption in figure looks somewhat different, with the highest signature of CO_2 consumption from grid points covered by igneous rocks. This is because these lithologies consume most CO_2 during weathering due to their high content of weatherable primary minerals. Previously glaciated areas in Eastern North America and Scandinavia, yield higher CO_2 consumption and silicate weathering rates than tropical regions of similar lithological and topographic setting.

3.4.3 River waters

Concentrations of dissolved elements in rivers reflect the weathering rates of the regoliths in the river catchment (Goddris et al., 2006). Here we compare the model output of average Ca^{2+} and HCO_3^- concentrations for large river catchments to the measured concentrations of Ca^{2+} and HCO_3^- in rivers described in (Gaillardet et al., 1999). We do this in order to assess if the model is able to capture variation in chemical weathering rates between different climates.

Figure 3.10 shows the relationship between river concentrations of Ca^{2+} and HCO_3^- as well as the absolute concentration of these ions in large tropical, temperate and arctic rivers. The rivers chosen are the same as covered by Holland (1978) except the Rio Grande, which is not included in the dataset used here (Gaillardet et al., 1999). Most of the rivers are American, though a few European and African rivers have been included as well. A qualitative comparison between the two plots presented in figure 3.10 reveals that most values of Ca^{2+} and HCO_3^- concentrations locate model output and observed data in the same area of the graph with a few exceptions (Congo, Dvina and Rhine). In general temperate and arctic rivers display higher Ca^{2+} and HCO_3^- concentrations than tropical rivers. Rivers that are located close to the charge balance (stapled red line in figure 3.10) drain larger carbonate formations.

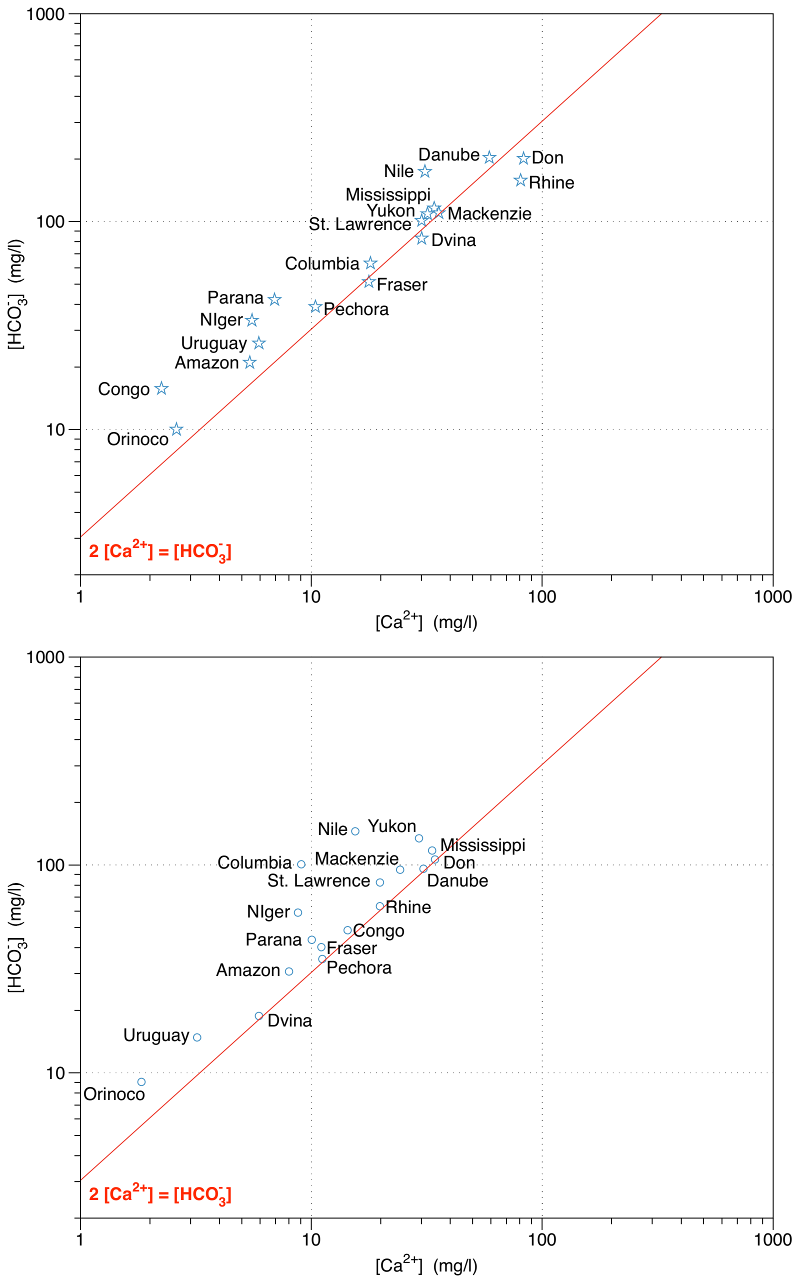

Figure 3.10: The annual mean concentration of calcium and bicarbonate of some major rivers. The relationship between the calcium and bicarbonate concentration of many rivers is close to the charge balance $2[Ca^{2+}]=[HCO_3^-]$ (red line) characteristic of $CaCO_3$ dissolution. Top: data from (Meybeck and Ragu, 1995; Gaillardet et al., 1999), bottom: model output.

3.5 Discussion

In this study we have investigated the potential for modeling global chemical weathering rates in terms of the limitations set by the important physical transports. We thereby include both eco-hydrological (i.e. climatic) drivers of weathering and tectonic control through mineral supply limitation. Parameterizations for these processes have been implemented in a simple, yet mechanistic model of the regolith and the model has been applied to both local, regional and global scales. We have compared the model output to observations on regional and global scales and find that results are reasonable. The model thus captures global patterns of Ca^{2+} and HCO_3^- fluxes across climatic and tectonic gradients.

The global pattern of Ca^{2+} (figure 3.9) reflects the occurrence of orogens and carbonate rocks. The highest fluxes occur where carbonates are combined with a warm, wet climate. This is because these environments sustain a high biotic productivity and yield high weathering rates year round as opposed to the seasonal variations of the polar regions. For silicate weathering, areas with high topographic relief sustain the highest weathering rates. CO_2 consumption (figure 3.9) is thus high in the orogens, but also in a large part of the arctic and temperate regions, where the regolith is still relatively fresh after the last glaciation.

We have shown that chemical weathering can be modeled by considering only limitations associated with physical transports of the important weathering ingredients: water, carbon and minerals. The simulated weathering rates result from the two limitations (defined in section 3.2.7): the eco-hydrological limitation and the supply limitation. The eco-hydrological limitation includes the formulation of potential chemical weathering in terms of a chemical saturation state given by CO_2, mineral composition and temperature. The physical transport of water through the regolith controls the rate at which minerals are dissolved and exported. In this respect a transport limitation is always assumed. The supply limitation is implemented through the modification of erosion on regolith depth. As regoliths accumulate, less weatherable minerals become available through physical weathering processes: the pulverization of bedrock into particles of the regolith. In section 3.4.1 (figure 3.5) it was established that the formulation of the physical weathering rate with depth has no impact on the chemical weathering rate at steady state. It does, however, affect the rate at which steady state is reached.

The advantage of our approach is the inherent simplicity and low control through input parameters. As opposed to many contemporary models (e.g. Goddris et al. 2006), it does not require detailed input data regarding regolith mineral composition, mineral surface area and kinetic rate laws. We have tried to implement a minimum of large scale empirical laws, the erosion parameterization is the exception. In spite of this simplicity the model produces reasonable results and moreover, reasonable spatial variability.

3.5.1 Limitations

Even though the model captures regional patterns and produces reasonable estimates of global weathering fluxes, there are some inherent limitations to the approach taken. In the following these limitations will be further discussed.

The global output of dissolved calcium fluxes from land to ocean in table 3.7 are in general on the low side of previous estimates (9.3×10^{12} vs. 13.1×10^{12} moles pr. year, Gaillardet et al. 1999) but reasonable. We could minimize this discrepancy by some fine tuning of the model, e.g. by changing the parameterization for physical erosion. This would add to the potential for chemical weathering in areas that are limited by mineral supply, e.g. the Amazon basin. However, since our estimates of river concentrations are not in general lower than observations, we decided to keep the model as it was first constructed without further fine tuning.

The partitioning of global Ca^{2+} fluxes between silicate and carbonate minerals differs from Berner and Berner (1987) but agrees with Gaillardet et al. (1999). This partitioning is very sensitive to the definition of lithological composition, especially for sedimentary rocks in which it can be very variable. Here, we have only three classes, which all are represented by high carbonate mineral weight fractions. This can lead to an overestimate of the carbonate contribution to the global scale Ca^{2+} flux, and thus to an underestimate of

CO_2 consumption. On the other hand, we have not considered the potentially important role of disseminated calcite in granite (White et al., 1999). This may lead to an underestimate of the carbonate fraction for that lithological class, and hereby to an overestimate of the CO_2 consumption.

The riverine concentrations of Ca^{2+} and HCO_3^- in figure 3.10 reflects the overall pattern of concentrations for large rivers across climatic gradients, for both field data (Meybeck and Ragu, 1995; Gaillardet et al., 1999) and the model. The tropical rivers generally exhibit lower concentrations than the temperate rivers for both data and model. This indicates that the overall patterns of weathering is reasonably modeled on this large regional scale. For a few rivers there is a larger discrepancy between model and data (e.g. Congo, Dvina and Rhine, figure 3.10). There are more possible reasons for these discrepancies including coarse lithological representation and factors that have not been included in the model such as anthropogenic impacts and dissolution of organic matter in rivers. The latter would especially influence the HCO_3^- concentration. Note that the river concentrations cannot be explained by the carbonate equilibrium $2\ [Ca^{2+}] = [HCO_3^-]$ alone, because weathering of silicate minerals that do not contain Ca also contributes to the HCO_3^- concentration.

A substantial simplification of the model concerns the treatment of uplift and erosion. In the model erosion is treated as an empirical function of topographic relief in line with previous work (Hilley and Porder, 2008). Because we do not model the response of the topographic relief to erosion, we implicitly assume that uplift equals erosion plus weathering. We can thus make a first order estimate of uplift rates by considering the mass balance of the regolith. A mechanistic representation of erosion should also include a runoff dependence and lateral sediment transport and deposition in order to capture weathering in foreland sedimentary basins (Moquet et al., 2011). However, because we only allow secondary minerals to be eroded, hydrological effects are already considered to some extent through their impact on chemical weathering. Nevertheless, we may underestimate erosion rates and thus chemical weathering rates by turning an empirical function into a potential, because the empirical formulation already includes all effects on erosion, including those of hydrology and vegetation. A substantial improvement to the model could potentially be achieved through a mechanistic representation of erosion.

In the model the partial pressure of CO_2 in the regolith, together with the composition of the regolith and bedrock are the primary controls on the chemical saturation state as described in equation 3.12. This indirect biotic impact on weathering illustrates some general dynamics of biotic enhancement of weathering. It does not include biotic uptake or enhancement by vegetation, fungi and bacteria. In order to model initial biotic increases in weathering and nutrient uptake, we would need a layered model. This is because the layers dominated by biotic recycling have much larger pools of Ca, K, Na and P, which easily floods the rest of the system if not separated in the model. This level of model complexity is not matched by the vegetation model and therefore beyond the scope of this study. Furthermore, in order to model biotic enhancement in steady state we would need to know the amount of leaching of nutrients that does not go back into the soil. It has previously been shown that biotic enhancement of weathering might not be detectable in steady state, and that disturbance is important, e.g. fires, harvests and landslides (Balogh-Brunstad et al., 2008). Also, the impact of vegetation on physical erosion is most likely a decrease, due to the stabilizing effect of root systems on the regolith (Reubens et al., 2007). This would also lead to a corresponding decrease in chemical weathering rates in steady state, unless microbial activity is able to reverse this effect by dissolution of secondary minerals (Sokolova, 2013). The relative importance of these processes is unknown, but should be considered in future studies implementing more advanced process based models for long time scales.

Finally, we do not consider the case where reaction kinetics are important. In order to establish in which cases reaction kinetics are important, we need detailed information about the flow paths and residence time of water in regoliths. The appropriate model for this would have multiple regolith layers and a more detailed formulation of water transports for the shallow soils where reaction kinetics may control weathering rates. This level of complexity is beyond the scope of this study. Also, as mentioned in the introduction, verification in large scale datasets would be difficult, because a clear temperature dependence has not been observed (Kump et al., 2000; Hartmann et al., 2010). Therefore it is difficult to establish and verify the importance of reaction kinetics at the global scale.

3.5.2 Implications and perspectives

We have illustrated that for steady state scenarios of chemical weathering, only two limits seem to matter for continental scale fluxes. These limits are imposed by the physical and chemical processes that govern the active weathering zone of the regolith. By equally emphasizing chemical and physical drivers, this simple model simulates overall patterns of chemical weathering reasonably well. The implications for our understanding of steady state chemical weathering will be discussed in the following.

The single point simulations illustrate the response of the model to changes in different parameters and drivers. If we are to consider only steady state scenarios (which are appropriate for geological time scales) only the parameters and parameterizations that have a direct influence on the steady state become important. Thus the formulation of regolith production is irrelevant for the simulated steady state by the model. The regolith production function may have an influence on the thickness of the regolith, but not on the chemical weathering rate in steady state. Calculating steady state scenarios thus may be simplified to a comparison of the limitations on weathering as in Arens and Kleidon (2011) (Chapter 4), where the potential eco-hydrological rates are compared directly to the potential supply limited rates. The overall potential chemical weathering rate is thus the minimum of these two limits. This approach is useful for calculation of long term scenarios, because the focus is on the steady state response. Slow transient simulations are unnecessary for these scenarios as the fluxes are controlled by the two limits of the steady state approach.

In the model we assume that dissolution rates are fast enough, that we do not need to consider a kinetic impact on a large regional scale. This assumption is applicable only at large spatial and temporal scales, and not at short time scales, when meteoric water first comes into contact with the weatherable minerals of the regolith. There could be more reasons why the signature of kinetic control, a temperature dependence of river concentrations of dissolved loads, is indistinguishable in observations. This could be the case if the dissolved load in large proportions of the water in rivers are controlled by saturated states or a supply limitation on weathering rates, i.e. by the physical transport of water and minerals. If a large part of the water does not come into contact with the active chemical weathering zone of the regolith, a perturbation to this water flux could mask the response from a covarying kinetic control.

The sensitivity of climate and particularly temperature to atmospheric carbon dioxide has been the backbone of the silicate weathering feedback hypothesis for three decades since the work of Walker et al. (1981). As a result, kinetic weathering laws have been extensively applied in weathering models (e.g. West et al. (2005), Hilley and Porder (2008)). If we consider that kinetic weatherings laws may not be suitable for application on a large scale and thereby in models of the global carbon cycle, we also need to reconsider the silicate weathering feedback and how it may function. If the silicate weathering feedback is primarily controlled by the interactions between climate, vegetation and the water cycle, a smooth feedback as formulated in Walker et al. (1981) might be a gross simplification, due to feedbacks and thresholds associated with these interactions. The silicate weathering feedback could therefore also exhibit thresholds and perhaps even shift between positive and negative feedback regimes. However, because we did not explicitly consider kinetic limitations, their role on a large scale needs to be further explored, preferably in a process oriented model that integrates both climatic and tectonic drivers of wethering.

The strength of our approach is in the integrated view of the controls of weathering, equally emphasizing the hydrologic controls from above and the tectonic controls from below. There is therefore the potential for testing the impacts of interactions between climate and crustal uplift on chemical weathering rates by using the regolith model coupled to a climate model. The role of crustal uplift in the silicate weathering feedback can be evaluated as well as the potential strength of the silicate weathering feedback itself during different time periods in Earth history. This would add to our understanding of the role of silicate weathering in the carbon cycle and thereby climate variability on geological time scales.

3.6 Conclusion

We have presented an alternative approach to quantifying global chemical weathering rates in a dynamic global regolith model. The approach distinguishes itself from previous work (e.g. Goddris et al. 2006; Godderis et al. 2008) through the focus on limitations. It does not implement the usual factorial approach, in which established empirical laws for each driving factor is multiplied or implemented as a correction to chemical weathering rates (e.g. Taylor et al., 2012). The problem with such an approach is that it is inherently assumed that every point on the surface responds to a change in any driving factor. Conversely, our approach is able to disseminate the combined impact of simultaneous adverse effects.

The global regolith model specifically considers the limitations associated with the physical transport of water, carbon and minerals through calculations of the water balance and potential erosion. Biotic effects are considered through the dependence of chemical weathering on the carbon balance of the regolith. The model is able to simulate large scale geographical variations in chemical weathering rates as indicated by dissolved calcium and bicarbonate in rivers consistent with observations. Detailed input on regolith composition is not necessary. Instead the evolution of a bulk regolith is modeled given the controls and limitations set by the physical transports. The model allows us to calculate transient responses towards steady state on long time scales up to 1Ma. We find that topographic and eco-hydrological controls are equally important in defining modeled steady states.

The model presented here can be used to evaluate Earth system hypotheses, such as the silicate weathering feedback hypothesis. If we are to re-evaluate the strength of the silicate weathering feedback globally, we need to do it in terms of limitations, by considering the drivers in an integrated framework. Our approach presents the means to do this.

4 Eco-hydrological versus supply-limited weathering regimes and the potential for biotic enhancement of weathering at the global scale

Biotic enhancement of weathering (BEW) has been proposed to substantially alter the geologic carbon cycle but the large scale impact of small scale biotic processes remains elusive, especially when compared to large scale drivers of weathering such as climate and crustal uplift. We used a global land surface model to estimate the potential strength of BEW for two contrasting types of weathering regimes that are either limited by the supply of fresh parent material by uplift or controlled by the climatic and eco-hydrological conditions. We then removed the biospheric effect on soil CO_2 in the model in order to determine the reduction of weathering rates and hereby to infer BEW. We find that only those areas that are not supply limited are susceptible to biotic enhancement and conclude that the potential for BEW depends directly on the supply of fresh material and thus on crustal uplift.

4.1 Introduction

On geological time scales the amount of CO_2 released into the atmosphere by volcanic activity must be balanced by removal of CO_2 from the atmosphere in steady state. The silicate weathering hypothesis (Walker et al., 1981) suggests a negative feedback that involves the climatic effects on dissolution of silicate minerals on land and the subsequent formation of carbonate minerals $(Ca,Mg)CO_3$ in the oceans as a sink for CO_2. The flux of calcium and magnesium from land to ocean thus plays a critical role.

The global climatic effects of temperature and runoff on weathering have previously been parameterized empirically (Walker et al., 1981) (Berner, 1991) (Godderis et al., 2008) as has the effects of erosion/uplift and the biosphere (Hilley and Porder, 2008) (Schwartzman and Volk, 1989). In these studies each process has been treated separately, because a global scale process based model of rock weathering remains elusive due to the complexity of the Earth's surface and the range in scale of processes involved. In order to understand the role of climate, uplift and biota at the global scale we first need to consider their relative importance and potential interactions regionally. This is due to the high spatial variability in climatic and tectonic conditions (see also West et al. 2005).

Here we compare the climatic and tectonic forcings in order to estimate the dominant control on weathering rates in steady state, and classify the Earth's surface accordingly. We view the continental export of dissolved calcium from land to ocean as being primarily limited either by the uplift of fresh parent material (which balances weathering and erosion in steady state), or by the saturated soil water discharge given by eco-hydrological conditions and bedrock mineralogy. These two limitations have been implemented into the JeSSy-SimBA land surface model (Porada et al., 2010) in order to quantify and compare the corresponding weathering rates and classify regions according to the dominant limitation. Finally, we characterize the potential for BEW by excluding the impact of the terrestrial biosphere on soil CO_2.

4.2 Method

4.2.1 Supply-limited Weathering Flux

The supply-limited weathering flux is calculated based on a steady state assumption in which the rate of crustal uplift is balanced by denudation. To calculate this rate, we use an empirical erosion parameterization (Hilley and Porder, 2008; Montgomery and Brandon, 2002), which relates erosion ε (mm/yr) to topographic relief R_Z

$$\begin{aligned} \varepsilon &= 2.0 \times 10^{-4} R_z \qquad \text{for} R_z \leq 494 \text{ m} \\ \varepsilon &= 1.4 \times 10^{-6} R_z^{1.8} \qquad \text{for} R_z \geq 494 \text{m} \end{aligned} \tag{4.1}$$

If we assume that only secondary minerals are eroded, erosion will depend directly on the intensity of weathering. The calculated erosion fluxes are normalized to the relative abundance of their source minerals in the bedrock lithology, and the corresponding weathering flux FCa_{sl} is then

$$FCa_{sl} = FSiO_2 \cdot xCa/xSiO_2 \tag{4.2}$$

where $FSiO_2$ is the calculated erosion flux of SiO_2 and xCa and $xSiO_2$ are the fractions of calcium and SiO_2 in the bedrock.

4.2.2 Eco-hydrological Controlled Weathering Flux

To calculate the eco-hydrological controlled weathering flux, we assume that the maximum concentration of dissolved calcium is given by the saturation with respect to carbonate. This is a reasonable assumption because the equilibrium concentration with respect to primary minerals such as anorthite is much higher than that of carbonate and carbonate would thus precipitate before this equilibrium concentration is reached. Precipitation of secondary silicate minerals such as montmorillonite also binds Ca^{2+}, especially in dry steppe soils, but not at a rate to match weathering and thereby define an upper limit for Ca^{2+} concentration (Shvartsev, 2008a). Since we consider the large-scale weathering rate to be proportional to the flux of Ca^{2+} in drainage and river discharge R, we ignore the potential weathering hidden in formation of carbonate and clay precipitates in soils. Weathering reactions of minerals that do not contain calcium are included indirectly by assuming that they occur at the same rate, so the composition of primary minerals remain the same over time. We use the formulation of equation (3.12):

$$[Ca^{2+}]^3 = \frac{K_{eq} \cdot pCO_2}{c_{min}} \Big(\frac{m_{Ca}}{m_p}\Big) \tag{4.3}$$

where pCO_2 is the partial pressure of CO_2 in the soil and c_{min} is a correction term for the simultaneous dissolution of other minerals. We use the molal fraction m_{Ca}/m_p of Ca-minerals m_{Ca} to all reacting primary minerals of the bedrock m_p to define the activity of dissolving Ca minerals. Note that $c_{min} = 4$ yields the carbonate equilibrium solution of pure carbonate dissolution. The eco-hydrological controlled weathering flux FCa_{eco} is then given by:

$$FCa_{eco} = R \cdot [Ca^{2+}] \tag{4.4}$$

4.2.3 Model Setup

We use the JeSSy-SimBA land surface model (Porada et al., 2010) forced with climate data from the NASA Land Surface and Hydrology archive from 1960 to 1989. (Sheffield et al., 2006). JeSSy-SimBA simulates carbon and water fluxes including vegetation productivity, respiration, evapotranspiration and runoff/drainage. We use the lithologies of Amiotte Suchet and Probst (1995) rescaled to a resolution of $1.125^o \times 1.125^o$. The mineralogy of each lithological class is defined in table 3.5[1]. We assume that local topographic relief scales with topographic gradient between grid cells with a maximum of 2000 m.

We have made three runs of the model in which the model was spun up to an inter-annual steady state for carbon and water pools. In the control run, we calculated the weathering rates as described above. In the mono-lithological run, the lithology was defined as granitic in all grid points for illustration purposes (figure 4.1). In the "no biota" run soil CO_2 levels were kept at 360 ppm.

4.3 Weathering regimes and biotic enhancement of weathering

Figure 4.1 shows the two potential weathering fluxes due to the eco-hydrological conditions (fig. 4.1 (a)) and due to uplift (fig. 4.1 (b)), as well as the minimum of both fluxes (fig. 4.1 (c)) for a mono-lithological run. While the eco-hydrological rate reflects mostly the global distribution of continental

---

[1] Shale is defined as *shale a* in table 3.5

(a) Potential climatically driven calcium flux

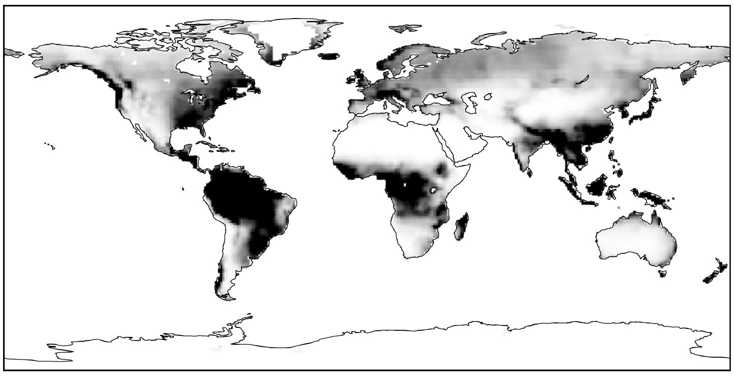

(b) Potential erosion equivalent calcium flux

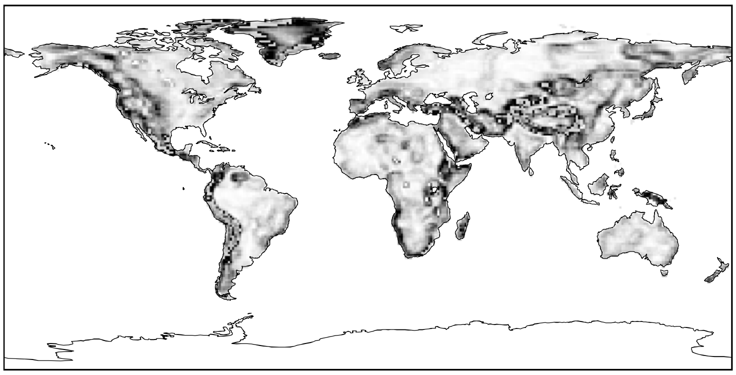

(c) Steady state calcium flux

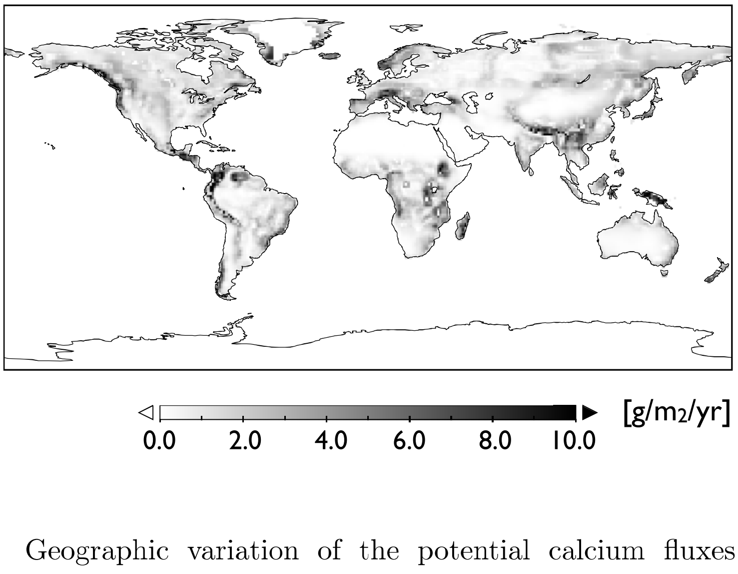

Figure 4.1: Geographic variation of the potential calcium fluxes for mono-lithological (granite) simulation due to (a) eco-hydrological control and (b) the supply limit by continental uplift. The minimum of both rates is shown in (c). See Method section for description of rate calculation.

precipitation, the supply-limited rate maps the topographic relief. The total global calcium fluxes calculated by this minimization method ($5 - 18 \times 10^{12}$ moles/year depending on lithology) are within the range of previous estimates (e.g. Holland, 1978).

Figure 4.2 (a) shows the regional classification according to the dominant limitation of weathering, with areas of carbonate lithology excluded, because dissolution of carbonate is congruent. This lithology does not form the same amount of soil residues and is per definition always in an eco-hydrological controlled regime. Noteworthy is that a large part of the boreal zone on the northern hemisphere is in the supply-limited regime for the steady state solution. However, soils in this region are still far from steady state due to recent glaciations.

To evaluate the potential for BEW in the context of these two limitations, we excluded the effect of the biota on soil CO_2. Note that there are other impacts of the biota on weathering rates, such as microbial effects and the impact of vegetation on runoff and drainage (Taylor et al., 2009). The biota may also impact erosion rates (Dietrich and Perron, 2006). Here, the "no biota" run has excluded only the impact of the biota on soil CO_2 levels. Figure 4.2 (b) shows the classification for the "no biota" run and figure 4.2 (c) shows the ratio in calcium transport between the control and the "no biota" run, (i.e. in fig. 4.2 (c) = (a)/(b)). Note that the biotic increase in soil CO_2 shifts a large part of the eco-hydrological controlled areas to the supply-limited regime (black areas in fig. 4.2 (b) become grey in fig 4.2 (a)). This suggests that only areas that are not supply-limited are susceptible to BEW. There is also an upper bound to the possible enhancement by biotic processes in a given area, and this upper bound depends on the topographic relief. Since topographic relief is maintained by crustal uplift on geological time scales, we conclude that the long term potential for BEW depends on the rate of continental uplift.

(a) Weathering vs. erosion limited regimes for control run

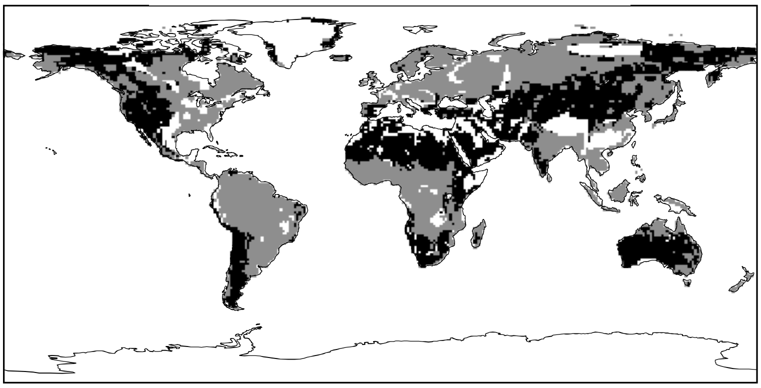

(b) Weathering vs. erosion limited regimes for ACO2 run

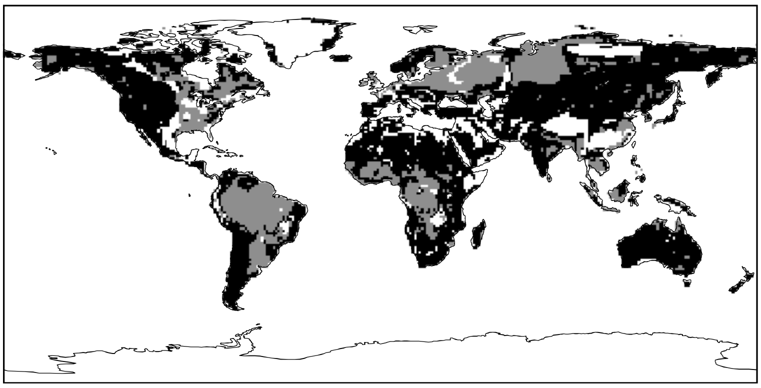

(c) Biotic enhancement of weathering

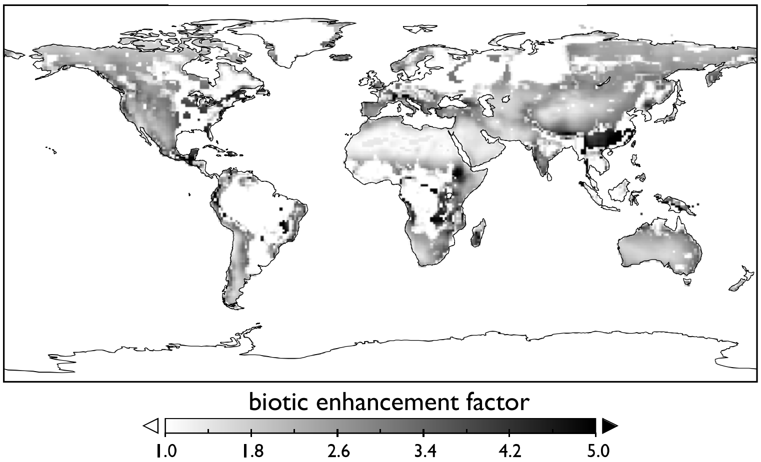

Figure 4.2: (a) Supply limited (grey) and eco-hydrological controlled (black) regimes for control run. Carbonate and ice covered regions (white) are excluded. (b) Same as (a) but for the "no biota" run, see Method section. (c) The biotic enhancement is calculated as the ratio of (a) to (b).

4.4 Conclusions

We classified regions according to the dominant limitation on weathering - supply of parent material or eco-hydrological conditions - in order to differentiate the importance of tectonic and climatic processes and the role of the biota for the flux of calcium to the oceans. Our results suggest that the biota primarily affects regions under climatic control, and that biotic effects may shift such regions from an eco-hydrological regime to a supply-limited regime.

The ultimate limitation on weathering and thus BEW is crustal uplift, because it controls erosion and thus exposure of bedrock to the surface. Process based models that include both climatic/biotic forcing and tectonic forcing on weathering are needed in order to understand coupling between these large scale processes and the resulting spatial weathering patterns. The strength of the silicate weathering feedback depends on the inherent limitations in the response of the Earth's surface to varying atmospheric CO_2 levels and climate. It would seem that process based models can be of great utility to understand weathering dynamics beyond the range of current conditions, and thus also to estimate the variability of atmospheric CO_2 levels and climate on geological time scales.

5 The impact of mineral supply limitation on the silicate weathering feedback

The sensitivity of global silicate weathering rates to a large range of atmospheric CO_2 levels is investigated with a model that combines climatic and tectonic controls on chemical weathering. In the model chemical weathering is seen as a co-limited process defined by the minimum of two rate limits. A climatic rate limit associated with runoff and an erosion rate limit associated with topographic relief. We find that mineral supply-limitation in areas of low topographic relief reduces the weathering sensitivity and thus the strength of the global scale silicate weathering feedback. Only areas that are not supply limited are sensitive to CO_2 induced changes in chemical weathering rates through climatically driven ecological and hydrological effects. Not only does supply-limitation reduce the size of these climatically controlled areas, the relative weathering flux from these areas decreases gradually with increasing CO_2. An analysis of the resulting feedback reveals that supply-limitation consistently reduces the impact of each of the global climatic drivers of weathering: CO_2, temperature, and precipitation. This supports the notion that uplift plays an important role in shaping the strength of the silicate weathering feedback through the impact on supply of weatherable minerals. It also suggests that models of the long term carbon cycle may overestimate the extent to which climate shapes silicate weathering rates on the land surface.

5.1 Introduction

Silicate weathering plays an important role in stabilizing atmospheric CO_2 and climate on geological time scales (Ebelmen, 1845; Urey, 1952; Walker et al., 1981). The vast amount of CO_2 released into the atmosphere by volcanic activity and metamorphic degassing on geological time scales $(4 - 10 \cdot$

10^{18} mol/m.y. Marty and Tolstikhin, 1998) would result in very high and ever increasing atmospheric CO_2 levels, unless CO_2 was removed from the atmosphere at roughly the same rate. The process most commonly deemed responsible for the stabilization of atmospheric CO_2 is weathering of silicate minerals on the land surface of the Earth (Walker et al., 1981; Berner, 1991). Silicate weathering releases dissolved Ca and Mg into rivers leading to the consecutive formation of $(Ca,Mg)CO_3$ in the oceans. As a result atmospheric CO_2 is bound in carbonate on the ocean floor. The sensitivity of silicate weathering to climate is essential in shaping the range of possible atmospheric CO_2 levels and associated climate states. Thus silicate weathering constitutes an important negative feedback on atmospheric CO_2 on geological time scales.

The global silicate weathering sensitivity has previous been estimated using a range of laboratory and field data (Walker et al., 1981; Schwartzman and Volk, 1989; Berner, 1991; West et al., 2005) to describe the dependence on CO_2, temperature, runoff, biotic effects and erosion. The common approach is to find empirical relationships for each of the driving factors and then multiply these parameterizations in a factorial approach to achieve an overall weathering sensitivity function. Walker et al. (1981) presented the first of this type of parameterizations in which global silicate weathering rate (W) was related directly to CO_2 (P), difference in global mean temperature (ΔT) and runoff (expressed in terms of the sensitivity of runoff to ΔT):

$$\frac{W}{W_0} = \left(\frac{P}{P_0}\right)^{0.3} e^{0.056 \cdot \Delta T} e^{0.017 \cdot \Delta T} \tag{5.1}$$

where the subscript 0 refers to a reference state. This type of silicate weathering sensitivity or feedback function can then be implemented into a carbon cycle model. By using a factorial approach one inherently applies the assumption, that every point on the land surface responds to a change in any of the driving factors, because each factor is weighed evenly. However, as pointed out by West et al. (2005), areas that are limited by the supply of weatherable minerals should not respond to small changes in runoff or temperature, and this needs to be considered in global models of the carbon cycle, because only areas where silicate weathering is sensitive to climatic change will shape the silicate weathering feedback.

Here, we use a global model of chemical weathering (Arens and Kleidon, 2011) that considers both climatic and tectonic limitations on weathering to estimate the impact of supply limitation on the silicate weathering feedback. We force the model with sensitivity simulations of an atmospheric GCM (Arens and Kleidon, 2008; Kleidon, 2009) for a large range of atmospheric CO_2 levels in order to determine the model sensitivity of chemical weathering rates to atmospheric CO_2 and climate for the present day geologic setup of the Earth. We then use the model output to parameterize a global silicate weathering feedback function and compare this to previous parameterizations used in global models of the carbon cycle. As we shall illustrate, supply limitation has a direct impact on the strength of the silicate weathering feedback by setting limitations for the effects of all other drivers of weathering. This is supported by our analysis of the global parameterizations for each of the drivers precipitation, temperature and CO_2. Also, as atmospheric CO_2 levels are gradually increased, a gradually smaller fraction of the weathering fluxes comes from areas that shape the silicate weathering feedback. Finally, we show that biotic enhancement of weathering decreases with increasing atmospheric CO_2 due to the impact of mineral supply limitation.

5.2 Method

In order to estimate the sensitivity of global scale chemical weathering rates to atmospheric CO_2 we need to consider spatial variation of the climatic and tectonic drivers of weathering. We use models to relate this variation to available data on climate and topographic relief. Figure 5.1 presents an overview of the models for atmosphere, eco-hydrology and weathering and their inputs and outputs. The weathering model calculates steady state weathering rates based on parameterizations of limitations associated with the climatic and tectonic setup for the present day geography of the Earth. In the following the steady state solution is presented in more detail.

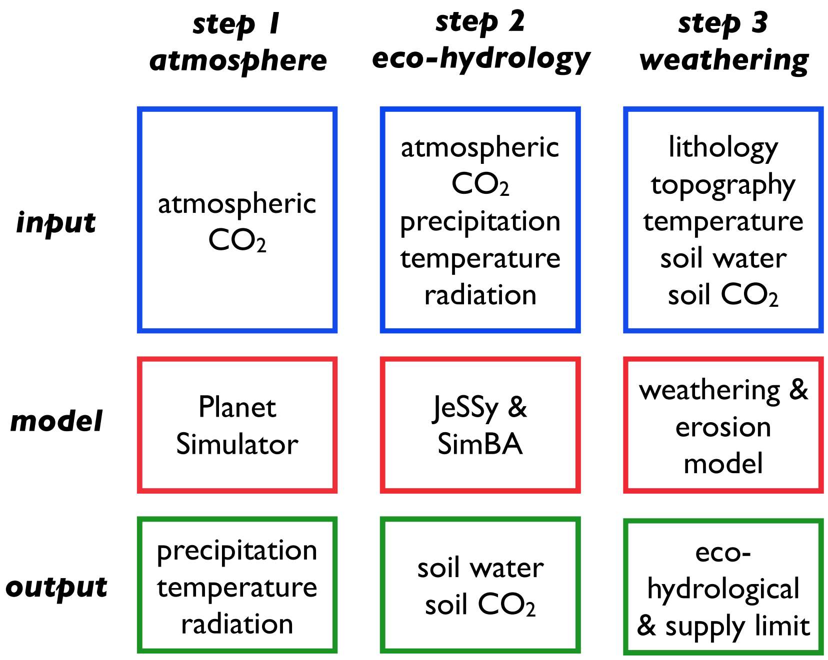

Figure 5.1: The three steps of the model setup. Output generated by the atmosphere and eco-hydrological models is used in the weathering and erosion model.

5.2.1 Steady state weathering rate

In steady state regolith production balances chemical weathering and physical erosion, i.e.

$$\begin{aligned} \frac{dM_p}{dt} &= P_r - W_r = P_r - (W_s + W_l) = 0 && (5.2) \\ \frac{dM_s}{dt} &= W_s - \varepsilon = 0 && (5.3) \\ \frac{dM}{dt} &= \frac{dM_p}{dt} + \frac{dM_s}{dt} = P_r - W_l - \varepsilon = 0 && (5.4) \end{aligned}$$

where M_p is primary mineral mass, M_s is secondary mineral mass, M is regolith mass, P_r is regolith production rate, $W_r = W_s + W_l$ is chemical weathering or transformation rate from primary to secondary minerals W_s and dissolved load W_l and ε is physical erosion rate. Here, we have disregarded any external inputs such as dust deposition. Note that where W_s is low ε also becomes low and vice versa. The production and loss of regolith thus balance each other. The limitations set by topographic relief on ε and climate on W_s can be used to answer the critical question what controls W_l. Essentially we solve eq. 5.3 and since $W_l \propto W_s$:

$$W_l \propto min(W_s, \varepsilon) \tag{5.5}$$

which means that the dissolved load is proportional to the minimum of the limitations set by climate on W_s and topographic relief on ε. If topographic relief is high, there is a potential for high physical erosion rates, i.e. the physical transport and deposition elsewhere of solid material from the regolith. In this case chemical weathering may become a limiting factor on physical erosion rates, because chemical weathering affects the structural integrity of the material (Carson and Kirkby, 1972). Essentially, ε cannot exceed W_s in steady state. We define the landscape as under *eco-hydrological control*, if the physical transport of sediment ε is limited by chemical weathering W_s (Arens and Kleidon, 2011). Conversely, at low topographic relief the potential for physical transport of sediment is low and chemical weathering may outpace physical erosion. However, the resulting accumulation of regolith slows down chemical weathering rates due to supply limitation of weatherable minerals from the bedrock. This supply limitation occurs because the bedrock is isolated from chemical and physical weathering agents by the regolith. Thus, W_s cannot exceed ε in steady state. We define this as the *supply-limited regime* (Riebe et al., 2004; West et al., 2005; Arens and Kleidon, 2011).

The steady state solution is calculated based on the potential fluxes of chemical weathering and physical erosion. The potential chemical weathering is what we would have if there is no supply limitation on weatherable minerals from the bedrock, i.e. no accumulation of regolith to the point where it isolates the bedrock from weathering agents. In the following formulation we concentrate on Ca fluxes because Ca fluxes are important for the silicate weathering feedback. The upper limit to the concentration of dissolved Ca depends on the water and carbon balance of the regolith and on the lithology of the bedrock. It is variable during the year and calculated according to:

$$[Ca^{2+}]^3 \backsimeq \frac{K_{eq} \cdot pCO_2}{c_{min}} \left(\frac{m_{Ca}}{m_p} \right) \tag{5.6}$$

where pCO_2 is the partial pressure of CO_2 in the regolith, $\frac{m_{Ca}}{m_p}$ is the relative abundance of Ca-minerals in the bedrock, K_{eq} is the equilibrium constant for calcite equilibrium and c_{min} is a correction term for simultaneous weathering of other minerals (cf. eq. (3.12)).

We express the potential chemical weathering rate as the export of dissolved calcium from the regolith by

$$FCa_{eco} = R \cdot [Ca^{2+}] \tag{5.7}$$

which is just the drainage R multiplied with the concentration of calcium ions in the soil/regolith water. Note that this weathering flux is not limited by regolith production rate, it assumes ample abundance of bedrock minerals in the regolith.

The potential physical erosion is defined given the topographic constraint:

$$\varepsilon = 0.05 + 7.5 \times 10^{-4} \frac{R_z}{1 - (R_z/2000)^2} \tag{5.8}$$

where ε is in units of mm/yr and R_z is the topographic relief in meters. Equation 5.8 has the general form suggested by Montgomery and Brandon (2002) but has been tuned to yield reasonable global weathering rates for the steady state solution of the reference simulation. Thus 360 ppm atmospheric CO_2 yields a silicate Ca flux of $4.14 \cdot 10^{12}$ mol/yr.

In principle the steady state equation must be valid for each element of the regolith. The erosional fluxes of secondary minerals are normalized to correspond to the relative abundance of their sources in the bedrock, whereby the composition of the eroded material corresponds to that of the regolith resulting from weathering the bedrock lithology. We express the chemical weathering needed to support the potential erosion through the formation of secondary minerals in terms of the dissolved calcium fluxes. We hereby assume that all Ca is exported from the regolith in dissolved form. Thus

$$FCa_{sl} = FSiO_2 \cdot \frac{xCa}{xSiO_2} \tag{5.9}$$

where FCa_{sl} is the calcium export calculated for each grid point, $FSiO_2$ is the erosion of SiO_2 (quartz) and xCa and $xSiO_2$ are the fractions of calcium and SiO_2 in the bedrock.

The steady state solution of the model reveals which areas are in the supply-limited regime and which areas are under eco-hydrological control. In order to find the steady state chemical weathering rate FCa_{ss}, we consider chemical weathering as co-limited by mineral supply and climate. We do this by comparing the potential fluxes FCa_{sl} and FCa_{eco} as we compared the solid fluxes in equation 5.5:

$$FCa_{ss} = min(FCa_{eco}, FCa_{sl}) \tag{5.10}$$

On a yearly basis one of the two will be less than the other, thereby defining the dominating weathering regime. Thus if $FCa_{sl} < FCa_{eco}$ weathering is defined as supply-limited, and conversely if $FCa_{eco} < FCa_{sl}$ chemical weathering rate is controlled by eco-hydrology.

5.2.2 Model Setup

We used climate model output generated by the Planet simulator (Lunkeit et al., 2004; Fraedrich et al., 2005a,b) for atmospheric CO_2 levels between 100 ppm and 10.000 ppm (Arens and Kleidon, 2008; Kleidon, 2009). We extrapolated the climate model output to 1.125° × 1.125° and used it to calculate the soil/regolith eco-hydrology (i.e. carbon and water balance) including partial pressure of CO_2, evapotranspiration and runoff with the coupled JeSSy and SimBA land surface model (Porada et al., 2010). Finally, we used the output of JeSSy-SimBA together with land maps of topography and lithology to calculate the upper limits on chemical weathering set by eco-hydrology and supply of weatherable minerals with a simple model of chemical weathering and physical erosion. A comparison of these two limits yields the steady state weathering rate and thus the sensitivity of chemical weathering to atmospheric CO_2.

Climate sensitivity

The global mean temperature and precipitation sensitivity to CO_2 of the climate model (Lunkeit et al., 2004; Fraedrich et al., 2005a,b) and the resulting surface water fluxes of the land surface eco-hydrological model (Porada et al., 2010): evapotranspiration, total runoff and drainage are shown in figure 5.2.

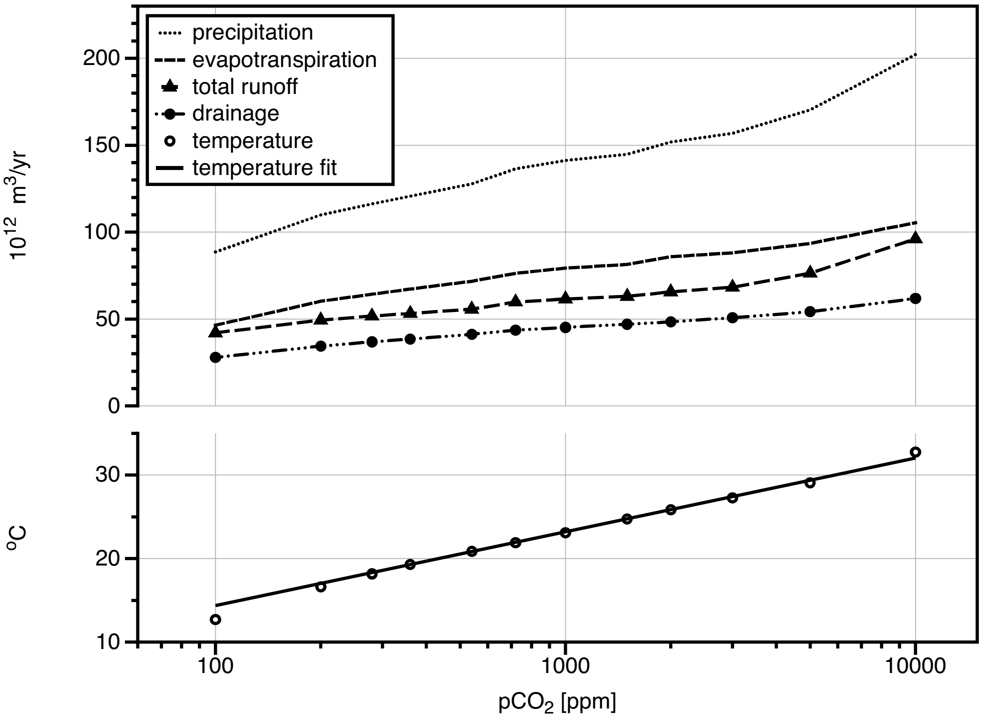

Figure 5.2: Sensitivity of global land precipitation, evapotranspiration, total runoff, drainage and global mean temperature to atmospheric CO_2. Total runoff is the sum of surface runoff and drainage. Global mean temperature is fitted with equation (5.11) (Arens and Kleidon, 2008; Kleidon, 2009).

The relationship between atmospheric CO_2 and global mean temperature can be fitted by the relation (cf. Chapter 2):

$$\Delta T = 3.833 \times ln\left(\frac{pCO_2}{360}\right) \tag{5.11}$$

which is consistent with other climate models (e.g. Oglesby and B. (1990); Kothavala et al. (1999)).

Lithologies and topography

In order to calculate how much Ca is available for chemical weathering, we need a description of the composition of the bedrock. We use a map of lithologies (Amiotte Suchet and Probst, 1995) scaled to 1.125° × 1.125° and the bulk composition for each lithology (table 5.1). The mineralogy has been simplified to consists of a combination of non-weatherable and weatheable minerals, of which a part form secondary minerals when weathered. This is achieved by representing the rock as a combination of quartz, carbonate, pyroxenes and feldspars including Ca containing anorthite, which forms the secondary mineral kaolinite when weathered.

Class	Ca-feldspar	K,Na-feldspar	Pyroxenes	Quartz	Secondary	Carbonate
1 - sandstone	0.01	0.11	-	0.86	0.01	0.01
2 - carbonate	-	-	-	-	-	1.0
3 - shale	0.0005	0.0055	-	0.104	0.8405	0.0495
4 - granite	0.05	0.55	-	0.40	-	-
5 - acid volcanic	0.05	0.55	-	0.40	-	-
6 - basalt	0.25	0.55	0.20	-	-	-

Table 5.1: Characterization of lithologies by mineral weight fractions. After Nockolds (1954).

We assume that local topographic relief (Farr et al., 2007) scales with topographic gradient between grid cells. The topographic relief has been scaled to yield a maximum of 2000 meters consistent with the range in the formulation of physical erosion (eq. 5.8).

5.3 Results

5.3.1 Global patterns of weathering

The global patterns of Ca weathering rates are displayed in figure 5.3. Figure 5.3a shows the Ca fluxes for all lithologies and figure 5.3b for only silicate weathering. Also, the difference in Ca weathering for a doubling of CO_2 is shown (figure 5.3c). This is the steady state scenario, which is not necessarily comparable to present day weathering rates as many areas are not in a steady state, e.g. due to recent glaciations in North America and Scandinavia. It is worth noting that carbonate is most sensitive to a doubling of CO_2 because carbonate is by definition not supply limited in our approach. However, carbonate weathering has no direct impact on the silicate weathering feedback,

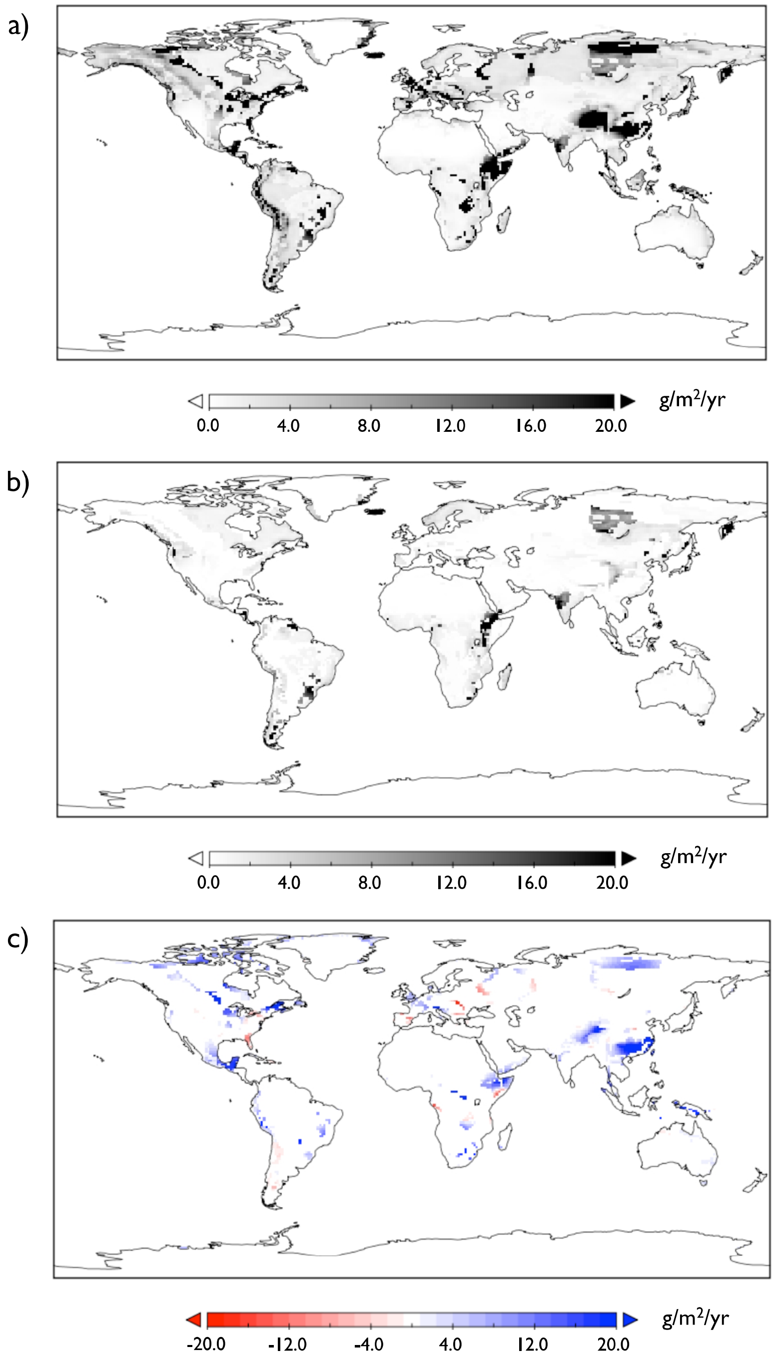

Figure 5.3: a): Total calcium fluxes (maximum Ca flux is 140.7 g/m^2/yr). b): Silicate calcium fluxes (maximum silicate Ca flux is 59.6 g/m^2/yr). c): change in calcium fluxes for doubling of atmospheric CO_2 (360 → 720ppm).

because there is no net consumption of CO_2 in the dissolution of carbonate on land and reformation of carbonate in the oceans. For silicate weathering the large basalt covered igneous provinces exhibit the highest weathering rates, e.g. Iceland, the African Rift Valley and the Deccan and Siberian Traps.

5.3.2 Weathering regimes

Figure 5.4a shows the classification of different regions into the two weathering regimes: eco-hydrological control (black) or supply-limited (grey). The eco-hydrological controlled areas are largely consistent with regions experiencing drought, whereas most of the shields are in the supply-limited weathering regime. Carbonate covered areas are not included in this classification.

Figure 5.4b shows the shifts in weathering regimes for a doubling of CO_2. Most shifts are from eco-hydrological controlled to supply-limited (red), e.g. for the Deccan Traps. However, some areas shift from supply-limited to eco-hydrological controlled (blue). This indicates a decrease in either drainage or biospheric productivity or both for these locations.

Finally, figure 5.4c shows the change in silicate Ca fluxes for a doubling of CO_2. A comparison of figure 5.4c and figure 5.4a reveals that overall, only eco-hydrologically controlled areas are susceptible to the changes in Ca weathering rates for a doubling of CO_2.

5.3.3 Global weathering sensitivity

The model output for global calcium weathering fluxes for the range of atmospheric CO_2 levels is displayed in figure 5.5. The three panels are organized from total Ca flux when only the eco-hydrological limit is considered (figure 5.5a), to Ca flux from silicate weathering alone when only the eco-hydrological limit is considered (figure 5.5b), to Ca flux from silicate weathering when both the eco-hydrological and the supply limit are considered (figure 5.5c). In order to attribute the effect of different forcings on the Ca weathering sensitivity, we ran a series of simulations, in which the isolated effects of precipitation (blue bullets), temperature (red circles) and atmospheric CO_2 (purple triangles) were considered as well as the combined effects (black squares). For each input factor (precipitation, temperature,

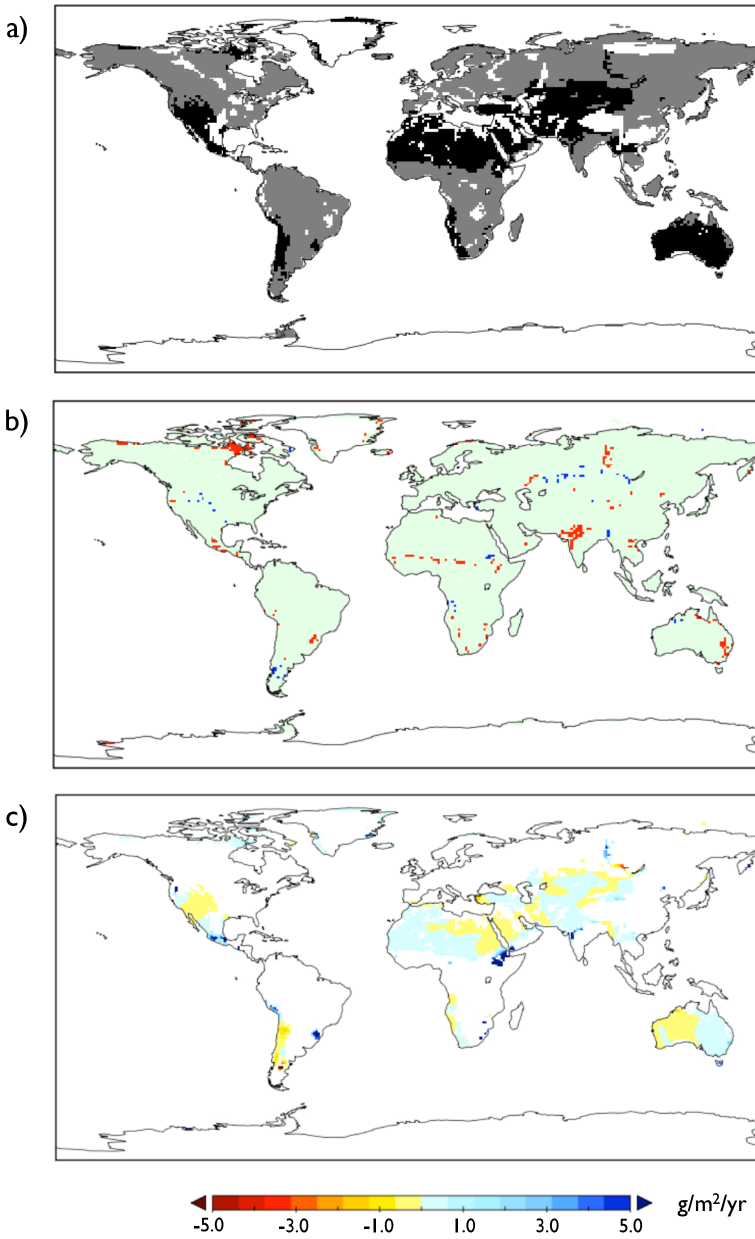

Figure 5.4: a): Weathering regimes for simulation with 360 ppm atmospheric CO_2. Black: eco-hydrological, grey: supply limited, white: carbonate. b): Change in weathering regime with a doubling of atmospheric CO_2 (360 → 720ppm). Red: shift from eco-hydrological control to mineral supply limitation, blue: shift from mineral supply limitation to eco-hydrological control. c): Change i silicate Ca fluxes for a doubling of CO_2 (360 → 720ppm).

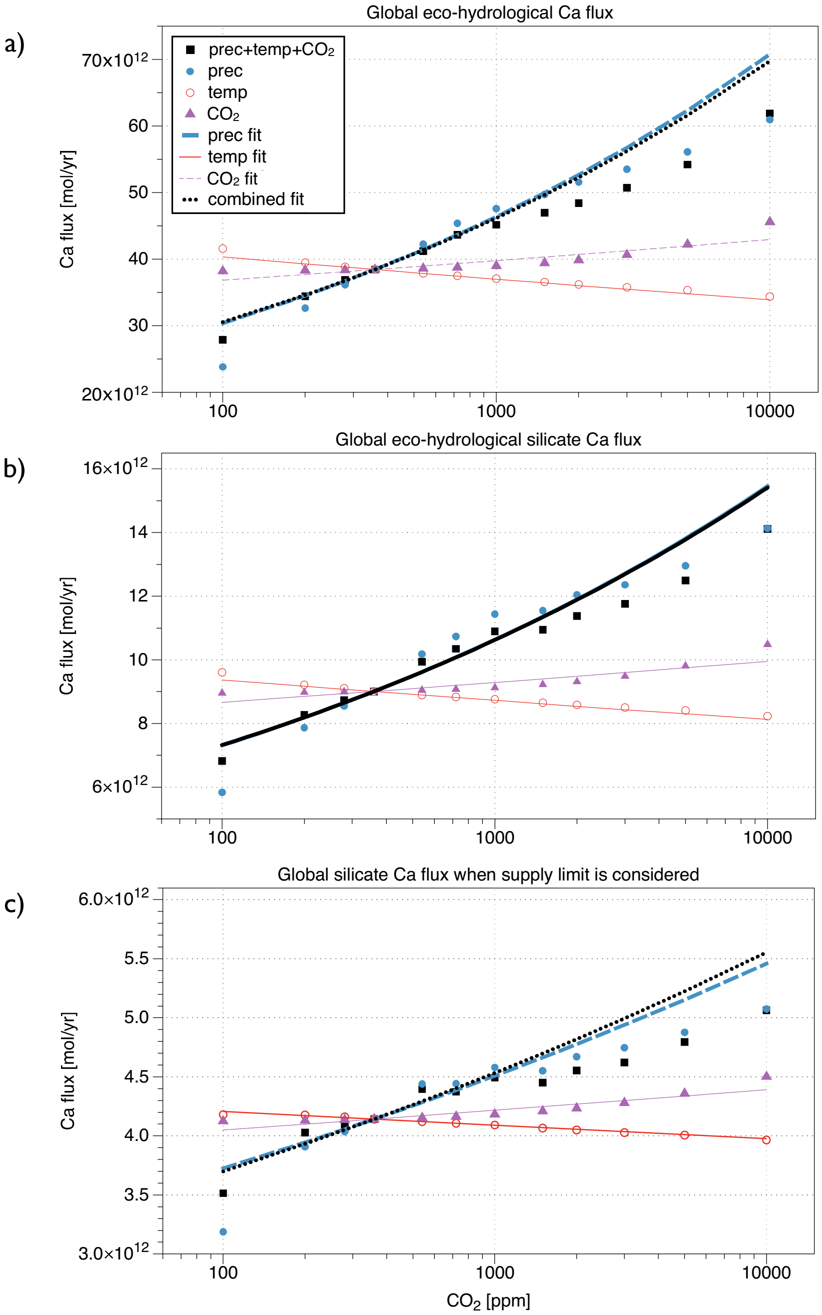

Figure 5.5: Global weathering sensitivity of Ca fluxes (control) for a) eco-hydrological Ca flux, b) eco-hydrological Ca flux resulting from silicate weathering and c) Ca flux from silicate weathering when supply limitation is considered, i.e. the steady state scenario. See text for explanation of line fits and table 5.2 for parameterizations.

simulation	figure	weathering function	r^2
eco-hydrological Ca flux	4.a	$\frac{W}{W_{360}} = \left(\frac{P}{P_{360}}\right)^{0.03} \cdot e^{-0.010 \cdot \Delta T} \cdot e^{0.048 \cdot \Delta T}$	0.81
eco-hydrological silicate Ca flux	4.b	$\frac{W}{W_{360}} = \left(\frac{P}{P_{360}}\right)^{0.03} \cdot e^{-0.008 \cdot \Delta T} \cdot e^{0.042 \cdot \Delta T}$	0.88
silicate Ca flux with supply-limitation	4.c	$\frac{W}{W_{360}} = \left(\frac{P}{P_{360}}\right)^{0.02} \cdot e^{-0.003 \cdot \Delta T} \cdot e^{0.022 \cdot \Delta T}$	0.57

Table 5.2: Parameterizations of silicate weathering fit functions in figure 5.5. The first term is the atmospheric CO_2 sensitivity, the second term is the global mean temperature sensitivity and the third term is the weathering sensitivity to global precipitation on land.

CO_2) a fit was made to the model output corresponding to the form of the Walker et al. (1981) weathering sensitivity parameterization in equation 5.1. These fits are also displayed in figure 5.5, and the parameterizations are listed in table 5.2.

If the eco-hydrological limitation on chemical weathering and transport of weathering products was the only active limitation, the present day Ca flux would be 38×10^{12} [mol/yr] (figure 5.5a). This is roughly 2.5 times higher than estimates of the transport of dissolved Ca in rivers (Livingston, 1963). We expect the calculated global eco-hydrological flux to be higher than observations, because it does not take supply limitation into account. Overall this Ca flux increases with increasing atmospheric CO_2, which supports the idea of a feedback, if CO_2 is consumed as a result of the weathering. The sensitivity analysis of the Ca flux to the climatic forcings reveals that most of the sensitivity in Ca flux is caused by precipitation (table 5.2).

The middle panel of figure 5.5 shows the sensitivity of Ca fluxes from silicate weathering if the eco-hydrological limitation is the only control. The silicate Ca flux is approximately 25% of the total Ca flux in figure 5.5a. Again, there is an increase in the Ca flux with increasing atmospheric CO_2, and most of the sensitivity is attributable to precipitation. The sensitivity of the Ca flux from silicate weathering is similar to that of the total Ca flux (table 5.2). Since silicate weathering leads to a net consumption of CO_2 from the atmosphere, it is this flux that is relevant from a weathering feedback perspective.

The bottom panel of figure 5.5 displays the Ca flux sensitivity to atmospheric CO_2, when supply limitation is also considered. The silicate Ca flux for the close to present day CO_2 levels of 360ppm is 4.14×10^{12} [mol/yr], which is 18.5% of the simulated total Ca flux (22.4×10^{12} [mol/yr], not displayed). This is in agreement with the fraction of Ca originating in silicate weathering estimated in Berner and Berner (1987). Thus when supply limitation is considered, the fraction of the global Ca flux that originates in silicate weathering is decreased. Also, the variation in Ca fluxes is clearly smaller than for the pure eco-hydrological silicate Ca flux, yielding an increase by 6% for a doubling of atmospheric CO_2. The corresponding increase for the eco-hydrological silicate Ca flux is 15%. This indicates that supply limitation decreases the global sensitivity of silicate weathering to atmospheric CO_2. This is also evident in table 5.2 as the sensitivity of each term in the weathering function is decreased. The largest impact is on the precipitation term, which no longer represents most of the overall sensitivity. Note that including supply limitation also greatly affects the quality of the fit as expressed by r^2. This is to be expected because the geographical distribution of topography does not correlate with the climatic variables of the weathering function. The weathering sensitivity does support the existence of a silicate weathering feedback, albeit a weaker one than indicated by the simulations in which we only consider the eco-hydrological limitation.

5.4 Discussion

In the following we will discuss the results of our weathering sensitivity study and what they imply for the silicate weathering feedback. We will focus on the roles of supply limitation and biotic effects on weathering. First, however, we consider a few simplifications and assumptions in our approach, that need further attention.

Climate

As most climate models are built to simulate present day climate, extrapolation to very high or low atmospheric CO_2 should consider potential changes in ice-cover and sea-level. Because of the many feedbacks involved, there is no state-of-the-art method for doing so, and the sensitivity of any climate model to a large range of atmospheric CO_2 should be considered with reservation.

Our climate model input was generated by a model with constant land surface area and glacial cover. This means, that the modeled weathering sensitivities are also only valid for a scenario with constant land surface area. As our range of CO_2 levels span 100 to 10000 ppm, it is unlikely that land surface area should be constant. Atmospheric CO_2 has a significant impact on the radiation balance of the atmosphere, especially in polar regions, where ice sheets exist. For both low and high atmospheric CO_2 levels the extent of the polar ice sheets is not going to be the same as is presently observed. Higher CO_2 levels would lead to the exposure of land areas presently covered by ice, and these areas would be subjected to chemical weathering. This would lead to an increase in global weathering rates with increasing CO_2 levels. Conversely, as a larger fraction of the ice sheet melts at higher CO_2 levels, sea levels would increase, leading to the submergence of coastal areas in the ocean. This decrease in land area, would lead to a decrease in global chemical weathering rates on land. Which of these effects is larger depends on the area of the exposed/submerged land and on the topography and lithology of the affected areas.

Another effect of keeping the land area and ice sheets constant, is in the climate model itself. As the large scale circulation of the atmosphere is driven by differences in the radiation balance and temperature between the Equator and the poles, keeping the poles artificially cold, through the influence of the constant ice sheets on the polar radiation balance, influences global atmospheric circulation and the capacity of the atmosphere to transport water.

The overall sensitivity of the model is adequate for our purposes. A doubling of atmospheric CO_2 leads to a global mean temperature increase of 2.7°C, which is close to the 'most likely value of about 3°C' of the IPCC (2007). A more complex climate model, with a stronger or weaker sensitivity to atmospheric CO_2, should not change the overall conclusion concerning the impact of supply limitation on the silicate weathering feedback.

Supply limitation

Our formulation of supply limitation is based on a simple function of physical erosion, which depends only on topographic relief. However, physical erosion also depends on precipitation, as runoff is largely responsible for the lateral transport of solid material on the surface of the Earth. This coupling between climate and erosion could potentially weaken the effect of supply limitation on the global silicate weathering feedback, as increased precipitation would lead to increased erosion, a decrease in regolith depth and thus increased exposure of weatherable minerals from the bedrock. However, the basic principle that erosion can set an upper limit to chemical weathering is supported by global observations (West et al., 2005). Conversely, a decoupling between chemical weathering and physical erosion is observed for very high physical erosion rates (Dixon and Von Blanckenburg, 2011) of tectonic active mountainous regions. This suggests that weathering in these areas are not controlled by supply limitation, but rather by climate. Overall, our approach captures these global features by considering and comparing the limitations set by climate and tectonic features separately.

Biotic effects

There has been a large number of studies concerning biotic enhancement of weathering, e.g. Knoll and James (1987); Schwartzman and Volk (1989); Berner (1992); Taylor et al. (2009). When biotic effects are included in a model it is important to consider at what time scales these effects will be important, and if the impacts are transient in nature. As the silicate weathering feedback is based on a steady state premise, transient effects should only be considered to the extent where they can be maintained on long time scales, for instance through continued disturbance (Balogh-Brunstad et al., 2008). Also, not all processes are representative of most surface areas. One example is lichen weathering, which occurs directly on primary rock and therefore depends on the surface area of rock exposure.

Here, the inclusion of biotic effects has been simplified to only contain effects on soil/regolith CO_2. Cycling of Ca (and other nutrients) has not been included. Our approach specifically considers the steady state chemical and physical limitations and boundary conditions for a regolith box, which renders internal cycling beyond the scope of this study. However, leaching of nutrients by surface runoff and erosion of organic matter should be considered in process oriented models of chemical weathering. Although we do not consider biotic effects in great detail, we do consider biotic effects associated with CO_2. We should therefore be able to capture the overall dynamics of biotic effects, because we focus on the sensitivity of chemical weathering to CO_2.

5.4.1 Implications for the silicate weathering feedback

The weathering functions of table 5.2 have the same form as the Walker et al. (1981) parameterization of eq. (5.1), which makes them comparable. In our model most of the sensitivity of silicate chemical weathering is attributable to the change in precipitation, whereas Walker et al. (1981) ascribed most of the silicate weathering sensitivity to CO_2 and temperature. This is because the terms are derived from different assumptions. The temperature dependence as formulated by Walker et al. (1981) (eq. 5.1) is derived from dissolution kinetics under far-from-equilibrium laboratory conditions and therefore positive, whereas our representation of the temperature dependence is based on saturated states and therefore negative. As a clear temperature dependence has been difficult to establish in the field (Kump et al., 2000; Hartmann et al., 2010), we cannot say to which degree natural regolith solutions are controlled by dissolution kinetics or saturated states. Most likely they are a combination of the two. The dependence on atmospheric CO_2 is considerably weaker in our model than the Walker et al. (1981) formulation. This is because chemical weathering rates are only sensitive to CO_2 in areas under eco-hydrological control, and because of biotic effects on the concentration of CO_2 in the regolith. The role of biotic effects will be explained in more detail in section 5.4.1. The precipitation term in our approach and the runoff term in eq. (5.1) (Walker et al., 1981) have both been derived from global climate models. Considering supply limitation in our model brings the hydrological contribution to the weathering sensitivity close to the rather conservative estimate of Walker et al. (1981). In the following section we will elaborate on the role of supply limitation.

Supply limitation

That tectonic uplift should have an impact on the silicate weathering feedback through the impact on physical erosion and mineral supply has been a fundamental theory of the geological carbon cycle since the work of Raymo et al. (1988). This has led to the inclusion of parameters and parameterizations for the role of uplift and erosion in models of the geological carbon cycle (e.g. Berner (1994); Wallmann (2001)). These parameterizations are based on a factorial approach in which each driving factor is parameterized separately, often by a constant for each point in time, and then multiplied to give an overall weathering feedback function. The choice of the constant is most often based on limited and highly uncertain proxies, as previously pointed out by Boucot and Gray (2001), and the model setup leaves little room for the consideration of interactions between processes. Overall this makes models of the geological carbon cycle highly speculative.

Supply limitation has previously been considered in global models of chemical weathering (West et al., 2005; Hilley and Porder, 2008; Taylor et al., 2012). In West et al. (2005) and Taylor et al. (2012) supply limitation was considered through a normalized correction term, which described the deviation from a mean physical erosion rate. This approach is good in capturing variability in weathering rates based on empirical observations. In Hilley and Porder (2008) an empirical function of physical erosion was used to calculate mineral supply rate and residence time in the regolith/weathering zone. These terms were then implemented in a standard empirical kinetic function depending on mineral surface area and reaction time. Our approach differs from these previous models by considering supply limitation through a limitation comparison or minimization process (eq. 5.10). Instead of prescribing a factorial global weathering function, in which each term is derived separately from empirical data, the global parameterization emerges from a sensitivity study of the model. Supply limitation is not represented by a separate term in the weathering function (table 5.2). Instead we observe that the strength of the sensitivity of each term corresponding to one of the drivers: atmospheric CO_2, temperature and precipitation, is weakened by supply limitation. Also, the quality of the fit is greatly diminished with r^2 decreasing from 0.88 to 0.57 (table 5.2). This suggests that the type of function chosen for the global weathering sensitivity is not able to capture limitations and thresholds associated with supply limitation.

The weakening of the impact of each separate driver of weathering suggests that supply limitation cannot simply be added as an additional term to a global formulation of weathering. This is further substantiated by the change in the fraction of Ca flux from supply limited areas with increasing atmospheric CO_2 shown in figure 5.6a. As atmospheric CO_2 increases a larger part of the Ca flux comes from areas that are in the supply limited weathering regime. This indicates that the potential for further increase in weathering rates decrease as CO_2 levels increase, and that a global function for supply limitation must depend on atmospheric CO_2 as well as tectonic activity.

Biotic enhancement of weathering

There are many ways in which vegetation and microorganisms may have an impact on or control chemical weathering rates. These include but are not limited to: the addition of reactive species, such as H^+ and organic acids to the soil solution; impacts on soil CO_2 through respiration; removal of dissolved species though root water uptake; effects on precipitation on regional scales; and stabilization of soils and regolith by roots. For a thorough review see Taylor et al. (2009).

We implemented biotic enhancement of weathering in terms of the indirect effect of the biosphere on soil CO_2. The biospheric effect tends to decrease with increasing atmospheric CO_2 levels, shown in figure 5.6b. This is inconsistent with previous formulations (e.g. Berner and Kothavala (2001)), in which biotic enhancement of weathering often increases with increasing

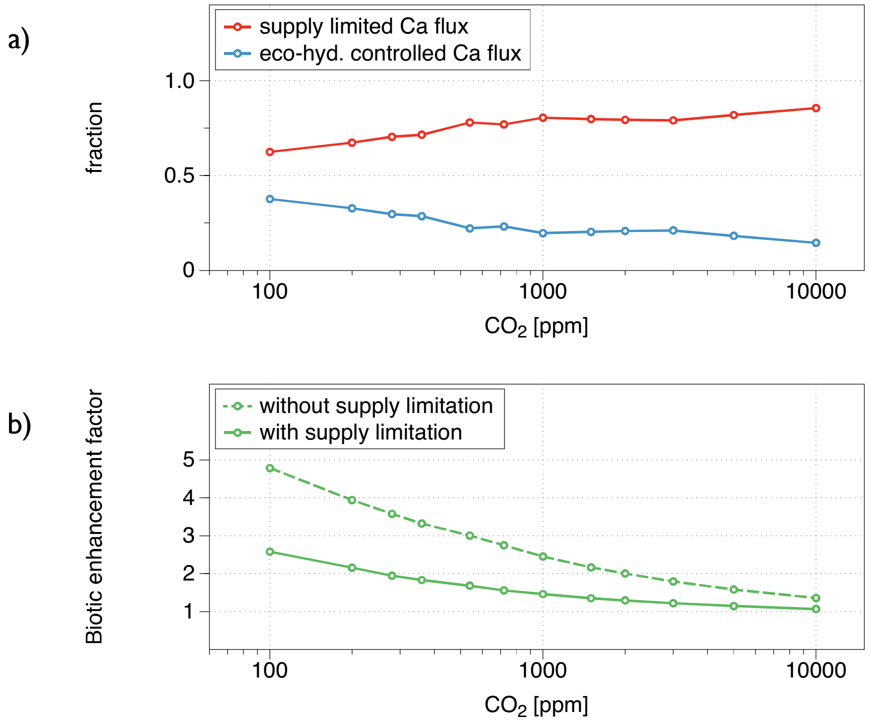

Figure 5.6: a) Fraction of total silicate Ca flux from eco-hydrological controlled areas (blue) and supply-limited areas (red). As the atmospheric CO_2 level increases, the fraction of the silicate Ca flux that comes from supply-limited areas increases as well. b) Biotic enhancement of silicate weathering (solid line). Silicate Ca fluxes of the control was divided by silicate Ca fluxes from a set of simulations where the biosphere does not affect regolith CO_2. Also shown is the biotic enhancement of the eco-hydrological silicate Ca flux, i.e. when supply limitation is not included (stapled line).

atmospheric CO_2. These formulations assume that biotic enhancement of weathering increases with an increase in biospheric productivity through fertilization effects associated with increasing CO_2 levels. There are two reasons why this is not the case in our approach. First of all, our vegetation model does not consider fertilization effects on biospheric productivity and the biotic effect is solely expressed in terms of the somewhat passive impact on soil CO_2, which affects the saturation state of Ca^{2+} in the soil solution and thus potential Ca weathering rates. As atmospheric CO_2 levels increase, the difference between soil CO_2 levels and atmospheric CO_2 levels decreases, and the biotic effect thus becomes smaller. Also, as atmospheric CO_2 levels increase, a larger part of the weathering flux comes from areas in which weathering is limited by mineral supply (figure 5.6a). Since Ca fluxes increase with increasing CO_2 this means that the area of the land surface that is in the supply limited regime must increase as well. This decreases the potential for biotic enhancement of weathering at the global scale (illustrated by the difference in biotic enhancement with and without supply limitation, figure 5.6b), because only areas in which weathering is not supply limited are sensitive to this biotic effect. In itself, biotic enhancement of weathering may lead to mineral supply limitation as was previously shown in Chapter 4 (published as Arens and Kleidon 2011). As mineral supply limitation can lead to a shift in biospheric functioning, and a focus on biotic investment in recycling of nutrients (Chadwick et al., 1999), supply limitation may be something the biosphere cannot overcome, leading to decreasing biospheric productivity over time (Wardle et al., 2004). Thus, even if other effects of biotic enhancement of weathering were included, such as selective weathering of minerals containing important nutrients, or effects associated with biospheric impacts on the hydrological cycle, it is not safe to assume that biotic enhancement of weathering should increase with increasing CO_2 levels. In order to further elucidate if supply limitation can lead to a decrease in biotic enhancement with increasing atmospheric CO_2 levels, we test three additional scenarios. The sensitivity of biotic enhancement of weathering to atmospheric CO_2 for these scenarios is illustrated in figure 5.7. In the first scenario we assume constant biotic enhancement by multiplying the eco-hydrological Ca fluxes of the simulation where the biosphere does not affect soil CO_2 with a biotic enhancement factor of 3.3. This corresponds to the biotic enhancement at 360ppm for the eco-hydrological Ca flux of the control run. In the second scenario we implement a fertilization effect on the control simulation as it is formulated in the GEOCARB model (Berner, 1991, 1994; Berner and Kothavala, 2001):

$$f_B(CO_2) = \frac{2 \cdot RCO_2}{1 + RCO_2} \tag{5.12}$$

Here, the CO_2 concentration of the atmosphere $[CO_2]$ is considered by RCO_2

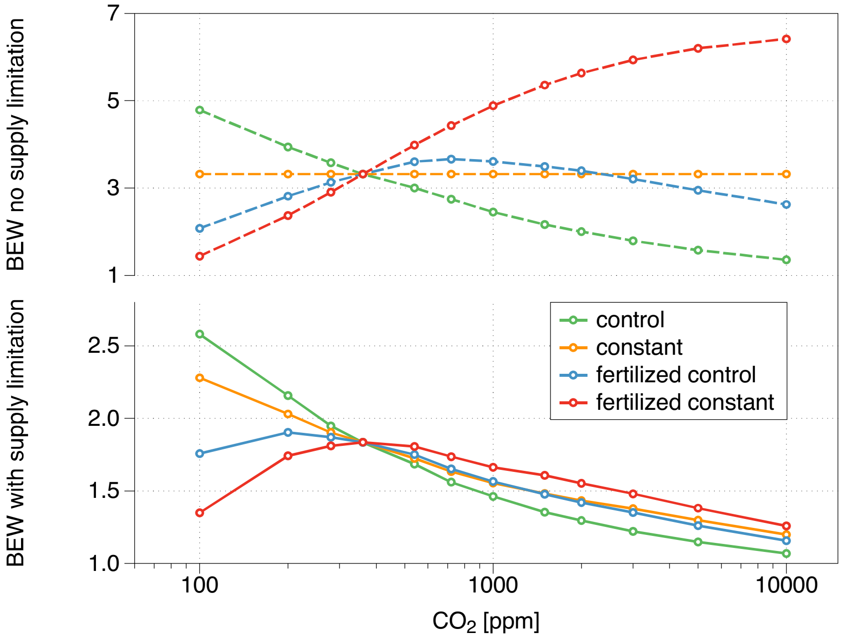

Figure 5.7: Biotic enhancement of silicate weathering (BEW) for four scenarios. The top panel shows the biotic enhancement of the global eco-hydrological Ca flux, i.e. what the Ca flux would be without supply limitation. The bottom panel shows the biotic enhancement of weathering when supply limitation is considered. The four scenarios are: 1) The control simulation (green), 2) constant biotic enhancement of eco-hydrological Ca fluxes by a factor 3.3 (yellow), 3) biotic enhancement through an additional CO_2 fertilization effect on the control simulation (blue), 4) biotic enhancement through an additional CO_2 fertilization effect on the constant BEW scenario (red). Supply limitation leads to decreasing biotic enhancement of weathering with increasing CO_2 above 360ppm in all four scenarios.

which is $[CO_2]/360$ppm, thus for $[CO_2] = 360$ppm, $RCO_2 = 1$ and the fertilization feedback becomes $f_B(CO_2) = 1$. We multiply this effect with the eco-hydrological Ca fluxes of the control run, i.e. what the Ca fluxes would be without supply limitation. We thereby assume that all plants respond to fertilization effects. This means that for preindustrial $[CO_2]$ of 360 ppm, weathering rates remain unchanged, for lower CO_2 levels weathering rates decrease and for higher CO_2 levels, weathering rates increase compared to the control run. Thus the silicate weathering feedback is potentially strengthened by the fertilization feedback function f_B. In the third scenario we multiply the fertilization feedback function f_B with the constant biotic enhancement eco-hydrological Ca flux in order to get a scenario in which biotic enhancement of weathering increases with increasing atmospheric CO_2 when supply limitation is not considered. The biotic enhancement of the eco-hydological fluxes for the three scenarios plus the control simulation is shown in the top panel of figure 5.7. We finally implement supply limitation in the three scenarios by applying eq. (5.10). The resulting biotic enhancement is depicted in the bottom panel of figure 5.7 along with the biotic enhancement of the control simulation.

From our results in figure 5.7 it is evident that supply limitation has a significant impact on the extent to which the biosphere can increase chemical weathering. Even in the scenario where the biotic enhancement of the eco-hydrological Ca flux increases with increasing CO_2, supply limitation leads to an overall decrease in biotic enhancement of weathering with increasing CO_2. In this context it is worth noting that our definition of physical erosion and thus supply limitation only depends on topographic relief and not on climate. A direct dependence of physical erosion on climate would lead to a different sensitivity of biotic enhancement of weathering to atmospheric CO_2, but that mineral supply limitation should affect biotic enhancement seems inevitable.

5.5 Conclusion

We investigated the role of supply limitation in the silicate weathering feedback. To do so we modeled chemical weathering as a co-limited process, and used spatially explicit representation on limits to map regions of supply limitation. We then analyzed the resulting global weathering fluxes to deduce a global silicate weathering function. Our approach illustrates the impact of mineral supply limitation on the silicate weathering sensitivity. Not only does mineral supply limitation weaken the silicate weathering feedback, it also defines the geographical areas that contribute most strongly to the silicate weathering feedback. These areas are not a fixed proportion of continental land areas, but may be different for even small differences in atmospheric

CO_2. Thus global mineral supply limitation is not a simple function independent of atmospheric CO_2. We have shown that mineral supply limitation has an increasing effect on silicate weathering fluxes with increasing atmospheric CO_2, leading to a weakening of the silicate weathering feedback.

A similar observation is made for the role of biospheric enhancement of weathering. At higher concentrations of CO_2 in the atmosphere biotic enhancement, as it is expressed here, plays a smaller role, because the difference to a non-biotic state becomes smaller. As weathering rates become increasingly limited by mineral supply, the potential for biotic enhancement of weathering decreases as well. This indicates that biotic enhancement of weathering is probably not a simple increasing function with CO_2. Even if we assume increasing biotic enhancement with increasing atmospheric CO_2, the impact of a finite mineral supply is to counteract and even reverse this sensitivity.

Our model study indicates that mineral supply limitation has a dampening effect on the response of chemical weathering rates to climatic and biotic drivers. As continents changed positions in the past and the biosphere evolved, a finite mineral supply played a significant but variable role in shaping the response of silicate weathering rates to excursions in atmospheric CO_2 and climate. By considering chemical weathering as a co-limited process, we have illustrated that the silicate weathering feedback function is unlikely a simple factorial expression of the drivers and limitations involved in shaping global silicate weathering rates. Thus process limitations and interactions would need to be considered more explicitly in future models of silicate weathering and the geological carbon cycle.

6 Conclusion and Outlook

This study focusses on the role of physical transport mechanisms in controlling chemical weathering rates at the global scale. We have investigated this issue with global spatially-explicit models, including a climate model, an integrated vegetation and soil hydrology model and a new model of the regolith. We have examined how limitations associated with the physical transport of water, carbon and minerals affect chemical weathering rates and the potential for biotic enhancement of weathering. Finally, we have analyzed the implications mineral supply limitation has for the silicate weathering feedback and evaluated the common approach for the application of empirical laws in global models of the carbon cycle. In the following the main results of this study are summarized followed by an outlook on directions for future research. The summary is formulated in the framework of the research questions posed in the introduction.

6.1 Summary

1. How does transport limitation of dissolved compounds shape the response of global chemical weathering rates to atmospheric CO_2?

Chemical weathering rates are reflected in the concentration of dissolved load in rivers, which integrate chemical weathering rates over the whole catchment. Concentrations of Ca^{2+} and HCO_3^- of many rivers are close to saturation of $CaCO_3$ at atmospheric CO_2 levels and the world average is only slightly below (Holland, 1978). This suggests that the transport limitation associated with runoff is a dominant effect on large scales. We have therefore calculated the capacity of runoff/rivers to transport Ca^{2+} to the oceans, when assuming saturation of $CaCO_3$ at atmospheric CO_2 levels (Chapter 2). The sensitivity of this transport capacity to atmospheric CO_2 is a result of the combined effects of CO_2, temperature and precipitation on runoff and the concentration of Ca^{2+} at saturation ($[Ca^{2+}]_{sat}$). We are therefore able to express this sensitivity in terms that are comparable to the silicate weathering sensitivity of Walker et al. (1981) and make a direct comparison. We find that the transport capacity of rivers supports the existence of a negative feedback for silicate weathering due to the responses of runoff and $[\mathrm{Ca}^{2+}]_{sat}$ to atmospheric CO_2 (equation 2.7). However, the warmer temperatures of high CO_2 climates reduces the potential strength of the feedback, because $[\mathrm{Ca}^{2+}]_{sat}$ decreases with temperature. We thus get a combined sensitivity that is weaker than that of Walker et al. (1981) (equation 2.8). Because we only consider saturated states, the obtained relationship should serve as an upper limit of the global dissolved Ca^{2+} flux into the oceans. As the sensitivity of this upper limit to atmospheric CO_2 is weaker than the kinetic feedback of Walker et al. (1981), this indicates that there is a risk of overestimating the the strength of the silicate weathering feedback if it is considered dominantly kinetic. That transport limitation of dissolved load is a dominant effect on chemical weathering rates is further substantiated by our model output of river concentrations of $[\mathrm{Ca}^{2+}]$ and $[\mathrm{HCO}_3^-]$ in Chapter 3 (figure 3.10), in which we do not consider kinetic effects. Finally, when we add the biotic impact on soil CO_2 as reflected in the parameterizations of eco-hydrological Ca fluxes in table 5.2, the weathering sensitivity to atmospheric CO_2 is decreased. The overall dominant effect on the weathering feedback thus becomes the precipitation/runoff. This happens because biotic activity increases soil CO_2, whereby the differences in soil CO_2 and thus chemical weathering between climatic states are decreased. Biotic processes potentially enhances chemical weathering rates, whereby the soil/regolith solution is brought closer to saturation. This could lead to a similar weakening of the kinetic feedback, as kinetic limitations are replaced by transport limitations, when saturation is reached.

2. Can global spatial variability of chemical weathering be modeled by considering only transport limitation of liquid and solid phases?

The modeled concentrations of Ca^{2+} and HCO_3^- of rivers in Chapter 3 (figure 3.10) suggests that we are able to capture overall spatial variability of chemical weathering of minerals containing calcium on a regional scale by considering only transport limitations. The model specifically considers the limitations associated with the physical transport of water, carbon and minerals in regoliths through calculations of the water balance and potential erosion. Biotic effects are considered through the dependence of chemical weathering on the carbon balance of the regolith. The model captures variability in weathering rates and CO_2 consumption across climatic and tectonic gradients, and by considering the timing of Holocene glaciations also captures latitudinal variations. This variability in the physical drivers of weathering is reflected in observed spatial variability of Ca^{2+} and HCO_3^- concentrations in rivers (figure 3.10). Rivers draining old soils/regoliths of flatland terrains yield lower Ca fluxes compared to rivers draining the younger soils/regoliths of mountainous areas (figure 3.9). A sensitivity study of the response of the regolith model to variation in essential parameters establishes the physical transport/erosion of secondary minerals as an important control, specifically for areas where weathering is limited by mineral supply. Conversely, the physical transport of dissolved elements by regolith drainage and runoff is an important control in areas, where weathering is not limited by mineral supply.

3. What effect does mineral supply limitation have on the potential for biotic enhancement of weathering at the global scale?

Biotic enhancement of weathering can only occur where there is a potential for further weathering. This means that areas that are already limited by mineral supply are not susceptible to further biotic enhancement, unless mineral supply is directly affected by biotic effects. As mineral supply is controlled by physical erosion, topographic gradients and thus tectonic uplift has a direct impact on mineral supply. From this we can infer that the potential for biotic enhancement of weathering ultimately must have a strong connection to tectonic uplift. In Chapter 4 we have produced a global map of the two contrasting weathering regimes: supply limited weathering and eco-hydrologically controlled weathering (figure 4.2). In the latter, biotic enhancement of weathering is possible. However, biotic processes may only enhance weathering as far as mineral supply permits. Thus biotic enhancement of weathering may shift the weathering regime from eco-hydrologically controlled weathering to supply limited weathering.

4. How does mineral supply limitation affect the global sensitivity of silicate weathering rates to atmospheric CO_2 and climate?

Mineral supply limitation has a dampening effect on sensitivity of silicate chemical weathering to atmospheric CO_2. By considering chemical weathering as a co-limited process, both potentials for physical transport (of dissolved and solid weathering products) play important roles in defining modeled steady states (Chapter 5). Thus not only the purely climatic effects on the dissolved fluxes shape the response of chemical weathering rates to changes in atmospheric CO_2. Areas that are limited by the physical transport of solid weathering products, and thus by mineral supply, do not contribute to the silicate weathering feedback, except to the extent to which physical erosion is directly affected by climate. To consider the climatic effects on physical erosion would require a more process based approach to modeling solid transports. Nevertheless, we may conclude that supply limited areas are not a fixed proportion of continental land areas, but may be different for even small differences in atmospheric CO_2, as the limitations associated with the physical transports shift the balance towards or away from supply limitation. This feature is reflected in the increase in the fraction of the global Ca^{2+} flux that comes from supply limited areas with increasing CO_2 (figure 5.6). Essentially this means that a smaller and smaller fraction of the land surface contributes to the silicate weathering feedback as atmospheric CO_2 levels increase. Thus supply limitation may inhibit the response of chemical weathering rates to any climate related driver, be that atmospheric CO_2, precipitation or temperature.

5. How does mineral supply limitation affect the global sensitivity of biotic enhancement of weathering to atmospheric CO_2?

Biotic enhancement of weathering as formulated in this study primarily works through the impact on soil/regolith CO_2 and the concentrations of Ca^{2+} and HCO_3^- at saturation. Thereby increased biotic productivity leads to increased $[Ca^{2+}]$ and $[HCO_3^-]$. In Chapter 5, we showed that the global biotic enhancement factor by this formulation of biotic impacts on chemical weathering rates depends on atmospheric CO_2 levels (figure 5.6). At higher levels of atmospheric CO_2, the biotic enhancement factor decreases. There are two reasons for this. First, the difference between soil CO_2 levels and atmospheric CO_2 levels decreases as atmospheric CO_2 levels increase. Second, as weathering rates increase with increasing CO_2 a larger and larger proportion of the weathering flux comes from areas that are limited by mineral supply and thus not susceptible to biotic enhancement of weathering. Even in a scenario where biotic enhancement of eco-hydrological Ca fluxes increases with increasing atmospheric CO_2 levels because of a fertilization effect (figure 5.7), the impact of mineral supply limitation is an overall decrease in biotic enhancement of weathering with increasing CO_2. The decrease in biotic enhancement of weathering at higher CO_2 levels is thus directly linked to the transport limitations associated with a finite mineral supply. This conclusion is in contrast to previous assumptions regarding the sensitivity of biotic enhancement of weathering to atmospheric CO_2 (e.g. Berner (1994); Berner and Kothavala (2001)) and is a direct result of using an approach that disseminates the combined impact of simultaneous adverse effects.

6. Can a spatially explicit model of silicate weathering be simplified into a factorial law applicable in a box model of the geological carbon cycle?

In principle it is possible to represent the behavior of a more complex process-based model with factorial laws, as was done in Chapter 5. However, as the complexity of the model increases and other non-climatic drivers are included, choosing the right form of the function becomes more challenging. A purely climatic function as used in Walker et al. (1981) and in Chapter 5, will become less appropriate as other drivers are included. This is reflected in the ability of the function to fit the output of the model, a feature that was clearly observed in our analysis with the inclusion of supply limitation, which led to a decrease in r^2 from 0.88 to 0.57. Thus adding another limitation of weathering weakens the impact of other drivers. From the viewpoint of co-limitation, the impact of each driver of chemical weathering cannot easily be represented by a factor, because one factor may potentially increase chemical weathering rates but will have no impact due to limitations associated with other factors. Thus a change in one driver will change the conditions and might lessen the impact of the other drivers. Furthermore, if important controls of weathering are left out, we risk overestimating the sensitivity of chemical weathering to atmospheric CO_2, because we do not consider the limitations associated with these unknown controls. In order to find the overall sensitivity of chemical weathering to atmospheric CO_2 an integrative approach that considers all drivers simultaneously is needed. This can only be achieved with process based models.

6.2 Outlook

The work presented in this thesis has focussed on the potential global scale impact of local limitations on chemical weathering rates. However, because of the large gap in resolution between local catchment scale models and global models, there is a need to better understand how local limitations in general may be scaled up to the global level. It would therefore be worthwhile to look more closely at how local limitations shape the potential for a silicate weathering feedback locally and regionally. In order to enhance our understanding of the weathering dynamics of catchments of various sizes, I suggest the following three research projects, which all build on the regolith models developed in this study:

(1) A process-based model of erosion coupled with our dynamic regolith model to assess the role of variable erosion and associated limitations on a catchment scale. By coupling the process based erosion model with our view of limitations on weathering associated with physical transport, we should be better able to understand where in the catchment there is a potential for a silicate weathering feedback.

(2) An analysis of the role of kinetic limitations on a catchment scale. This requires an expansion of our model to include kinetic limitations. Also, a more advanced hydrological model that considers the route and residence time of water in soils and regoliths is needed.

(3) An investigation of the influence of biotic recycling of nutrients on the chemical weathering budget and chemical weathering rates. It has previously been shown that biotic enhancement of weathering might not be detectable in steady state (Balogh-Brunstad et al., 2008), and that disturbance is im-

portant, e.g. fires, harvests and landslides. Therefore, this analysis should also include an investigation of how stochastic variability of disturbances may influence chemical weathering rates on long time scales.

Furthermore, as a global scale study:

(4) A test of the impacts of interactions between climate and tectonic uplift on chemical weathering. This can be done by including feedbacks on topography in the regolith model and coupling it to a climate model. The role of crustal uplift in the silicate weathering feedback and geological carbon cycle, i.e. the Raymo Hypothesis (Raymo et al., 1988), can thereby be evaluated.

Ultimately, these suggested studies are steps towards an extensive model, which could be used to investigate couplings between drivers of weathering. An example is the coupling between kinetic limitations and biotic processes. Whether or not weathering is transport limited by runoff depends on whether or not the soil/regolith solution reaches saturation. This may depend on biotic effects, because biotic processes potentially enhances chemical weathering rates, whereby the soil/regolith solution is brought closer to saturation. Thus by considering saturated states we could inherently be considering biotic effects that are efficient up to this transport limit. This indicates that biotic enhancement of weathering is likely connected to kinetic limitations, as it is in kinetically limited weathering regimes that biotic effects may have the largest impact. Therefore kinetic limitations should be considered in a comprehensive model of biotic enhancement of weathering.

Another example is the coupling between erosion and biotic processes. We have already shown in Chapter 4 that mineral supply and thus erosion affects the potential for biotic enhancement of weathering. Vegetation most likely decreases physical erosion, due to the stabilizing effect of root systems on the regolith. This would also lead to a corresponding decrease in chemical weathering rates in steady state, unless other biotic processes are able to reverse the effect. However, if erosion is decreased because of biotic processes, this could lead to a change in topography, which again would affect erosion rates. Dietrich and Perron (2006) suggests that life sets a signature on topography, which is difficult to detect and requires mechanistic modeling that specifically includes biotic effects on erosion. With the suggested extensions to our model, it could be used as a first step towards answering the question of how life may influence not just chemical weathering rates, but also entire landscapes.

Bibliography

Ahnert, F. (1977). Some comments on the quantitative formulation of geomorphological processes in a theoretical model. *Earth Surface Processes*, 2:191–201.

Amiotte Suchet, P. and Probst, J.-L. (1995). A global 1 degree by 1 degree distribution of atmospheric/soil co_2 consumption by continental weathering and of riverine HCO_3 yield. Technical report, Centre National de la Recherche Scientifique, Center de Geochemie de la Surface, Strasbourg Cedex, France.

Anderson, G. (2005). *Thermodynamics of Natural Systems.* Cambridge University Press.

Arens, S. and Kleidon, A. (2008). Global sensitivity of weathering rates to atmospheric CO_2 under the assumption of saturated river discharge. *Mineralogical Magazine*, 72:305–308.

Arens, S. and Kleidon, A. (2011). Eco-hydrological versus supply-limited weathering regimes and the potential for biotic enhancement of weathering at the global scale. *Applied Geochemistry*, 26:S274–S278.

Balogh-Brunstad, Z., Keller, C., Bormann, B., O'Brien, R., Wang, D., and Hawley, G. (2008). Chemical weathering and chemical denudation dynamics through eosystem development and disturbance. *Global Biogeochemical Cycles*, 22.

Berner, E. and Berner, R. (1987). *The Global Water Cycle.* Prentice Hall, Englewood Cliffs, New Jersey.

Berner, R. (1991). A model for atmospheric CO_2 over phanerozoic time. *Amer. J. Sci.*, 291:339–376.

Berner, R. (1992). Weathering, plants, and the long-term carbon cycle. *Geochim. Cosmochim. Acta*, 56:1099–1102.

Berner, R. (1994). GEOCARB II: A revised model of atmospheric CO_2 over phanerozoic time. *Amer. J. Sci.*, 294:56–91.

Berner, R. (1999). A New Look at the Long-term Carbon Cycle. *GSA Today*, 9:1–6.

Berner, R. and Caldeira, K. (1997). The need for mass balance and feedback in the geochemical carbon cycle. *Geology*, 24:955–956.

Berner, R. and Kothavala, Z. (2001). Geocarb iii: A revised model of atmospheric co_2 over phanerozoic time. *Amer. J. Sci.*, 301:182–204.

Bluth, G. and Kump, L. (1994). Lithologic and climatologic controls of river chemistry. *Geochimica et Cosmochimica Acta*, 58:2341–2359.

Boucot, A. and Gray, J. (2001). A critique of phanerozoic climate models involving changes in the CO_2 content of the atmosphere. *Earth-Science Reviews*, 56:1–159.

Brantley, S. (1992). Kinetics of dissolution and precipitation - experimental and field results. In *Water-Rock Interaction*. Park City.

Carson, M. and Kirkby, M. (1972). *Hillslope Form and Process*. Cambridge University Press.

Chadwick, O., Derry, L., Vitousek, P., Huebert, B., and Hedin, L. (1999). Changing sources of nutrients during four million years of ecosystem development. *Nature*, 397:491–497.

Dietrich, W. and Perron, T. (2006). The search for a topographic signature of life. *Nature*, 439:411–418.

Dixon, J. and Von Blanckenburg, F. (2011). Speed limits to soil weathering and CO_2 withdrawal. *Mineralogical Magazine*, 75:767.

Donnadieu, Y., Godderis, Y., Pierrehumbert, R., Dromart, G., Fluteau, F., and Jacob, R. (2006). A GEOCLIM simulation of climatic and biogeochemical consequences of Pangea breakup. *Geochemistry Geophysics Geosystems*, 7(11).

Drever, J. (1994). The effect of land plants on weathering rates of silicate minerals. *Geochimica et Cosmochimica Acta*, 58:2325–2332.

Ebelmen, J. (1845). Sur les produits de la decomposition des especes minerales de la famille des silicates. *Annales des Mines*, 7:3–66.

Edmond, J. and Huh, Y. (2003). Non-steady state carbonate recycling and implications for the evolution of atmospheric PCO_2. *Earth and Planetary Science Letters*, 216:125–139.

Fang, C. and Moncrieff, J. (1999). A model for soil CO_2 production and transport 1: Model development. *Agricultural and Forest Meteorology*, 95:225–236.

Farr, T., Rosen, P., Caro, E., Crippen, R., Duren, R., Hensley, S., Kobrick, M., Paller, M., Rodriguez, E., Roth, L., Seal, D., Shaffer, S., Shimada, J., Umland, J., Werner, M., Oskin, M., Burbank, D., and Alsdorf, D. (2007). The shuttle radar topography mission. *Rev. Geophys.*, 45.

Fouke, B., Farmer, J., Marais, D., Pratt, L., Sturchio, N., Burns, P., and Discipulo, M. (2000). Depositional facies and aqueous-solid geochemistry of travertine-depositing hot springs (Angel Terrace, Mammoth Hot Springs, Yellowstone National Park, U.S.A.). *Journal of Sedimentary Research*, 70:565–585.

Fraedrich, K., Jansen, H., Kirk, E., Luksch, U., and Lunkeit, F. (2005a). The planet simulator: towards a user friendly model. *Meteorologische Zeitschrift*, 14:299–304.

Fraedrich, K., Jansen, H., Kirk, E., and Lunkeit, F. (2005b). The planet simulator: green planet and desert world. *Meteorologische Zeitschrift*, 14:305–314.

Gaillardet, J., Dupr, B., Louvat, P., and Allgre, C. (1999). Global silicate weathering and CO_2 consumption rates deduced from the chemistry of large rivers. *Chemical geology*, 159:3–30.

Gaillardet, J., Rad, S., Rive, K., Louvat, P. amd Gorge, C., Allegre, C., and Lajeunesse, E. (2011). Orography-driven chemical denudation in the Lesser Antilles: Evidence for a new feed-back mechanism stabalizing atmospheric CO_2. *American Journal of Science.*

Gislason, S., Arnorsson, S., and Armannsson, H. (1996). Chemical weathering of basalt in southwest Iceland: Effects of runoff, age of rocks and vegetative/glacial cover. *American Journal of Science*, 296:837–907.

Godderis, Y., Y., D., M., T., and C., D. (2008). Shield effect on continental weathering: Implications for climatic evolution of the earth at the geological time scale. *Geoderma*, 145:439–448.

Goddris, Y., Franois, L., Probst, A., Schott, J., Moncoulon, D., Labat, D., and Viville, D. (2006). Modelling weathering processes at the catchment scale: The WITCH numerical model. *Geochimica et Cosmochimica Acta*, 70:1128–1147.

Hartmann, J. (2009). Bicarbonate-fluxes and CO_2-consumption by chemical weathering on the Japanese Archipelago - Application of a multi-lithological model framework. *Chemical Geology*, 265:237–271.

Hartmann, J., Jansen, N., Drr, H., Kempe, S., and Khler, P. (2009). Global CO_2 consumption by chemical weathering: What is the contribution of highly active weathering regions? *Global and Planetary Change.* doi:10.1016/j.gloplacha.2009.07.007.

Hartmann, J., Jansen, N., Dürr, H., Harashima, A., Okubo, K., and Kempe, S. (2010). Predicting riverine dissolved silica fluxes to coastal zones from a hyperactive region and analysis of their first-order controls. *Int. J. Earth Sci.*, 99:207–230.

Hartmann, J. and Moosdorf, N. (2011). Chemical weathering rates of silicate-dominated lithological classes and associated liberation rates of phosphorus on the Japanese Archipelago - Implications for global scale analysis. *Chemical Geology*, 287:125–157.

Hartmann, J. and Moosdorf, N. (2012). The new global lithological map database GLiM: A representation of rock properties at the Earth surface. *Geochemistry Geophysics Geosystems*, 13.

Heimsath, A., Dietrich, W., Nishiizumi, K., and Finkel, R. (1997). The soil production function and landscape equilibrium. *Nature*, 388:358–361.

Hilley, G. and Porder, S. (2008). A framework for predicting global silicate weathering and CO_2 drawdown rates over geologic time-scales. *PNAS*, 105(44):16855–16859.

Holland, H. (1978). *The Chemistry of Oceans and Atmosphere.* Wiley, New York.

Holland, H. (2004). The geologic history of seawater. In Elderfield, H., Holland, H., and Turekian, K., editors, *Treatise on Geochemistry, Vol. 6. The Oceans and Marine Geochemistry*, pages 583–625. Elsevier Pergamon, Kidlington, Oxford.

Humphreys, G. and Wilkinson, M. (2007). The soil production function: A brief history and its rediscovery. *Geoderma*, 139:73–78.

IPCC (2007). *Fourth Assessment Report: Climate Change 2007: The Physical Science Basis.* Cambridge University Press.

Kasting, J. and Catling, D. (2003). Evolution of a Habitable Planet. *Annu. Rev. Astron. Astrophys.*, 41:429–463.

Kleidon, A. (2009). Climatic constraints on maximum levels of human metabolic activity and their relation to human evolution and global change. *Climatic Change*, 95:405–431.

Knoll, M. and James, W. (1987). Effect of the advent of and diversification of vascular land plants on mineral weathering through geologic time. *Geology*, 15:1099–1102.

Kothavala, Z., Oglesby, R. J., and Saltzman, B. (1999). Sensitivity of equilibrium surface temperature of ccm3 to systematic changes in atmospheric co_2. *Geophys. Res. Lett.*, 26:209–212.

Kump, L., Brantley, S., and Arthur, M. (2000). Chemical weathering, atmospheric CO_2, and climate. *Annu. Rev. Earth Planet. Sci.*, 28:611–667.

Lenton, T., Crouch, M., Johnson, M., Pires, N., and Dolan, L. (2012). First plants cooled the Ordovician. *Nature Geoscience*, 5:86–89.

Livingston, D. (1963). *Data of Geochmistry*, chapter G. USGS Prof. Paper 440-G, 6 edition. (M. Fleischer ed.).

Lunkeit, F., K., F., Jansen, H., Kirk, E., Kleidon, A., and Luksch, U. (2004). *Planet Simulator Reference Manual.* Meteorological Institute, University of Hamburg. http://www.mi.uni-hamburg.de/Planet-Simulator.216.0.html.

Marty, B. and Tolstikhin, I. (1998). CO_2 fluxes from mid-ocean ridges, arcs and plumes. *Chemical Geology*, 145:233–248.

McKenzie, J. and Vasconcelos, C. (2009). Dolomite Mountains and the origin of the dolomite rock of which they mainly consist: historical developments and new perspectives. *Sedimentology*, 56:205–219.

Meybeck, M. and Ragu, A. (1995). GEMS/Water Contribution to the Global Register of River Inputs (GLORI. Technical report, UNEP/WHO/UNESCO, Geneva.

Montgomery, D. and Brandon, M. (2002). Topographic controls on erosion rates in tectonically active mountain ranges. *Earth Planet. Sci. Lett.*, 201:481–489.

Moosdorf, N., Hartmann, J., and Lauerwald, R. (2011a). Atmospheric CO_2 consumption by chemical weathering in North America. *Geochimica et Cosmochimica Acta*, 75:7829–7854.

Moosdorf, N., Hartmann, J., and Lauerwald, R. (2011b). Changes in dissolved silica mobilization into river systems draining North America until the period 2081-2100. *Journal of Geochemical Exploration*, 110:31–39.

Moquet, J. et al. (2011). Chemical weathering and atmospheric/soil CO_2 uptake in the Andean and Foreland Amazon basins. *Chemical Geology*, 287:1–26.

Morse, J. and MacKenzie, F. (1990). *Geochemistry of Sedimentary Carbonates*, volume 48 of *Developments in Sedimentology*. Elsevier, Amsterdam.

Moulton, K., West, J., and Berner, R. (2000). Solute flux and mineral mass balance approaches to the quantification of plant effects on silicate weathering. *American Journal of Science*, 300:539–570.

Nockolds, S. (1954). Average chemical compositions of some igneous rocks. *Bulletin of the Geological Society of America*, 65:1007–1032.

Oglesby, R. and B., S. (1990). Sensitivity of the equilibrium surface temperature of a gcm to systematic changes in atmospheric carbon dioxide. *Geophys. Res. Lett.*, 17:1089–1092.

Porada, P., Arens, S., Buandia, C., Gans, F., Schymanski, S., and Kleidon, A. (2010). A simple global land surface model for biogeochemical studies. Technical Report 18, Max-Planck-Institute for Biogeochemistry, http://www.bgc-jena.mpg.de.

Raymo, M. and Ruddiman, W. (1992). Tectonic forcing of late Cenozoic climate. *Nature*, 359:117–122.

Raymo, M., Ruddiman, W., and Froelich, P. (1988). Influence of late Cenozoic mountain building on ocean geochemical cycles. *Geology*, 16:649–653.

Regenauer-Lieb, K., Yuen, D., and Branlund, J. (2001). The Initiation of Subduction: Criticality by Addition of Water? *Science*, 294:578–580.

Reubens, B., Poesen, J., Danjon, F., Geudens, G., and Muys, B. (2007). The role of fine and coarse roots in shallow slope stability and soil erosion control with a focus on root system architecture: a review. *Trees*, pages 385–402.

Ridgwell, A. and Zeebe, R. (2005). The role of the global carbonate cycle in the regulation and evolution of the earth system. *Earth Planet. Sci. Lett.*, 234:299–315.

Riebe, C., Kirchner, J., and Finkel, R. (2004). Erosional and climatic effects on long-term chemical weathering rates in granitic landscapes spanning diverse climate regimes. *Earth Planet. Sci. Lett.*, 224:547–562.

Schlesinger, W. (1997). *Biogeochemistry. An Analysis of Global Change.* Academic Press, 2nd edition.

Schnoor, J. (1990). Kinetics of chemical weathering: a comparison of laboratory and field rates. In Stumm, W., editor, *Aquatic Chemical Kinetics*, pages 475–504. Wiley, New York.

Schwartzman, D. and Volk, T. (1989). Biotic enhancement of weathering and the habitability of Earth. *Nature*, 340:457–460.

Sheffield, J., Goteti, G., and Wood, E. (2006). Development of a 50-yr high-resolution global dataset of meteorological forcings for land surface modeling. *J. Climate*, 19:3088–3111.

Shvartsev, S. (2001). The water-rock synergy. *Earth Science Frontiers*, 8:36–45.

Shvartsev, S. (2008a). Geochemistry of fresh groundwater in the main landscape zones of the earth. *Geochemistry International*, 46:1285–1398.

Shvartsev, S. (2008b). Interaction in the Water-Rock System as a New Basis for the Development of Hydrogeology. *Russian Journal of Pacific Geology*, 2:465–475.

Sokolova, T. (2013). Decomposition of clay minerals in model experiments and in soils: Possible mechanisms, rates, and diagnostics (analysis of literature). *Eurasian Soil Science*, 46:201–218.

Stallard, R. and Edmond, J. (1983). Geochemistry of the Amazon 2: The influence of geology and weathering environment on the dissolved load. *JGR*, 88:9671–9688.

Taylor, G. and Eggletom, R. (2001). *Regolith Geology and Geomorphology.* Wiley.

Taylor, L., Banwart, S., Valdes, P., Leake, J., and Beerling, D. (2012). Evaluating the effects of terrestrial ecosystems, climate and carbin dioxide on weathering over geological time: a global-scale process-based approach. *Phil. Trans. R. Soc. B*, 367:565–582.

Taylor, L., Leake, J., Quirk, J., Hardy, K., Banwart, S., and Beerling, D. (2009). Biological weathering and the long-term carbon cycle: integrating mycorrhizal evolution and function into the current paradigm. *Geobiology*, 7:171–191.

Urey, H. (1952). *The planets, their origin and development.* Yale University Press.

Von Bloh, W., Franck, S., Bounama, C., and Schellhuber, H.-J. (2003). Biogenic enhancement of weathering and the stability of the ecosphere. *Geomicrobiology Journal*, 20:501–511.

Walker, J., Hays, P., and Kasting, J. (1981). A negative feedback mechanism for the long-term stabilization of earth's surface temperature. *Journal of Geophysical Research*, 86:9776–9782.

Wallmann, K. (2001). Controls on the Cretaceous and Cenozoic evolution of seawater composition, atmospheric CO_2 and climate. *Geochimica et Cosmochmica Acta*, 65:3005–3025.

Wardle, D., Walker, L., and Bardgett, R. (2004). Ecosystem properties and forest decline in contrasting long-term chronosequences. *Science*, 305:509–513.

West, A., Galy, A., and Bickle, M. (2005). Tectonic and climatic controls on silicate weathering. *Earth Planet. Sci. Lett.*, 235:211–228.

Whipple, K. (2001). Fluvial landscape reponse time: how plausible is steady-state denudation? *Am. Jour. Sci.*, 301:313–325.

White, A., Blum, A., Schulz, M., Bullen, T., Harden, J., and Peterson, M. (1996). Chemical weathering of a soil chronosequence on granitic alluvium: 1. reaction rates based on changes in soil mineralogy. *Geochim. Cosmochim. Acta.*

White, A. and Brantley, S. (2003). The effect of time on the weathering of silicate minerals: why do weathering rates differ in the laboratory and field? *Chemical Geology*, 202:479–506.

White, A., Bullen, T., Vivit, D.V. Schulz, M., and Clow, D. (1999). The role of disseminated calcite in the chemical weathering of granitoid rocks. *Geochimica et Cosmochmica Acta*, 63:1939–1953.

Willenbring, J. and von Blanckenburg, F. (2010). Long-term stability of global erosion rates and weathering during late-Cenozoic cooling. *Nature*, 465:211–214.

Willett, S. and Brandon, M. (2002). On steady states in mountain belts. *Geology*, 30:175–178.

Wollast, R. and Mackenzie, F. (1983). Global cycle of silica. In Aston, S., editor, *Silicon geochemistry and biogeochemistry*, pages 39–76. Academic, New York.

Zeebe, R. and Caldeira, K. (2008). Close mass balance of long-term carbon fluxes from ice-core CO_2 and ocean chemistry records. *Nature Geoscience*, 1:312–315.

Acknowledgements

There are many people to whom I am indebted, and without whom I would not have been able to accomplish the daunting task of writing a Ph.D. dissertation. When I started out I had no idea what I was embarking on. As the americans so like to say in anything that leads to their personal development “it has been a journey”. Corny and worn-out as this term may be, it really coins what it entails to pursue a doctoral degree. A journey is not a vacation, it means getting to where you are going, bumpy as the ride may be. In the end, you often find yourself forgetting the troubles you had on the way, and you might also have forgotten people you met, if the journey was long. Should that be the case in relation to my “journey” towards this document, I sincerely apologize.

To my advisor and group leader, Axel Kleidon, who gave me the opportunity to pursue a doctorate after a single meeting of a couple of hours: It was an exciting experience to join the group so early on and to watch it grow. Somehow you manage to always meet problems with fresh eyes, even when presented with them for the umpteenth time, and you are a master of spotting loose ends and tying them up, or pointing in the right direction. I have often left a meeting with you with a wealth of new ideas, which later developed into significant parts of this work. I especially want to thank you for your patience towards the end. For knowing when to push on, and when not to. Finally, I want to thank you for introducing me to Anke.

Anke Hildebrandt, my university supervisor, who joined in the 11th hour. Thank you for your enthusiasm and support. You made this all possible in the end.

I met Dr. Guy Munhoven at countless conferences. You were always interested in and supportive of my work. Thank you for providing the lithological data so crucial to my modeling efforts and for your feedback on the saturated rivers paper. Dr. Nils Moosdorf, Prof. Dr. Jens Hartmann, Dr. Yves Goddéris and Prof. Dr. Victor Brovkin also provided invaluable feedback at conferences and workshops. A special thanks goes to Nils for your comments on my manuscript on the regolith model, to Jens for your comments on an earlier version of this document, and to Prof. Dr. Jonas Kley for his interest and support when I first introduced my work at the Institut für Geowissenschaften.

Due thanks is owed to Dr. Uwe Mikolajewicz and Veronika Gayler for providing

ECHAM5 data used in glacial simulations.

I would also like to take this opportunity to thank the Helmholtz-Gemeinschaft as this work has been supported by the Helmholtz Association through the research alliance “Planetary Evolution and Life”.

I met many people during my time in Jena. Notably, the group members of the Biospheric Theory and Modelling group played a significant role in making my stays in Jena memorable on a number of occasions. Corina Buendía, thank you for many good discussions on weathering, especially on the role of vegetation. Eugenio Simoncini, thanks for taking the time to explain some basic geochemistry to me, this was really helpful. Lee Miller, you were a good help with troublesome data transformations. Thanks for your philosophical views and for generally creating a good atmosphere at group meetings. Fabian Gans, my german translator, particular thanks for translating the thesis abstract into german but also for your help with german in general. Philipp Porada, I thank you for your skewed view on things, your crazy tastes and your ability to remember ’90’s pop lyrics... one more time. Ryan Pavlick, I was very happy to share an office with you, especially in the beginning when you always knew the answers to my more or less stupid computing related questions. A special thanks for the gaming nights during my stay in 2012 is owed to Nathaniel Virgo, Philipp and Lena, Fabian and Alexandra. Other members of the group without whom Jena would not have been the same are/were: James Dyke, Kristin Bohn, Björn Reu and Stan Schymanski. Finally, a special thanks to Steffen Richter, Kerstin Sickel and the IT department at the Max Planck Institute for Biogeochemistry for technical support, and to Birgitta Wiehl for administrative support. Without you, Birgitta, we would not have gotten to where we were going, and we would all have been out of pens and paper. You are the backbone of “the tower”.

My friends in Jena, that are/were not a member of the Biospheric Theory and Modelling group, but nonetheless significant to me: Julia Marshall, Jeremi Thebeau, Bela Thebeau (and little Corvin), the Heimanns, Kerry Hinds and Myroslava Khomik. Thank you, Julia, for correcting the english of my introduction and summary. Any errors left are off course entirely my own responsibility. And thank you all for good company. I will leave our anecdotes for some other time.

At long last, I would like to thank my family: My parents for always believing in me, my siblings for always being right where I expect you to be, Robbert for introducing a new, albeit distractive dimension to my life and Calin Arens - I thank you for everything. Nothing less will do.

Selbständigkeitserklärung

Ich erkläre, dass ich die vorliegende Arbeit selbständig und nur unter Verwendung der angegebenen Hilfsmittel, persönlichen Mitteilungen und Quellen angefertigt habe.

....

Ort, Datum Susanne K. M. Arens